Titrimetric monitoring of chemical equilibrium and pH dynamics in a pilot-scale water resource recovery facility using PHREEQC and buffer capacity modelling

Mémoire

Maryam Tohidi

Maîtrise en génie des eaux - avec mémoire
Maître ès sciences (M. Sc.)

Québec, Canada

Titrimetric monitoring of chemical equilibrium and pH dynamics in a pilot-scale water resource recovery facility using PHREEQC and buffer capacity modelling

Mémoire

Maryam Tohidi

Sous la direction de:

Peter A. Vanrolleghem, directeur de recherche
Céline Vaneeckhaute, codirectrice de recherche

Résumé

L'augmentation considérable de l'eutrophisation des eaux de surface dans les dernières décennies a mené à la création de stations de récupération des ressources de l'eau (StaRRE) de plus en plus instrumentées pouvant procéder à l'élimination des nutriments. Pour assurer l'efficacité des procédés de récupération, plusieurs paramètres de qualité des eaux doivent être surveillés. Des méthodes en ligne et hors-ligne existent pour réaliser cette surveillance. Cependant, certains paramètres sont difficilement mesurés en ligne, alors des analyses en laboratoire sont toujours de mise. La titrimétrie est une méthode hors-ligne permettant la surveillance de la qualité des eaux en laboratoire.

Un appareil Titrino a été installé afin de procéder à l'analyse titrimétrique des eaux usées de l'usine pilEAUte, une StaRRE de traitement expérimentale de 12 m^3 située sur le campus de l'Université Laval. L'eau usée de cette station provient d'une résidence étudiante du campus et de ses environs. L'eau pompée vers la station est stockée dans un bassin de 5 m^3 avant d'être acheminée à un décanteur primaire. L'effluent du décanteur est alors envoyé vers deux chaînes de traitement biologique composées de cinq bioréacteurs chacune. Enfin, l'eau est acheminée vers deux décanteurs secondaires. Dans le cadre de ce projet, des campagnes de mesure ont été réalisées afin de comparer les données provenant de capteurs en ligne avec l'information extraite d'expériences de titrimétrie pour la mesure de la qualité des eaux usées de la station. Ces campagnes de mesure ont été réalisées en lien avec de projets menés avec des partenaires industriels.

L'objectif de cette étude est d'évaluer l'efficacité des analyses de titrimétrie pour la mesure de la qualité de l'eau à l'affluent et à l'effluent d'une StaRRE. Les données extraites de la titrimétrie sont analysées de deux façons différentes: la modélisation de la capacité tampon de l'eau et la modélisation de l'équilibre chimique via le logiciel PHREEQC. Ces méthodes ont été mises en place, puis comparées sur la base de leur efficacité pour mesurer la concentration de certaines substances tampon présentes dans les eaux usées. Pour améliorer les estimations des modèles, des améliorations au protocole d'utilisation du Titrino ont été développées. Il a été déterminé que l'utilisation d'une couverture d'azote gazeux et le stripage du CO_2 dissout dans les échantillons sont nécessaires à la réalisation de titrations fiables, et sont donc aussi

nécessaires à la mesure de substances tampon autre que l'alcalinité, soit l'ammoniaque et les acides gras volatils (AGV).

Afin de valider les résultats obtenus à l'aide du modèle de capacité tampon et afin d'obtenir une description complète de l'équilibre chimique des solutions analysées, un modèle de simulation de la procédure de titration a été développé avec le logiciel PHREEQC et l'interface PHREEQXCEL. Cet environnement de simulation a été supplémenté du solveur OpenSolver, un complément Excel à licence libre capable de réaliser les estimations de paramètres requises pour estimer la concentration de chaque espèce chimique présente dans les échantillons. De plus, la base de données de réactions chimiques de PHREEQC a été modifiée afin d'inclure toute l'information chimique nécessaire à la modélisation des spéciations se produisant dans les eaux usées. Après avoir proposé ces améliorations et avoir comparé les résultats des analyses de titration à des analyses chimiques conventionnelles, il a été déterminé que la titrimétrie est une alternative fiable pour la surveillance de la performance des procédés de récupération des nutriments des eaux usées.

Abstract

The considerable rise of eutrophication in water bodies has led to highly instrumented water resource recovery facilities (WRRFs) that can perform nutrient removal processes. To ensure the efficiency of these processes, several parameters that influence the performance of WRRFs need to be well thought out. The latter requires monitoring strategies composed of on-line and off-line methods. Lately, on-line measurements have contributed significantly to monitor and characterize the quality of water and wastewater. However, on-line measurements are not applicable or not implemented yet for some specific areas. For this, off-line laboratory methods are welcome alternatives. Titrimetry is one of the examples of a low-cost off-line method that allows characterizing aquatic streams.

Concerning titrimetric monitoring of wastewater, a Titrino device was installed in the laboratory of the 12 m^3 pilEAUte WRRF located at Université Laval. The wastewater feeding the plant is coming from a student residence building on campus. The water pumped to the station is feeding a storage tank with a volume of 5 m^3, from which it is then pumped to a primary clarifier. The influent stream is then split into two similar treatment lines, composed of several bioreactors. These two lanes are followed by two secondary settling tanks. In this work, sampling campaigns were performed to compare the sensor data and the off-line titrimetric measurements in a framework of research projects in which industrial partners are involved.

The goal of this study was to investigate the efficiency of using titrimetry to analyze and characterize influent and effluent samples of a WRRF. Two data interpretation methods, buffer capacity and PHREEQC, were tested and their performances in estimating the concentration of the concerned buffers were evaluated. For better model estimation, first, some of the lab procedures were improved. It was found out that nitrogen blanketing and CO_2 stripping are necessary to perform reliable titration, and thus, to measure other concerned buffers besides alkalinity, such as ammonia and volatile fatty acids (VFA).

Moreover, to validate the results of the buffer capacity model and to have a complete description of the equilibrium reactions of the chemical system under study, a titration simulation model was successfully built in PHREEQC with the PHREEQXCEL interface. This titration lab simulation was extended with the OpenSolver, an open-source Excel add-in,

which allows to reliably perform the parameter estimation needed to find the concentration of the different species in the sample. In addition, PHREEQC's database was modified to include all the model components and their essential chemical information for the speciation calculations.After introducing the mentioned lab and modelling improvements, the reliability of the titrimetric measurements for monitoring the performance of nutrient removal was enhanced.

Contents

List of Tables

List of Figures

"Let yourself be silently drawn by the stronger pull of what you really love. It will not lead you astray."

Rumi

Acknowledgments

I arrived in Québec, on a cold September night in 2017, terrified but mostly excited by all the unknowns of this journey and the new life I was beginning. What makes this journey unforgettable and most valuable for me is indeed beyond these handful of pages. On this journey, I got inspired by the people who walked alongside me. I would like to thank them here, with all my heart.

I would first like to thank my supervisor, Peter Vanrolleghem, who believed in me from continents away and gave me the privilege to work with him and his highly professional team.

Peter, I will never forget that on my first time in your office, you said that you would neither be my director, nor my professor, you would be my supervisor. You meant that you would never order me around, but instead guide me along my path. I would add that you were much more to me than a supervisor! Thanks for always leaving your door open for my 5-minutes-long questions and my Friday evening meetings! Thanks for all the time you said to me: "Don't run, I have time" when you caught me running in the corridor towards our meeting. For all the great moments of brainstorming together, and all the inspiring ideas you gave me. I learnt how to use my perfectionism constructively thanks to your positive attitude and thoughtful mentoring. But more importantly, thank you for believing in me when I didn't, and for listening and sympathizing with me in the hardest days.

I would like to thank my co-supervisor, Céline Vaneeckhaute, who always welcomed me warmly in her inspiring and fun research group. **Céline**, thanks for supporting me with all my PHREEQC questions. It is always inspiring seeing you and your passion for research.

I would especially like to thank the director of the department, **Prof. Paul Lessard**, for his precious comments on this work, and for his supportive attitudes towards learning French. J'ai toujours apprécié nos petites conversations en français dans le bus sur le chemin de l'école. Merci!

And my awesome colleagues and friends...

Elena Torfs, thank you for your warm presence in the very first days of this journey, for giving me that nodding smile in our first meeting with Peter, giving me the courage to say

what was in my head and not to be scared! For the very friendly environment that you welcomed me in that made me feel less far from home, for the beautiful days in the chalet, and all the nice and deep chats over coffee in the corridor. You were always there as a listening ear. I miss you a lot, and hoping selfishly to have you back in Québec soon!

Andreia Amaral, I can't say in words how much I am happy that you joined the team! You always inspired me with your wonderful talent for simplifying and breaking down big problems! Thanks for your precise, kind, and practical comments, Andreia! You always gave your compliments first, which made me receive your critics with an open heart and mind! Your positive energy is beyond all words, and it boosted me up every time I was down.

Thanks to all my friends in **model*EAU*** and our small office B, in particular **Romain**, for all the fun days in the lab and more, **Kamilia**, for all our *cherry on the top of the cake* chats, **Rania**, for your always calm presence and all your help with Titrino, **Feiyi**, for all the office neighbour brainstorms, **Bernard**, for all the chill coffee breaks, and **Sovanna**, for your open and kind heart. I am also grateful to **Gamze** and **Niels** for their irreplaceable help with the *AvN* project.

I especially want to thank **Christophe Boisvert** for his great help during his internship during our measuring campaigns and for his creative ideas for developing PHREEQC. Thanks also to **Michele Ponzelli** for our laboratory collaborations for the Primary Reactive Settler project.

I am grateful to my friends in Iran and Canada and all around the world, in particular **Fa**, for her warm presence in Canada. Living with her made home feel closer. I am grateful to **Shiva**, my best and oldest friend, for her presence, which is far in miles but closest to my heart.

And...

Thanks to my best colleague, friend, and lover, **Jean-David**, for all his support throughout this journey. First, thanks for your help translating the abstract of this work in French, and for all your technical and language support with my thesis. You were always introducing me to the coolest, most minimal, and applicable tools and platforms which lifted my motivation and creativity. I am so grateful for you making me feel understood every time I was hopeless and more than that, for your vital presence, and for lifting me up when I was low! Thank you for believing in me, for accepting me for who I am, and for continuing to dream with me. I keep loving you more and more every day.

Last but not least, my dad, **Bijan** whom, every day of my life here and back home, I wished was still among us. I wished I could hear his voice, wish I could get his advice... Still, I feel that he somehow sees me and shows me the way whenever I am lost. Baba, I want you to know that I am very proud of being your girl, you made me who I am, you made me feel

tall since I was only 3 when you framed my drawings. I love you and I hope I can make you proud.

My strongest mom, **Mansoureh**, who allowed me to find my voice, who knew when to hold me close and when to let me go. Maman, thanks for believing in me, and for raising me in such a way that I can now depend on myself. Without you, I may not be standing where I am, thanks for taking me to your chemistry lab classes where I was dreaming of being you one day. Thank you for encouraging me to follow my dreams. I love you and I can't wait to see you and jump into your arms.

My brothers, **Mohammad and Alireza**, thanks bros for supporting me in my decisions, for standing beside me, and for taking care of Mom! I love you, and I can't wait to see you all soon.

Maryam Tohidi

11 May 2020

Introduction

The considerable rise of eutrophication in water bodies has led to highly instrumented water resource recovery facilities (WRRFs) that can perform treatment processes resulting in high standard effluent quality. To ensure the efficiency of these processes, several parameters that influence the performance of WRRFs need to be well thought out. The latter requires monitoring strategies composed of on-line and off-line methods. Lately, on-line measurements have contributed significantly to monitor and characterize the quality of water and wastewater. For some specific areas where on-line measurements are not applicable or not implemented, off-line laboratory methods are welcome alternatives. Beyond instrumentation-based control strategies, the application of mathematical modelling of the wastewater treatment processes has led to a better understanding of these processes and the characterization of wastewater. Thus, more robust and efficient treatment strategies are developed and applied.

Amongst the existing treatment processes, the activated sludge process is one of the oldest and routinely used biological treatment processes, which is applied for industrial and municipal wastewater treatment. The activated sludge process as its name suggests, is built around the production of an activated mass of organisms capable of removing pollution (Metcalf & Eddy, 2014). During this process, in the biological reactors, these organisms use the pollutants present in the influent wastewater to grow. These organisms then flocculate and leave the water relatively free from suspended solids and soluble contaminants. Once the flocculated particles or sludge have settled, this water can be discharged into natural waters. The effluent stream should meet the discharge limits in terms of nutrients and other contaminants. However, the quality of the effluent depends on the treatment processes and the quality of the influent. Therefore, knowing the characteristics of the effluent together with the influent can help to increase the efficiency of the treatment, and thus meeting the discharge limits. Titrimetry is one of the examples of a low-cost off-line method that allows characterizing aquatic streams.

In view of the titrimetric monitoring of wastewater, a Titrino device was installed in the laboratory of the 12 m^3 pil*EAU*te WRRF located at Université Laval. The wastewater feeding the plant is coming from a student dormitory on campus. The water pumped to the station is feeding a storage tank with a volume of 5 m^3, from which it is then pumped to

a primary clarifier. The effluent of the primary clarifier is collected in a measurement tank, where a group of sensors is installed to characterize the influent water. The influent stream is then split into two similar treatment lines, composed of several bioreactors. These two lanes are followed by two secondary settling tanks, where another group of sensors is installed to measure the effluent quality of the treatment plant. Besides the on-line monitoring of the influent and effluent quality, off-line measurement campaigns are also performed to validate the sensors. Titrimetry is an off-line method that can replace wet chemical analyses for the measurement of some variables thanks to its simple procedure and cost-effectiveness. In this work, titrimetric analysis is used to measure bicarbonate alkalinity, volatile fatty acids (VFA), and ammonium concentrations.

The titrimetric analysis performed in this work uses an experimental titration setup to titrate wastewater samples with an acid or base titrant, connected to a portable computer (PC) that collects the titration data and plots the titration curve (pH changes as function of the consumed volume of titrant), to which, finally, a mathematical model is applied to interpret the titration data. One of the mathematical models used in this study is the buffer capacity model, which was used and developed by Van Vooren (2000). This Excel-based model calculates the buffer capacity as the inverse of the slope of the titration curve at each point of the titration. The measured buffer capacity values are then plotted as function of the pH values, generating the buffer capacity curve. A measured curve determined as the experimental buffer capacity curve, is used to estimate the chemical composition of the sample. Fitting the measured to the calculated buffer capacity curves, the concentration of the buffers in the model can be estimated.

PHREEQC is the other modelling tool used in this work, providing a more complete description of the equilibrium reactions of the chemical system under study. This software can engage with more complex and non-linear calculations comparing to the buffer capacity model that can only handle simple acid-base chemical equilibria. Therefore, PHREEQC is used to incorporate more parameters for better model estimation.

During this MSc study, the titrimetric analysis was applied to different measurement campaigns and case studies in the pil*EAU*te WRRF. The *primary reactive settler* and the *AvN project* are the two case studies in which titrimetry was used for characterizing the wastewater samples. These case studies and their objectives are introduced briefly within this work, and the results of the performed titrimetric analysis are presented and discussed.

Chapter 1

Literature review

1.1 Basic background

With the growth of the world population, the human contribution to waterbody pollution is ever increasing. This contribution manifests itself in different forms, such as in the discharge of domestic or industrial wastewater, or the application of fertilizers onto the soil (Von Sperling, 2007). All forms of discharge introduce pollutants into water affecting its quality. Suspended solids, biodegradable organic matter, nutrients and pathogenic organisms are the main pollutants in domestic wastewater, which is one of the most abundant type of wastewater.

As the need for reuse of water grows, the necessity of removing nutrients and other contaminants grows. In recent years, the awareness of the problems associated with nutrients in wastewater has drawn significant attention to scientific research and investments in modifying or renovating treatment processes. Indeed, wastewater must be subjected to certain treatment processes to meet discharge limits in terms of nutrient concentrations while remaining cost-effective.

Nitrogen is one of the nutrients of concern and is present in different wastewater compounds. For instance, human urine is one of the nitrogen sources and causes eutrophication, oxygen depletion and ammonia toxicity. Fertilizer nitrogen also ends up in receiving waters in the form of organic nitrogen, ammonium, nitrite, and nitrate. Their discharge into receiving waters eventually leads to irreparable environmental crises and health risks (Van Hulle, 2005).

Phosphorous is another nutrient that is essential for the growth of algae. However, at high loads it leads under certain conditions to eutrophication of lakes and reservoirs (Von Sperling, 2007).

In addition to nutrient contents various other parameters, can indicate the quality of wastewaters. The three main types of wastewater characteristics are physical, chemical and

biological in nature (Metcalf & Eddy, 2014). Some of these constituents of concern in the treatment of wastewater are briefly introduced later in this chapter.

Removal of the contaminants which are involved in various chemical and biological reactions, occurs within different treatment steps or unit processes. These unit process are split into different levels, beginning with preliminary and primary treatments which are mainly physical operations, followed by secondary treatment, and in some cases, tertiary treatment.

In preliminary treatment, large objects and gross solids in the wastewater are removed. In primary treatment, sedimentation is the main physical process that is used to remove a fraction of the suspended solids and organic matter. In secondary treatment, biological and chemical processes are applied to remove biodegradable organic matter and suspended solids. Tertiary treatment, uses advanced treatment options to further reduce pollutants, and could involve some type of physicochemical processes such as coagulation, filtration, reverse osmosis, disinfection, and etc.

For over 30 years, biological nutrient removal (BNR) has been integrated into the application and design of biological treatment systems (Metcalf & Eddy, 2014). It has thus become a part of the conventional secondary wastewater treatment. The reason for this addition to the treatment processes is the advantage of using BNR compared to chemical treatment processes, in which a lot of chemicals are consumed and a significant amount of waste solids are produced.

1.2 Wastewater composition

The most important characteristics of wastewater that deserve special consideration with regards to this study are:

- Solids
- Organic matter
- pH
- Alkalinity
- Nitrogen
- Phosphorous

These components may be classified based on different aspects, that indicate directly or indirectly the composition of the wastewater.

1.2.1 Solids

Excluding dissolved gases, all the water's contaminants contribute to loads of solids in wastewater (Von Sperling, 2007). The total solids content is the most important physical characteristic of wastewater in which various matters with different sizes and settleability are included. In fact, total solids can be classified based on size, chemical characterization and settleability.

According to their size, they can either be suspended (filterable) or dissolved (non-filterable). Colloidal solids have an intermediate size that is hard to identify with simple methods of filtration, while suspended and dissolved solids can be seperated easily in a single filtration step. Both total suspended solids (TSS) and total dissolved solids (TDS) include chemical forms of volatile solids and inorganic solids. Volatile solids represent the organic fraction in the total solids, which is volatilized under high-temperature conditions (550°C) (Metcalf & Eddy, 2014). The remaining non-volatile solids indicate the inorganic fraction of the total solids.

1.2.2 Organic matter

Organic matter is considered as one of the main causes of water pollution by sewage. Microorganisms cause depletion of oxygen, by oxidizing organic matter for metabolic processes (Von Sperling, 2007). Organic compounds, composed of carbon, oxygen, hydrogen and nitrogen, are present in the wastewater typically as proteins (40 to 60 %), carbohydrates (25-50 %), and fats (8-12 %) (Metcalf & Eddy, 2014).

Organic matter in wastewater can be divided in two fractions: biodegradable and non-biodegradable matter. Several analysis methods have been developed to quantify the organic content of wastewater reflecting the difficulties experienced with its determination due to its multiple forms and characteristics. Thus, direct or indirect methods of measurements are used to quantify the latter.

Measurement of oxygen consumption is an indirect laboratory method including (1) biochemical oxygen demand (BOD) and (2) chemical oxygen demand (COD) tests. The 5 day BOD (BOD_5) is a widely used indicator of organic pollution which measures the dissolved oxygen used by the microorganisms through the biochemical oxidation of organic matter (Metcalf & Eddy, 2014). It is also known as an indicator of biodegradable organic carbon (Von Sperling, 2007).

The COD test measures the consumption of oxygen for the chemical oxidation of organic matter with a strong oxidizing agent. For a better understanding of the biological treatment of wastewater, one needs to fractionate the COD. According to Metcalf & Eddy (2014), soluble and particulate COD are the main fractions that are further fractionated to evaluate

the treatability of wastewater. The readily biodegradable soluble COD (rbCOD) is one of the fractions that can be fermented to VFA. The produced VFA is an essential source of carbon in some treatment processes aiming at optimizing the efficiency of the plant.

1.2.3 pH

The concentration of hydrogen ions (H^+) is an important parameter both in treatment processes and in the effluent discharged to natural waters. The range of hydrogen ion concentration, which is expressed as pH and is defined as the negative of the logarithm of the hydrogen ion concentration (1.1), determines the intensity of acidic or basic (or alkaline) conditions of the water.

$$pH = -log_{10}[H^+] \tag{1.1}$$

The hydrogen ion concentration is defined by the dissociation of water, as follows:

$$H_2O \leftrightarrow H^+ + OH^- \tag{1.2}$$

Once this reaction reaches equilibrium, the concentrations of hydrogen and hydroxyl ions are related by:

$$K = \frac{[H^+][OH^-]}{[H_2O]} \tag{1.3}$$

Given the constant concentration of water in a dilute aqueous system, one can incorporate this concentration with the equilibrium constant (K) in (1.3) to give

$$K_w = [H^+][OH^-] \tag{1.4}$$

in which K_w is known as the ionization constant or the ion product of water with a value of approximately 10^{-14} at 25°C.

Most biological life is only possible within a very critical pH range of 6 to 9 (Metcalf & Eddy, 2014). Thus, biological treatment requires a certain pH range to occur. Moreover, for treated effluents discharged to natural waters, restrictions on the allowable pH range are developed to control the environmental impacts.

1.2.4 Alkalinity

Natural waters tend to have a narrow effective concentration or *activity* of hydrogen ions given the presence of buffers. Buffers are solutions of a weak acid and its salt (or a weak base and its salt) that resist pH changes and maintain the solution's pH at a stable value. The pH of many natural waters is affected by the presence of buffering systems, mainly dissolved inorganic carbon species including carbon dioxide (CO_2), bicarbonate (HCO_3^-), and carbonate (CO_3^{2-}) (Chapra, 2008).

CO_2 combines with water and forms carbonic acid (H_2CO_3) which, in turn, dissociates into ionic forms, as follows:

$$H_2CO_3 \leftrightarrow H^+ + HCO_3^- \tag{1.5}$$

with equilibrium constant K_1:

$$K_1 = \frac{[H^+][HCO_3^-]}{[H_2CO_3]} \tag{1.6}$$

The bicarbonate ion, in turn, dissociates to:

$$HCO_3^- \leftrightarrow H^+ + CO_3^{2-} \tag{1.7}$$

with equilibrium constant K_2:

$$K_2 = \frac{[H^+][CO_3^{2-}]}{[HCO_3^-]} \tag{1.8}$$

Given the concentration of the dissolved carbonate species within the aforementioned equations, one can express the total inorganic carbon concentration as:

$$c_T = [H_2CO_3] + [HCO_3^-] + [CO_3^{2-}] \tag{1.9}$$

A simple carbonate system can be illustrated as pure water in equilibrium with a gas phase, for instance, the CO_2 in the atmosphere, with constant partial pressure. Adding a strong acid or base will vary the pH, thereby keeping the solution in equilibrium with CO_2. Such a system of aqueous carbonate equilibrium with atmospheric CO_2 is shown in Figure 1.1. It can be seen that by adding an acid to the carbonate system, the equilibriums in the two equations (1.5) and (1.7) are shifted to the right side with more bicarbonate being converted to carbonic acid and more carbonate being converted to bicarbonate, respectively. Thus, once the pH changes, so do the amounts of carbonate solutes in the system.

Considering the presence of hydroxyl ions (OH^-) in the buffering system due to the dissociation of water itself (1.4), and the amounts of conjugate ions of the base (c_B) or acid (c_A) that have been added to the system respectively, the electroneutrality of the solution can be expressed as

$$c_B + [H^+] = [HCO_3^-] + 2[CO_3^{2-}] + [OH^-] + c_A \tag{1.10}$$

This charge balance equation can be formulated in a more practical way by introducing *alkalinity* as an alternative to the added amount of acid and base to the system (1.11):

$$Alkalinity = [HCO_3^-] + 2[CO_3^{2-}] + [OH^-] - [H^+] \tag{1.11}$$

In other words, alkalinity is the chemical capacity of water to neutralize acids. However, the above definition of alkalinity (1.11) is only applicable to systems with only inorganic carbon as buffering system. In fact, in wastewaters, other reactions and their compounds contribute

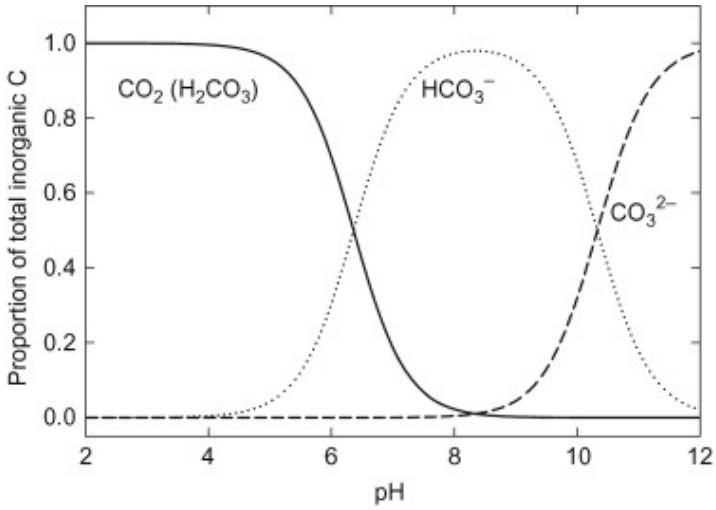

Figure 1.1: Proportion of total inorganic carbonous system as function of pH

to alkalinity, but these are present in very negligible levels in drinking water and are, thus, considered of less importance than the inorganic carbon in many systems (Chapra, 2008). For that reason, the alkalinity reported in this study is expressed as the bicarbonate alkalinity, which only indicates the concentration of the HCO_3^- buffer. It can be measured by titrating against a standard acid solution (see more in Chapter 3).

Alkalinity in wastewater is an important parameter in case chemical and biological treatment processes are used for the removal of nitrogen (see Section 1.3.2).

1.2.5 Nitrogen

Nitrogen is one of the essential elements for growth of microorganisms. It is considered the major nutrient of importance for the biological treatment of wastewater. Nitrogen alternates between various forms and oxidation states that each can be generated by organisms. Ammonia (NH_3, -3), ammonium (NH_4^+, -3), nitrite (NO_2^-, +3), and nitrate (NO_3^-, +5) are the most common forms of *inorganic* nitrogen with their different oxidation states.

The *organic* fraction of nitrogen consists of complex compounds such as amino acids, amino sugars and protein. These compounds of organic nitrogen can be either soluble or particulate. The nitrogen element in these components converts to ammonium thanks to the activity of microorganisms in aquatic systems. Urea, for instance, is mainly found in untreated wastewater (Metcalf & Eddy, 2014). This organic fraction of nitrogen, together with the inorganic fraction comprise *total nitrogen*.

Amino acids, a main fraction of biodegradable soluble organic nitrogen, are the monomers of complex proteins containing carbon and nitrogen. Like inorganic carbon species, these compounds together with total ammoniacal-nitrogen (TAN), nitrite (NO_2^-) and nitrate

(NO_3^-) dissociate in aqueous solutions. Thus, depending on the pH of the solution, different species of a buffering system can exist depending on their equilibrium constant. For instance, ammonia nitrogen equilibrates on an aqueous system with the following reaction:

$$NH_4^+ \leftrightarrow H^+ + NH_3 \tag{1.12}$$

It can thus be concluded that the distribution of the species is depending on the solution's pH.

1.2.6 Phosphorous

Besides nitrogen, phosphorous is the other essential nutrient for growth of algae and microorganisms. Total phosphorus in domestic wastewater is divided into two fractions, organic and inorganic, where the organically bound phosphorous occurs mainly in particulate form. On the other hand, the soluble phosphorus is dominated by inorganic phosphorus compounds, such as orthophosphates and polyphosphates.

Phosphate (PO_4^{3-}), hydrogen phosphate (HPO_4^{2-}), dihydrogen phosphate ($H_2PO_4^-$), and phosphoric acid (H_3PO_4) are the orthophosphates which, similarly to inorganic carbon, dissociate in the aqueous systems and have buffering effects. These buffers are readily available for biological metabolism, whereas polyphosphates must undergo hydrolysis to break-down into orthophosphates (Von Sperling, 2007).

1.3 Wastewater treatment processes

WRRFs generally consist of chemical, physical and biological unit processes that perform different types of treatment. In this section, primary clarifiers and their characteristics that can contribute to biological nitrogen removal are described. Subsequently, the removal processes of nitrogen and COD in the biological tanks are introduced.

1.3.1 Primary settling tanks

Primary settling tanks or clarifiers are used as part of the primary process of wastewater treatment with the purposes of settling and removing suspended particulate matter present in the influent. By removing the settleable solids, a large amount of energy that would have been used for the oxidation of particulates, is saved. Moreover, using a primary clarifier allows for a higher rate of soluble substrate removal during aeration in the biological treatment downstream, and lower overall sludge production (Lessard and Beck, 1988). Thus, an efficient primary clarification promotes the better operation of the biological treatment and sludge treatment units, respectively.

Reactive settling

As the performance of the primary clarifier directly influences the effectiveness of the treatment plant, understanding its dynamics is important. Several mathematical models have been proposed to describe the behaviour of primary clarifiers; however, only little attention has been given to their behaviour in dynamic terms (Lessard and Beck, 1988). In most of the primary clarifier models, no biological reactions are considered to take place in the reactor, and the main focus of the models is on simulating the behaviour of the suspended solids (Gernaey et al., 2001). Later, Bachis et al. (2015) successfully applied their new modelling approach, which was based on the particle settling velocity distribution (PSVD), in an improved primary settler model. It was illustrated that this approach can characterize primary effluent quality under addition of chemicals. Moreover, results of the fractionation of primary clarifier influent and effluent COD have shown changes in the wastewater composition and thus in their modelled fractionation of the wastewater.

Lessard and Beck (1988), during their 10-day measurement campaign at the Norwich WWTP (UK), obtained a complete dataset in which the impact of the biological phenomena in the settler was clearly shown. The biological reactions occuring in so-called reactive primary clarifiers perform best under different operational conditions than conventional clarifiers. Increasing hydraulic retention times or combining the excess biological sludge with the influent to settle in the primary clarifier are some examples of such operational conditions.

Given a long retention time in the primary clarifier, Lessard and Beck (1988) observed degradation and flocculation of the soluble COD. In fact, particulate COD and polymers first degrade through hydrolysis reactions, resulting in monomers that are often rbCOD. These soluble organic components, such as amino acids and fatty acids, are then converted to VFA through acidogenesis reactions (Appels et al., 2008). Fermentation of the primary sludge and consequently the production of VFA and rbCOD can eliminate the need for an external carbon source for the downstream biological nutrient removal processes. Later in this study (see Section 4.3), an application of a reactive primary clarifier in a pilot-scale plant aiming at enhancing VFA production will be discussed and evaluated.

In addition to flocculation and degradation of soluble COD, thanks to the long retention times of the clarifier and the anaerobic zones in the settled sludge, ammonium is released as a result of both hydrolysis and ammonification of organic nitrogen.

1.3.2 Biological tanks

Biological treatment through activated sludge consists of nitrogen and carbon removal which takes place in bioreactors. The active biomass can be divided into heterotrophic or autotrophic organisms depending on their carbon source, organic and inorganic, respectively. These groups of bacteria are responsible for carbon removal, nitrification and denitrification reactions, and

phosphorous removal. Both biomass use oxygen as an electron acceptor. Some heterotrophic organisms can also use nitrate as an electron acceptor under anoxic conditions, which makes denitrification possible. However, these organisms require readily biodegradable carbon, such as VFA or external carbon sources such as methanol, for the process rate to be high. The autotrophic biomass, on the other hand, uses inorganic carbon to produce biomass and ammonium as electron donor (Von Sperling, 2007). The biomass grows in the bioreactor and is maintained in the system for several days by decantation and recirculation.

Since denitrification needs readily biodegradable carbon which can be available in the primary effluent, the anoxic basins are often placed directly downstream of the primary treatment. Nitrates, which are formed downstream in the aerated basins, are sent to the anoxic basins through internal recirculation. If the available carbon is insufficient for complete denitrification, external carbon must be added.

Nitrification

Ammonium converts to nitrate in the two steps of this oxidation reaction:

$$NH_4^+ + 3/2O_2 \leftrightarrow NO_2^- + 2H^+ + H_2O \tag{1.13}$$

$$NO_2^- + 1/2O_2 \leftrightarrow NO_3^- \tag{1.14}$$

It can be seen from (1.13) that acidity is produced (H^+) in the first step. However, nitrifying bacteria can only be active in a specific range of pH, as can be seen in Figure 1.2 taken from Van Hulle et al. (2007). The authors measured the oxygen uptake rate (OUR) of nitrifying bacteria at different pH values. They found that bacteria are most active for pH between 6 and 8. The optimum pH value reported was 7.23 $\pm$ 0.03. Providing sufficient alkalinity is therefore essential to maintain pH around neutrality in nitrifying reactors. This can be provided by the carbonate buffering system present in the wastewater. Thus, the nitrification reactions can be rewritten as:

$$NH_4^+ + 2HCO_3^- + 2O_2 \leftrightarrow NO_3^- + 2H_2CO_3 + H_2O \tag{1.15}$$

where bicarbonate alkalinity acts as a buffering agent during nitrification.

Denitrification

Nitrate is reduced to nitrogen gas through denitrification according to the following reaction:

$$2NO_3^- + 2H^+ \leftrightarrow N_2 + 5/2O_2 + H_2O \tag{1.16}$$

Since this reaction is performed by heterotrophic microorganisms which, among others, consume VFA as carbon source, one can rewrite the aforementioned equation as follows:

$$NO_3^- + VFA + H_2CO_3 \leftrightarrow N_2 + biomass + HCO_3^- \tag{1.17}$$

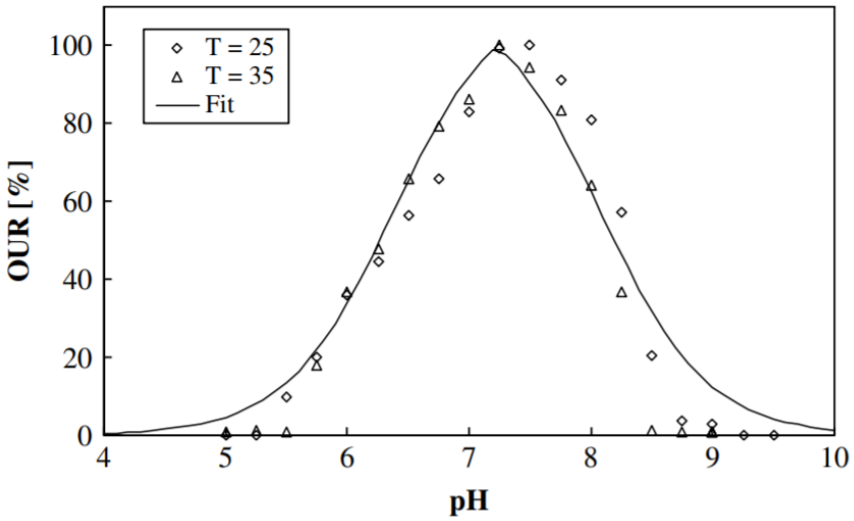

Figure 1.2: Influence of pH at 25°C and 35°C on nitrification-OUR (Van Hulle et al., 2007)

As a difference between nitrification and denitrification, one can notice the production of alkalinity in denitrification, whereas alkalinity is consumed during nitrification. Thus, denitrification partially compensates the acidity created by nitrification and lowers the need for external addition of alkalinity upstream.

1.4 Titrimetry in literature

Monitoring and control of WRRFs rely on a combination of a proper process model, reliable online data, and adequate control strategies (Vanrolleghem and Lee, 2003). Although within the last decades, sensor capabilities and control equipment have improved significantly, problems regarding treatment processes evolved too. The parameters of pollution which affect the quality of water need to comply with tighter standards. Therefore, advanced treatment systems are required not only for organic carbon but also for nitrogen and phosphorus removal.

This section briefly reviews the available equipment and analyzers for monitoring the quality of wastewater in terms of the compounds of interest for nitrogen removal. Titrimetry is then introduced as an easy, cost-effective method to measure and control different characteristics of wastewater. Therefore, the main focus of this section is on titrimetric analysis and its application. The concept of titration and buffer capacity interpretation method is introduced. Finally, the application of titration in wastewater treatment in the literature is reviewed.

1.4.1 Measurement of the compounds of interest for nitrogen removal

Alkalinity

The idea of measuring alkalinity originates from the difficulties of measuring the dissolved carbon and bicarbonate content of the mixed liquor on the basis of pH measurements (Vanrolleghem and Lee, 2003). Only in the last few decades, monitoring bicarbonate buffer, the main contribution to alkalinity, has been automated and applied in practice (Bouvier et al., 2002). According to Vanrolleghem and Lee (2003), two basic principles have been used to evaluate bicarbonate alkalinity. The first one is *titrimetry*, which will be particularly explained in Section 1.4.3. The second method is based on the *evolution of the CO_2 gas* as the sample is acidified. An application of this method can be found in the work of Di Pinto et al. (1990), where an instrument enabling the automatic semi-continuous determination of bicarbonate is developed for anaerobic process control.

VFA

Measurement of VFA is a matter of concern in on-line monitoring of unit processes, mainly anaerobic digestion. However, only a few of the proposed on-line sensors have been implemented in practice.

Pind et al. (2002) developed an in-situ filtration technique, which together with a gas chromatograph, made the on-line measurement of VFA possible for flows such as animal slurry or manure.

Steyer et al. (2002) used a Fourier Transform Infra-Red (FT-IR) spectrometer as an on-line sensor, to measure VFA, COD, total organic carbon (TOC), and partial and total alkalinity in an anaerobic digester. The results of the on-line measurement were very close and compatible with those provided by a titrimetric and TOC analyzer. However, for each component of the measurement, a carefully performed calibration is needed.

Recently, biosensors have been used for measurement of VFA at laboratory scale. Jin et al. (2017) presented an example of a biosensor-based VFA measurement, in which they developed on innovative biosensor based on a microbial electrolysis cell for rapid monitoring of VFA during anaerobic digestion. Such technologies could be considered as cost-effective and efficient for VFA monitoring; however, their applicability remains limited to lab-scale measurements.

According to Zaher (2005) and Vanrolleghem and Lee (2003), titrimetry can be considered as a more robust technique for measuring VFA. It is not only cost-effective but also accurate and commercially practical. This will be developed in this thesis.

Nutrients

A lot of efforts have been invested to automate typical laboratory methods for the on-line measurement of nutrients in wastewater. According to Vanrolleghem and Lee (2003), three implementations exist. Amongst them, flow injection analysis (FIA) is the most popular on-line measurement method (see more in Ruzicka and Hansen (1975)). The nutrients of interest in these methods are quantified colorimetrically. Pedersen et al. (1990), for instance, have developed an automatic measurement system for monitoring ammonia, nitrate and phosphate for control of an activated sludge plant with biological removal of nutrients. The analyzers used are based on colorimetric methods which are carried out in a system with the same principle as FIA.

1.4.2 Titration concept

When a weak acid (HA), or a salt of its conjugate base (MA, where M is representing the cation), is added to water, the dissociation reaction of the weak acid is described as follows:

$$HA + H_2O \leftrightarrow A^- + H_3O^+ \tag{1.18}$$

Assuming the system is closed and homogenous, a mass balance on all species gives

$$C_a = [HA] + [A^-] \tag{1.19}$$

Adding a strong base to the weak acid solution can shift the equilibrium in (1.18) to the right, leading to the consumption of more acid and consequently more conjugate base production. With this shift in the equilibrium, more protons (H_3O^+) are consumed, resulting in pH incrementing gradually. This change in equilibrium is the basis of titration.

Titration is the process of adding a strong base or acid to a weak acid/base solution and measuring the changes of pH at each addition. These changes in pH over the amount of strong base/acid can be plotted as a titration curve. In Figure 1.3, an example of a titration curve for 1 L of a 0.01 M acetic acid (weak acid, HA) titrated with Sodium hydroxide (strong base, $NaOH$) is presenetd. In this curve, points a, b and c can explain the chemical events which build the shape of the titration curve.

Point a represents the establishment of the equilibrium pH in the acetic acid solution. At this point, no base has been added and the concentration of the unionized form (HA) is dominant over the ionized form (A^-) (96 % HA against 4 % A^-) (Van Vooren, 2000).

Point b is where the concentration of unionized acid is equal to the concentration of the ionized acid ($[HA]$=$[A^-]$). From the curve, it can be observed that around this point changes in the solution pH are very small per unit of strong base added. In other words, acetate shows the highest resistance to pH change and the buffering effect is the highest at this pH.

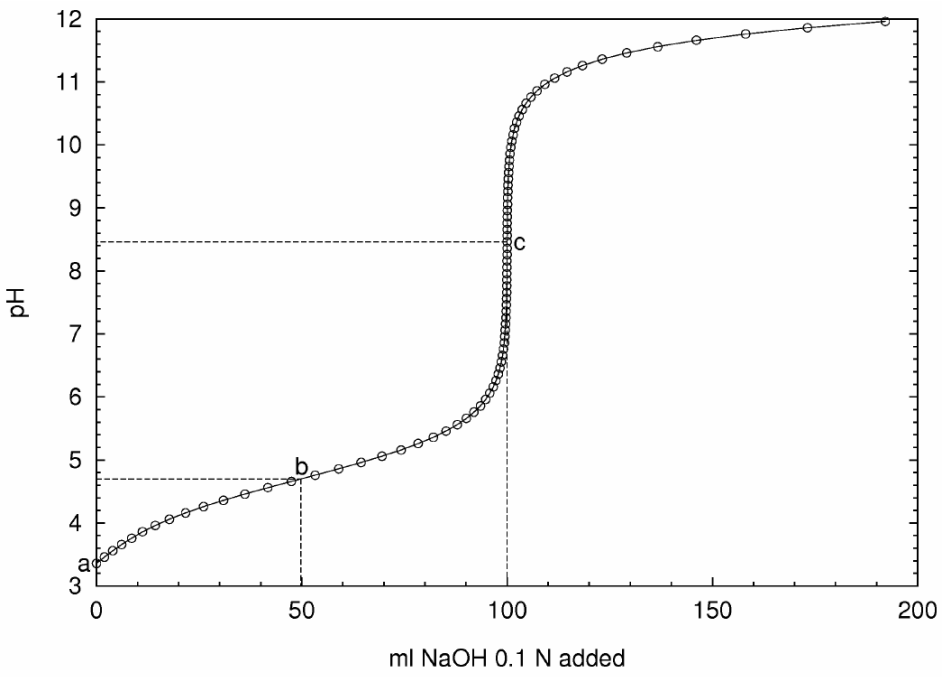

Figure 1.3: Titration curve for 1 L of a 0.01 M acetic acid solution (Benefield et al., 1982)

Point c represents the pH established when the concentration of the ionized acid approaches the initial acid concentration ($[A^-] \cong 0.01$ M). At this point, the pH reaches the equivalence-point for a 0.01 M acetate salt solution (MA). One will need to add a lot of base to get to the equivalence *point c* if a lot of buffer is present.

The buffering system in the aqueous solution shown in Figure 1.3 consists of only acetic acid which is a monoprotic (can interchange only one proton) buffer. However, in real life, wastewater samples contain more than one buffering system containing not only monoprotic but also poly-protic buffers. For instance, Figure 1.4 shows a titration curve for a more complex system where one no longer can detect points a, b, and c for each buffer in the system due to its complexity.

Buffer capacity curve

Getting the slope of a titration curve (pH-change versus added concentration of strong base/acid titrant), one can visualize the tendency of the solution at any point of the titration curve to change the pH upon addition of the titrant. The buffer capacity at any point of the titration is inversely proportional to the slope of its titration curve at that point, given as:

$$\beta = \frac{\delta C_B}{\delta pH} = -\frac{\delta C_A}{\delta pH} \tag{1.20}$$

where β is the buffer capacity in $eqL^{-1}pH^{-1}$, and C_B and C_A are respectively the concentrations of the base or acid dosed in mol/L (Van Vooren, 2000).

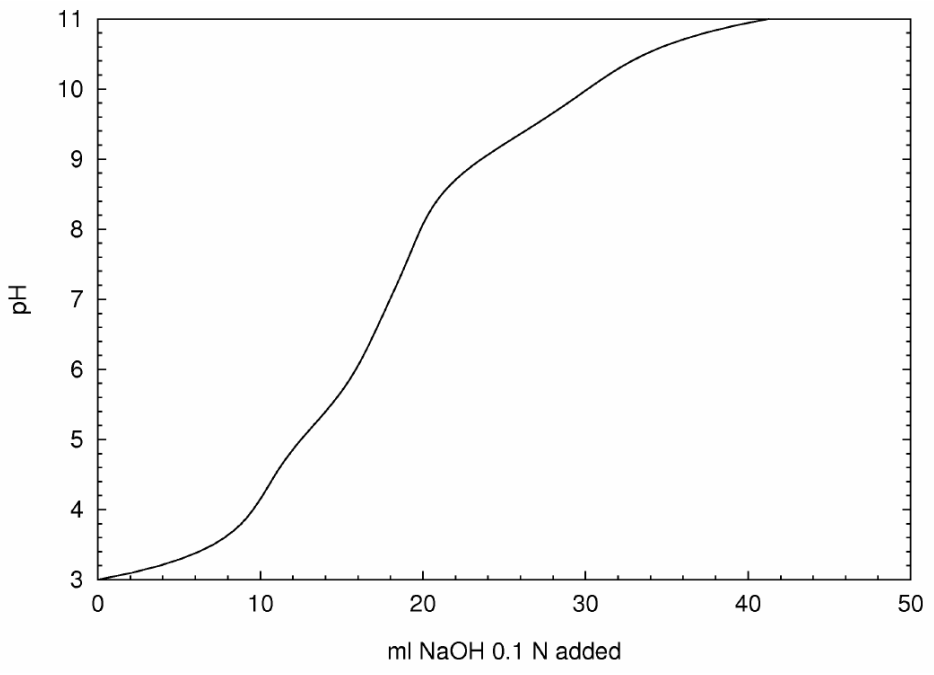

Figure 1.4: Titration curve for 1 L of an aqueous system comprising of 5 mgCO_2/L, 7 mg$oPO_4 - P$/L, 15 mg$NH_4^+ - N$/L and 0.6 meq/L of an unspecified soap (Van Vooren, 2000)

Plotting the inverse of the slope of the titration curve (β) at each point of the titration versus pH will lead to a graphical representation named buffer capacity curve. The buffer capacity curve corresponding to the titration curve in Figure 1.3 is shown in Figure 1.5. *Point b*, which represents the highest resistance to pH change in the titration curve, is the maximum point in the corresponding buffer capacity curve. In the buffer capacity curve, *Point c* clearly indicates that hardly any buffer is left in the system. Obtaining the area under the buffer capacity curve between a and c, one can determine the initial concentration of the buffer in this example.

The corresponding buffer capacity curve for the complex system shown in Figure 1.4, is presented in Figure 1.6. To obtain the buffer capacity curve of a system with more than one monoprotic buffer present, a more complex buffer capacity equation is required which is presented in the Methodology chapter (Section 3.3).

1.4.3 Application of titrimetry

In this section, standard procedures for measuring mostly bicarbonate alkalinity, VFA, and in some cases ammonium and other buffers in wastewater are highlighted. Then, the buffer capacity analysis is introduced as the most widely applicable and most accurate mathematical interpretation tool for titration data. Last, literature applications of titration for on-line and off-line measurement of different biological processes are discussed.

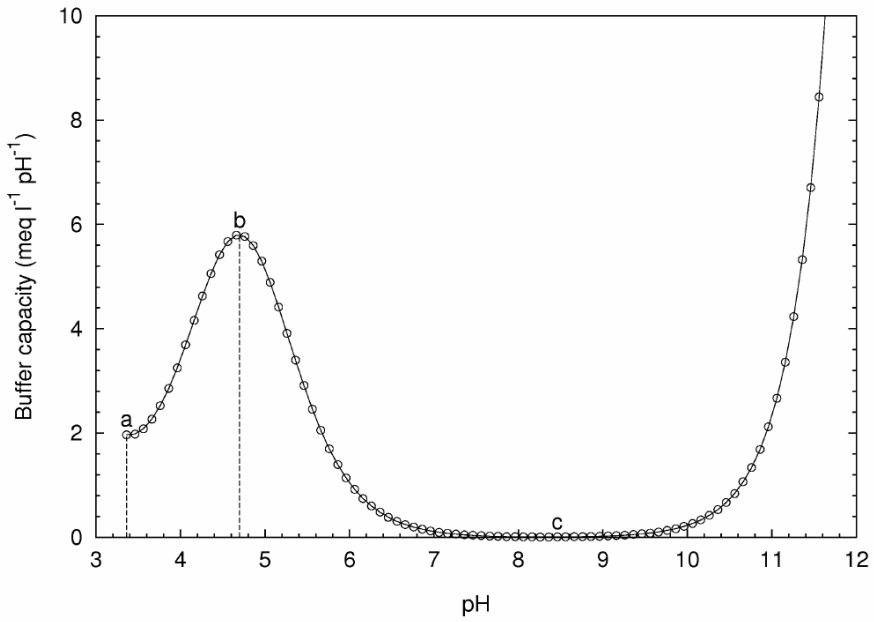

Figure 1.5: Buffer capacity curve for 1 L of a 0.01 M acetic acid solution (Van Vooren, 2000)

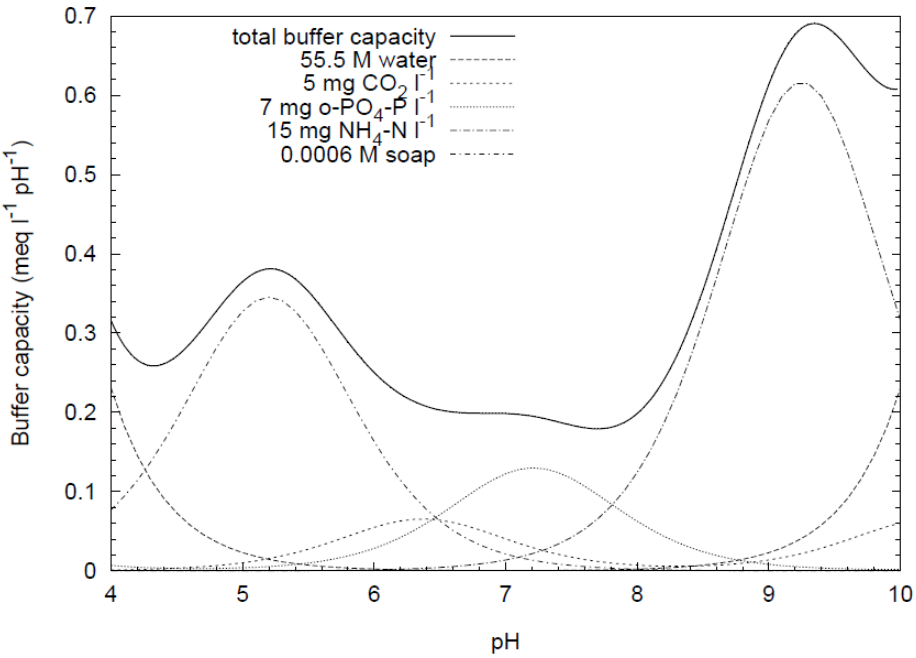

Figure 1.6: Buffer capacity curve for 1 L of an aqueous system comprising of $5mgCO_2l^{-1}$, $7mgoPO_4 - Pl^{-1}$, $15mgNH_4^+ - Nl^{-1}$ and $0.6meql^{-1}$ of an unspecified soap (Van Vooren, 2000)

Standard measurement methods and data interpretation

In a buffering system in which alkalinity is only due to the bicarbonate and carbonate buffers, the total alkalinity is determined by the equivalent acid added to the sample from pH 8.3

to 4.5 (Sawyer et al., 1994). However, in most cases (e.g in an anaerobic digester) total alkalinity includes all the bicarbonate and 80 % of VFA (Anderson and Yang, 1992). Since only bicarbonate is usable for neutralizing the VFA produced during digestion, total alkalinity does not represent the available buffering capacity of the system. Anderson and Yang (1992) thus suggested a simple, alkalimetric method that gives a direct measurement of both bicarbonate and VFA concentration by a two-stage titration: first from the pH of the initial sample to pH 5.1, then from pH 5.1 to 3.5 (Anderson and Yang, 1992).

A refinement of the aforementioned method, is using 5 points instead of 3 points. This 5 pH points acid titration experiment was suggested by Moosbrugger et al. (1993), and was aimed at measuring short chain fatty acids and inorganic carbon buffers in anaerobic systems. The 5 pH points include the initial pH (pH_0), a pair pH (pH_1, pH_2) located symmetrically around the first pK_a value of the inorganic carbon buffer, and a pH pair (pH_3, pH_4) located symmetrically around the pK_a value of the acetate buffer. An asymmetrical pH pair (for instance pH_1 and pH_3, see Figure 1.7) was considered as set-points around the theoretical pK_a, to correct for poor calibration or errors in pH. The bicarbonate and VFA estimates ranged around the expected values with an average standard deviation of 5 to 8 % (Moosbrugger et al., 1993).

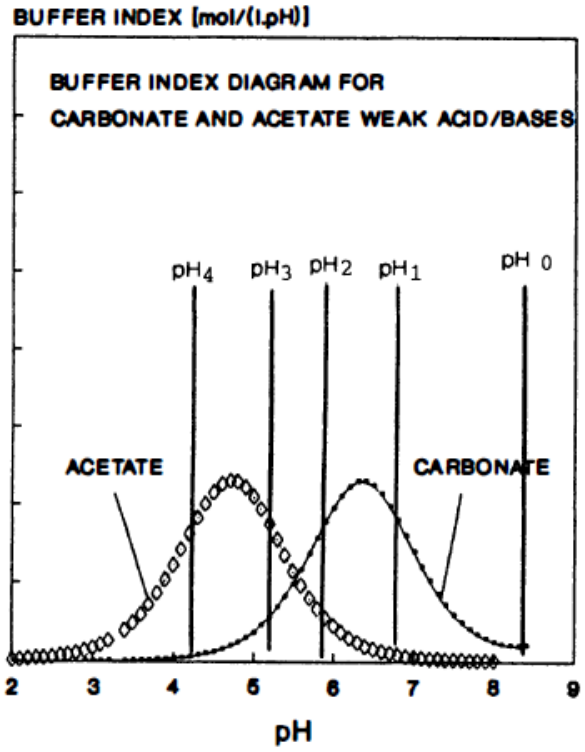

Figure 1.7: Buffer capacity (index) curve of carbonate and acetate buffer over the pH range 2 to 8.5 with 5 estimated pH points (Moosbrugger et al., 1993)

Other buffers in the system than bicarbonate and VFA (such as phosphate, ammonium, etc.) can affect the estimations derived from the 5 pH points The presence of these buffers can be taken into account once their concentrations are known. Wet chemical methods are suggested by the author as a way to measure these buffers and eliminate their influences on the estimations.

Zaher (2005) proposed the Kapp method (Kapp, 1984), together with the methods of Moosbrugger et al. (1993), as examples of two approximate titrimetric method classes. According to Zaher (2005), the Kapp method does not need base addition, and VFA can be estimated by using one equation which is simpler than the method described by Moosbrugger et al. (1993). In this method, the acid needed to titrate a sample from pH 5 to 4 can be considered proportional to the present VFA content in the sample (Zaher, 2005). This principle is valid because the only buffer system that exists and affects the consumption of acid between pH 5 and pH 4 is the acetate buffer. Indeed, other short-chain fatty acids can be present in the sample with very close pK_a values (4.75), but these buffers have similar buffering characteristics and can be lumped together as one buffer (Zaher, 2005).

According to Zaher (2005), the Kapp method considers the bicarbonate buffer (HCO_3^-/CO_2) with a pK_a of approximately 6.3 in addition to the VFA buffer. Other buffering subsystems such as NH_3/NH_4^+ (pK_a of 8.95) and $H_2PO_4^-/HPO_4^{2-}$ (pK_a of 7.2), are located relatively far from the pH ranges of bicarbonate and VFA. Therefore, their influence on the accuracy of the estimations can be assumed negligible, but only if their concentrations are low enough.

All interpretation methods mentioned above suffer from a major drawback: they all only take into account a limited number of components. A different approach was suggested by Van Vooren (2000) and further developed in the work of Van De Steene et al. (2002). According to this method, more accurate results can be provided if one interprets the whole titration curve. A buffer capacity model is then used for mathematical interpretation of the titration curves. In fact, a model can simulate the buffer capacity during the titration, based on the concentrations of the inorganic carbon buffer, VFA, ammonium and other buffers. An estimation of the concentration of these buffers is obtained by minimizing the error between the experimental and simulated buffer capacity curve. Later, Zaher et al. (2004) improved this method by using base addition; that is up-titrating the samples, often having removed the interfering inorganic carbon, and estimate other known buffers such as TAN. Moreover, they extended the model to approximate blind buffers (unknown buffers) to better fit the model to the experimental results.

Titration applications

According to the literature, titration has a wide application in wastewater treatment processes. In this work, these applications are classified into three main uses: effluent quality, nitrogen removal, anaerobic digestion.

Water quality

In 1996, Van Vooren et al. used an automatic online titration unit to monitor the effluent quality of domestic and industrial wastewater. In their work, the possibilities of a titration based sensor, together with the buffer capacity curves obtained from different effluent types were studied and evaluated. The buffer capacity model contained an undefined component, the bicarbonate buffer, the orthophosphate buffer, and the ammonium buffer. Two validation experiments were performed with the purpose of comparing the buffer concentrations obtained with the titration sensors with the one measured with an off-line analysis of the two effluent types (domestic and industrial wastewater).

Later, in 1999, Van Vooren et al. applied a pH buffer capacity based measurement system and evaluated its usefulness for multivariate monitoring of tertiary wastewater treatment with algae. In this work, both down- and up-titrations were performed. Therefore, two types of buffer capacity curves were processed. The inorganic carbon (IC) buffer concentration which is the only carbon source used by algae, was estimated from down-titration. The estimated IC buffer concentration was compared to different alkalinity measurements. It was found that the concentration of the IC buffer was 20 % lower than the (T-C) alkalinity ($CO_3^{2-} + HCO_3^- +$ other acting buffers between pH 8.3 and pH 4.5) measured by the titration curve. The authors point out that other buffering components than IC are included in the (T-C) alkalinity (e.g.: orthophosphate, ammonium, organic acids, etc.). In addition to the IC buffer, ammonium and orthophosphate were quantified from up-titration profiles and were found comparable with the laboratory analysis.

The buffer capacity model used in the above-mentioned application only contains a limited number of buffers. Therefore, all samples were assumed to contain the same buffering system. However, this assumption is not valid in real life. In 2001, Van Vooren et al. proposed a methodology aiming at developing a stepwise and automatically built buffer capacity model for each titrated sample. The application of these models resulted in better estimation of ammonium and orthophosphate concentrations compared to the fixed buffer capacity model. The automatic model building algorithm is implemented in the software *bomb* and has been evaluated as robust and fail-safe (Van Vooren et al., 2001).

In 2019, Guo et al. applied an interactive method, which involved a combination of computer modelling and field experimentation, to learn about the bacterial activity and process mechanisms affecting water composition in sewers. The main goals of this study were to better

understand the impact of biochemical processes such as fermentation and denitrification, and the interactions between biofilm and bulk-flow bacteria leading to changes in the water quality. Based on the results of a model-based experimental design, nitrate (NO_3^-) dosing tests were performed to lower VFA, sulfide, soluble organics and nutrient levels.

Nitrate addition also had the effect of increasing alkalinity. The VFA and the alkalinity in this work were measured by an on-line titrimetric analyzer named AnaSense (Hach, Loveland, Colorado, US). This device was monitoring hourly VFA and alkalinity changes under the existing operational conditions without chemical dosing, and under NO_3 dosing. Then, the VFA on-line data was validated by using ion chromatography (IC) analyzer (Metrohm, Herisau, Switzerland). It was concluded that the studied sewer system was reactive and that adding nitrate can contribute to managing these reactions and, for instance, reduce sulphide-induced corrosion.

Nitrogen removal

In the work of Van Hulle et al. (2006), research on the possibility of using a titrimetric set-up for monitoring the combined SHARON-Anammox process was carried out. The buffer capacity model used consisted of the monoprotic components total nitrite (TNO_2) and total ammonium (TAN), and the triprotic component phosphate. These buffers were successfully determined in the effluent of the SHARON reactor, whereas in the Anammox reactor, only TAN could be determined by the model due to the very low TNO_2 concentrations. The authors found the titrimetric results for the TAN and TNO_2 concentrations in the SHARON reactor comparable to the ones obtained by classic colorimetry. It was concluded that the titrimetric set-up can be a cheap, reliable, and easy to automate alternative to other analyses.

The experimental titration data obtained by Van Hulle et al. (2006) from the combined SHARON-Annamox process, which is a fully autotrophic nitrogen removal (ANR) process, were reused later in Van Hulle et al. (2009), in addition to the titration data obtained from an anaerobic solids digester (ASD) reactor. Similar to Van Vooren et al. (2001), the complete titration profiles were applied for buffer capacity interpretation to monitor certain components in the two mentioned reactors. In the ASD reactor, ammonium, VFA, and bicarbonate alkalinity are the components of concern. The interest of this study concerns the addition of a statistical analysis which was performed to assess the precision of the titrimetric results. For the purpose of this comparison, the samples were analyzed with another technique such as gas chromatography or colorimetry. According to the statistical tests, providing the correct titrant concentration, the titrimetric technique could be adequate for samples with concentrations ranging between 50 mg/L and 3000 mg/L.

Anaerobic digestion

Zaher et al. (2004) used titration to determine VFA and bicarbonate to assess the stability of an anaerobic digester. In their work, the potential on-line use of two sensors (Titrimetric Sensor and Buffer Capacity Sensor) were compared and evaluated. According to the authors, the Buffer Capacity Sensor, in which the advanced *bomb* interpretation method is used, can be considered as a good monitoring tool for anaerobic digestion, not only during normal operating conditions but also during exposure to buffering interferences.

A new titrimetric device named SNAC (System of titration for total ammonia Nitrogen, volatile fatty Acids and inorganic Carbon) has been developed by Charnier et al. (2016) with an improved accuracy to control anaerobic digestion plants. The additional feature of this device is the combination of measurements of electrical conductivity and pH. In this work, the buffer capacity method is chosen because it can consider many buffering components, as was previously done by Zaher et al. (2004). A conductivity sensor was implemented in the titration vessel. Since conductivity is influenced by the ionic charge of the components, it can easily distinguish components in the media. In the buffer capacity method, one knows that the effect of the compounds on the titration curves depends only on their concentrations and pK_a values. However, the effect on the electrical conductivity depends not only on the concentrations and pK_a values but also on the molar conductivity which is specific to the compounds (Charnier et al., 2016). Thus, according to the results of this work, the combination of electrical conductivity and pH sensors has improved the accuracy of estimating the buffers of interest.

1.4.4 Conclusion

During the last decades, titrimetry has been touted as a reliable, simple, and cheap method by many researchers to monitor biological nitrogen removal processes. Given the wide-ranging applications discussed in this review, titrimetry thus seems to be a valuable method to determine a wastewater's physicochemical characteristics.

Chapter 2

Objectives

The pilEAUte plant is a research-oriented treatment plant at Université Laval. It is equipped with a small laboratory, in which a Titrino device is available since 2005. Titration is so-called laboratory method that allows validating online data obtained from sensors installed in different zones of a treatment system. The aim of this MSc study therefore is to characterize influent and effluent samples from the pilEAUte plant in terms of $NH_4 - N$, VFA and alkalinity using efficient experimental and modelling methodologies based on titrimetry. To pursue this goal, several titration tests have been performed during sampling campaigns within different research projects on this facility, aiming at:

- developing an Excel-based buffer capacity algorithm for both down- and up-titration tests in which alkalinity and other buffers could be quantified.
- developing a titration simulation model in the PHREEQC-Xcel software aiming at better estimating the concentrations of the buffering components, and studying the chemical equilibria and reactions involved in the system under study.
- evaluating the efficiency of the developed titrimetric monitoring method under different operational conditions. In particular, the capability of the method is evaluated for estimating the concentration of the following buffers in this study: alkalinity, VFAs, and ammonia.
- evaluating the efficiency of the nitrification and denitrification processes in the biological reactors by performing down-titration and up-titration tests to monitor pH and alkalinity variations downstream and upstream of the bioreactors.

Chapter 3

Methodology

3.1 Study site

At Université Laval, a pilot-scale plant called pil*EAU*te was constructed and completed for treatment of wastewater in October 2014. The pil*EAU*te's equipment is installed in a laboratory of the civil and water engineering department in the Adrien Pouliot building on the University campus. The wastewater feeding the plant originates from a catchment that consists of a residence building on campus, and two childcare centers. The water in the catchment is pumped from the sewer system through a pumping station including two shredder pumps to the pil*EAU*te plant. In Figure 3.1, the location of pil*EAU*te and its catchment, in addition to the pumping station, is provided.

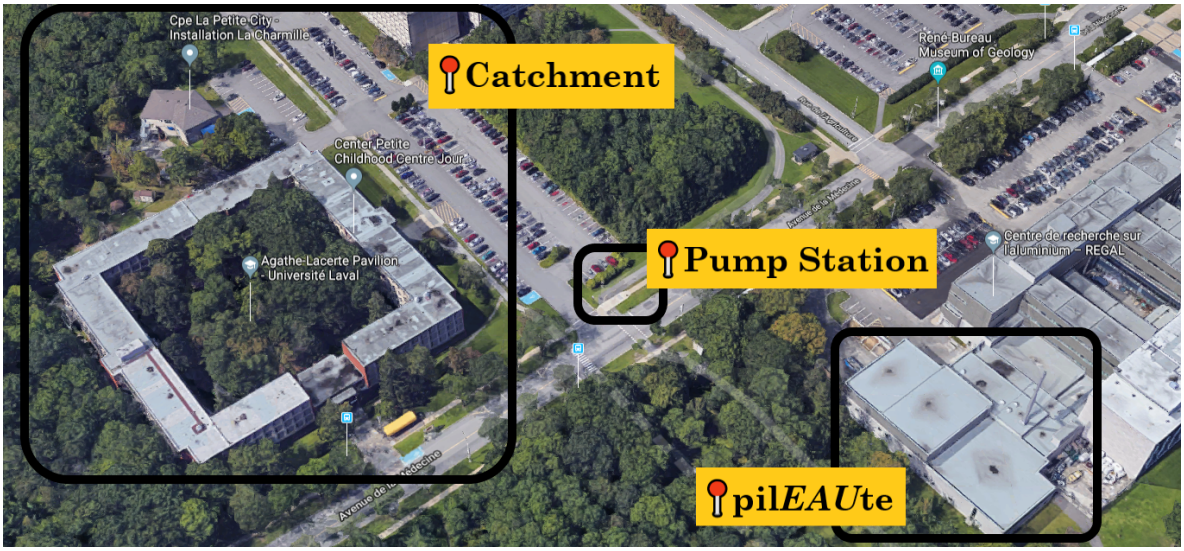

Figure 3.1: Location of the catchment, pump station, and the pil*EAU*te treatment plant (Google Inc., 2019)

The pilEAUte plant under study is composed of primary treatment to remove particulates followed by a biological treatment where COD and nitrogen removal take place. According to the schematic of the pilEAUte plant (Figure 3.2), the water pumped to the station is feeding a storage tank with a volume of 5 m^3. This tank is installed to provide sufficient flow during the night to feed the pilEAUte plant. The stored water is then pumped to a 2.1 m^3 primary clarifier using a pump with a fixed flow rate of 1.1 m^3/h. A large portion of the solid particles is removed there by physical settling operations.

The effluent of the primary clarifier is collected in a measurement tank, where a group of sensors is installed to characterize the influent of the secondary treatment. This water stream is distributed over two similar treatment lines named *pilot* and *co-pilot* where secondary treatment is carried out. These two tanks are followed by two secondary settling tanks, where another group of sensors is installed to measure the variables in the effluent.

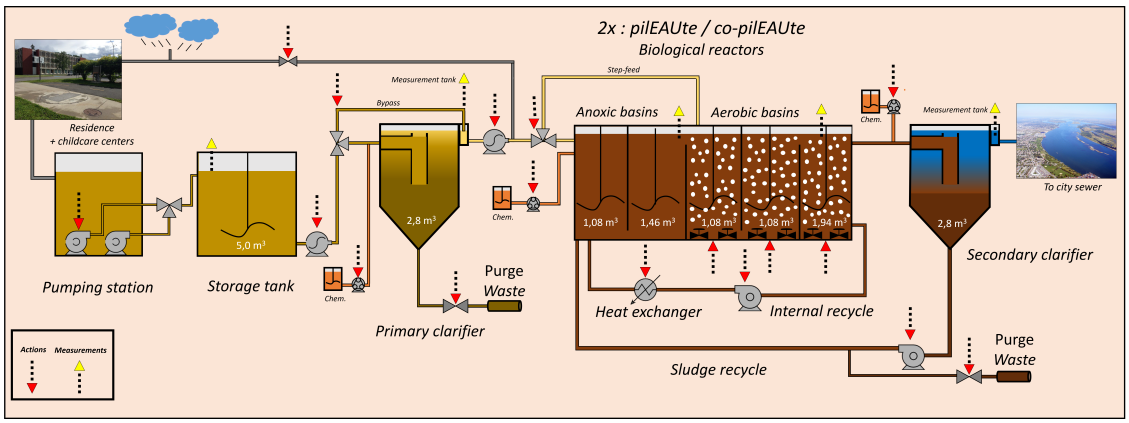

Figure 3.2: Schematic view of the pilEAUte treatment plant.

Various sensors are installed in the plant to track the performance of the process with respect to different parameters. All data collected by the sensors are integrated with two data collection systems: the monEAU base station and the SCADA (Supervisory Control And Data Acquisition) system, each linked to certain sensors. In Table 3.1, a list of the pilEAUte's sensors with regards to their measurement locations, as well as their data acquisition (DAQ) interfaces is given.

The SCADA system collects the data of four Solitax sensors located in the pilot and co-pilot reactor tanks and in their sludge recirculation lines. They measure the turbidity of water which is translated into Total Suspended Solids (TSS). Two oxygen probes are also connected to SCADA as well as several control loops of airflow and liquid flow rates. Conductivity and temperature are other water quality parameters collected by a conductivity meter in the primary effluent and monitored through this interface.

Table 3.1: Summary of the pilEAUte plant's sensors

Sensor	Brand	Parameter	Unit	Sensor's Location	DAQ Interface	Measurement principle
ammo::lyser	s::can	$NH_4 - N$ K pH Temperature	$mg.L^{-1}$ $mg.L^{-1}$ - $°C$	Primary effluent	monEAU station	ionophore membrane ionophore membrane non-porous reference electrode Thermocouple
spectro::lyser	s::can	TSS $NO_3 - N$ COD $sCOD$	$mg.L^{-1}$ $mg.L^{-1}$ $mg.L^{-1}$ $mg.L^{-1}$	Primary effluent	monEAU station	UV-Vis spectrometry
Conductivity	Hach	Conductivity Temperature	$\mu S.cm^{-1}$ $°C$	Primary effluent	SCADA	Potentiometry
Solitax	Hach	TSS	$mg.L^{-1}$	Anoxic tank of the bioreactors Sludge return flow	SCADA	Nephelometry
LDO	Hach	Dissoloved Oxygen Temperature	$mg.L^{-1}$ $°C$	Aerobic tank of the bioreactors Sludge return flow	SCADA	Luminescence
VARION	WTW	$NH_4 - N$ $NO_3 - N$ K Cl Temperature	$mg.L^{-1}$ $mg.L^{-1}$ $mg.L^{-1}$ $°C$	Secondary effluent	monEAU station	Ion selective electrode
pHmeter	WTW	pH Temperature	- $°C$	Secondary effluent	monEAU station	Potentiometry

Alongside the SCADA system, the mon*EAU* station plays an intermediate role between the data collection software and the sensors connected to it. The data of these sensors are collected by two different programs. For the spectro::lyser and ammo::lyser, the data are collected by the "Anapro" software (s::can, Vienna, Austria) and for the Varions, the "PrecisionNow BaseStation" software (Primodal Inc., Hamilton, ON, Canada) is used. Through a remote access software that is installed in the SCADA workstation, the mon*EAU* station PC is monitored.

The pil*EAU*te's N-removal facility is composed of two identical process lanes fed with the same wastewater. Using one lane as a reference process, the other lane can be manipulated for changes in the operational conditions and reactor configuration. Moreover, as mentioned before, it is highly instrumented with the data collection system. Consequently, its application on implementing different control strategies is significantly acknowledged. Over the last two years, two evaluation projects have been performed by the pil*EAU*te team, where various changes in the behavior of wastewater treatment have been studied. The two following projects are the case studies discussed further in this master thesis:

- **AvN Project**: AvN ammonia cascade control; a new control strategy developed by DC Water and HRSD (USA), aiming for maximizing nitrogen removal at minimal aeration, by controlling sludge retention time (SRT) and dissolved oxygen (DO).
- **Reactive Primary Clarifier Project**: Turning a primary clarifier into a fermentor; in a collaboration with Trojan Technologies and Ryerson University, this project aimed at enhancing the nutrient removal rate by increasing the soluble organic matter in the form of VFA by increasing the degree of fermentation in the primary sludge blanket.

The results of the two projects related to the context of this study are fully explained in the upcoming chapter of this thesis study. It is noted that data monitoring in pil*EAU*te is composed of both online and offline methods, where off-line measurements are validating the data obtained through the online method and contributed to sensor maintenance processes. One of the off-line methodologies applied in the laboratory of pil*EAU*te is titrimetric monitoring of wastewater characterization, performed through titration tests within a Titrino device which is installed since 2012. The configuration of this device and its application is fully explained in Section 3.2.

3.2 Titrimetry

The 794 Basic Titrino is an all-purpose titrator. This device is equipped with different input connections including two high-impedance measuring inputs for pH and potential measurements, one measuring input for polarized electrodes, and one measuring input for a

temperature sensor (Metrohm, 2002). A separate keypad and a magnetic stirrer are connected to the Titrino.

In the pil*EAU*te laboratory, a 778 Sample processor is connected to the Titrino for automatic multiple sample titration. A PC is then connected to the sampler which enables data exchange with the Metrodata VESUV Software, and data acquisition and evaluation through the Metrodata TiNet Software (Figure 3.3).

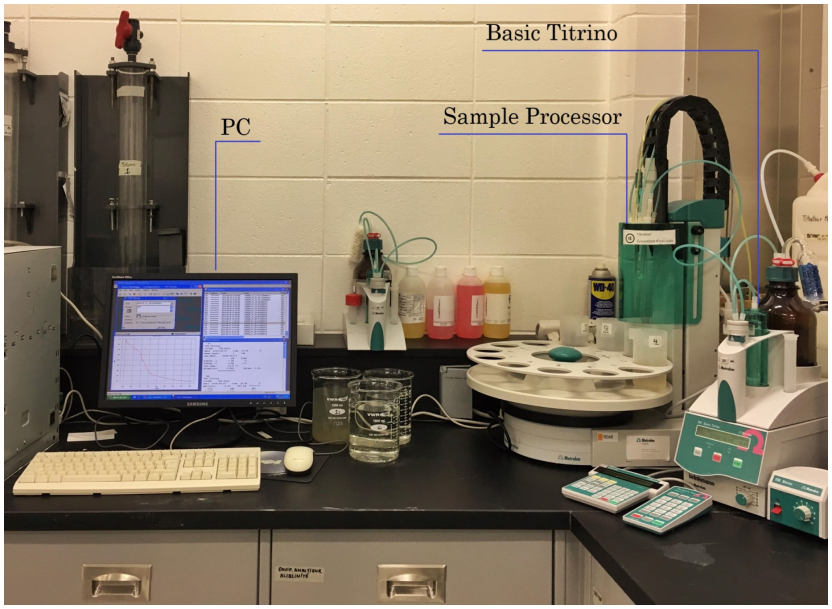

Figure 3.3: Titration devices in the pil*EAU*te laboratory

As shown in the schema of the Titrino instrument (Figure 3.4), the titrant solution is mounted on an exchange unit that can be easily removed by sliding it forward. Depending on the titration test, two exchange unit containers for acidic and basic titrant solutions are provided. The pH electrode is stored on the exchange unit, maintained in a guard cap containing a storage solution of potassium chloride (KCl) 3 M (mol/L). It can be used in the Titrino when there is only one sample to titrate, or used on the sample processor when more samples are to be titrated.

The Titrino is not only coupled to the sample processor; it could also be monitored by the sample processor. The sample processor can be equipped with different devices. As shown in Figure 3.5, the processor is connected to a keypad which enables changing the instrument's configurations, editing the run sequences, and changing the titration method's parameters. Moreover, lift operations and sample positioning, in addition to different command keys are provided on the keypad. The PC collects the titration data and evaluates it by plotting a titration curve for each experiment.

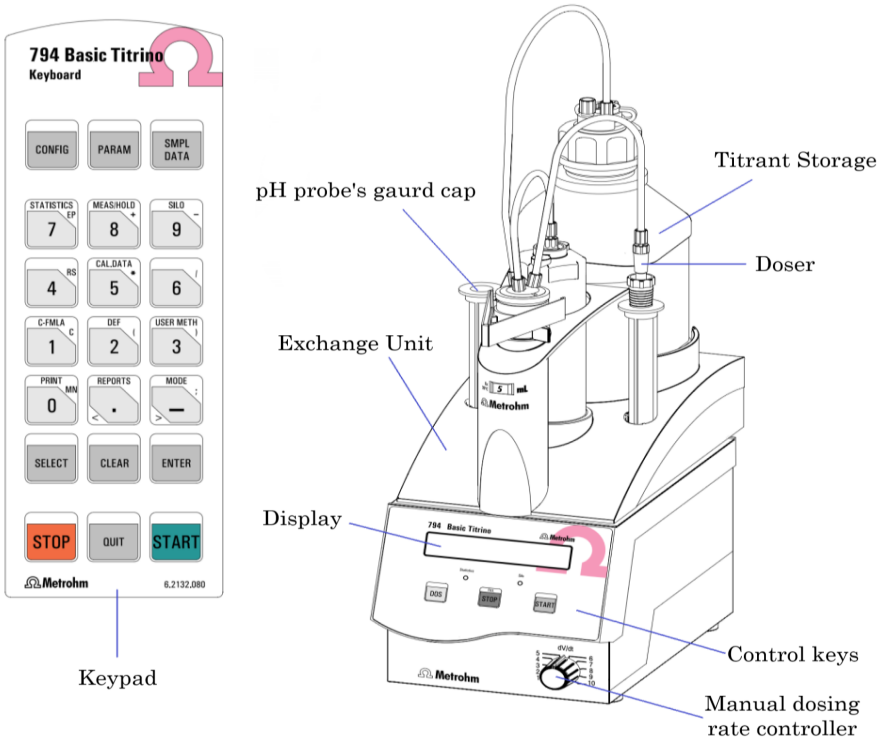

Figure 3.4: Schematic view of Titrino instrument and its keypad (Metrohm, 2002)

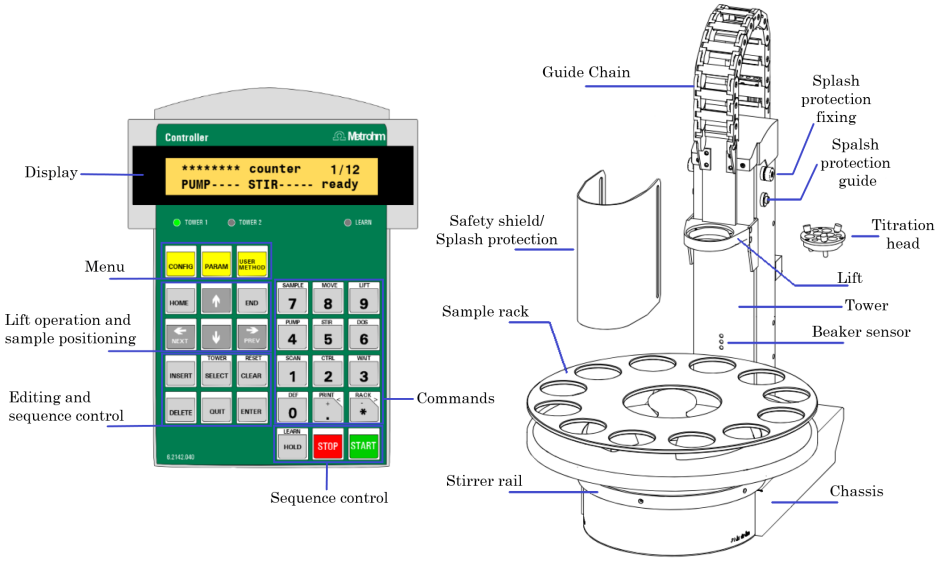

Figure 3.5: Schematic view of the Sample Processor and its keypad (Metrohm, 2007)

Depending on the components in the sample, the titration method is chosen. To characterize buffers with pK_a values in the acidic range (7 or less), down-titration is performed to acidify

Table 3.2: Optimal titrant concentration as function of the component concentration range (Van Hulle et al., 2009)

Titrant Concentration (mmol/L)	Concentration boundaries (mmol/L)
0.01	0.001-0.005
0.05	0.005-0.025
0.1	0.025-0.2

the sample. On the other hand, to measure the buffers in the basic range, the sample is up-titrated with a base solution.

The titrants used for the down- and up-titration tests are often weak sulfuric acid and weak sodium hydroxide respectively. They are prepared by adding an adequate amount of H_2SO_4(37 %) and NaOH pellets to distilled water. As discussed in the work of Van Hulle et al. (2009), the optimal titrant concentration is a function of the component concentrations. Given the results of their work (Table 3.2), and according to sensor data and laboratory data acquired from preliminary studies in the pilEAUte plant, the samples analyzed in this study are in the concentration range of 0.005-0.025 mmol/L. As such, an appropriate titrant of 0.05 mol/L is used to perform all titrations.

Before starting the titration, the parameters and the operational conditions in the experiment should be defined in the devices. The endpoint pH is one of the parameters that vary depending on the test, and it determines at which pH the titration should be terminated. For each buffer in the system, +/-1 pH unit of the equivalent point is considered, indicating the pH range where the buffer is present in the solution. As such, to determine the VFA concentration with a pK_a value of 4.75 (Bouvier et al., 2002), an endpoint of 3.5 could be considered.

To determine the total alkalinity, a down-titration to pH 4.5 should suffice. However, one needs to bring the pH down as much as possible to measure the alkalinity as good as possible. On the other hand, below pH 3 the buffer system is disturbed by the water buffer's overwhelming presence. Thus, to impede problem, and to avoid any under- or over-estimation of the buffers' concentration pH 3 seems to be a proper value. In addition, it is not an overly acidic point that may cause an additional error related to the H_2O buffering.

One drawback of the current method is the tendency of $CO2$ to be stripped to the atmosphere while the titration is performed. Indeed, a mixer is installed in the sample processor to stir the sample slowly during the titration.

For the up-titration test, the base is dosed until the sample reaches an endpoint pH of 11. This endpoint is chosen using the same procedure as for the down-titration. It allows to measure the $NH_4^+ - N$ buffer with a pK_a value of 9.24.

For both titration methods, 100 mL of the sample is titrated, and the volume of titrant dosed depends on the buffer concentrations, which varies along with the location where the samples are taken. If the samples are taken from the secondary effluent, the titrant's volume used is lower compared to samples of the raw wastewater or even primary effluent. This is explained by the buffer concentration dynamics in different sampling locations of the plant; buffers are more concentrated at the beginning of the treatment.

Once the sample's pH reaches the defined endpoint, the titration curve is plotted given the changes of pH for each dosing step and the volume of titrant consumed in each step. This curve and the report of the results are presented in the PC within the Vesuv software. To interpret the titration curve obtained, mathematical models are needed. For this, two different titration curve modelling approaches will be discussed in the following sections: Buffer capacity curve modelling and titration curve modelling using PHREEQC. The buffer capacity approach is an Excel-based mathematical model which will be elaborated more in detail in Section 3.3

3.3 Buffer capacity model

One of the readily available methods developed for analysing the titration data is the buffer capacity model. According to the work of Van Vooren (2000), modelling buffer capacity is preferred because the derivative data instead of the raw pH data is used. Thanks to this, measurement errors and pH calibration errors will not affect the model evaluation.

The derivative data applied in this approach is obtained from the slope of the titration curve (see Figure 1.3).Then, the capacity of buffer at each point of titration is calculated (see more in Section 1.4.2) as:

$$\beta = \frac{\delta C_B}{\delta pH} = -\frac{\delta C_A}{\delta pH} \tag{3.1}$$

where β is the buffer capacity in $eqL^{-1}pH^{-1}$, and C_B and C_A are respectively the concentrations of the base or acid dosed in mol/L.

Plotting the inverse of the slope of the titration curve versus pH, one may visually understand the dependency of β as function of pH (see Figure 1.5). A measured curve determined as the experimental buffer capacity curve, can be used as a basis for estimating the components of the sample. In fact, the area under each peak in the buffer capacity curve represents the concentration of the buffering component, and the position of the peak depends on its pK_a value(s).

As the sample is composed of different buffering systems such as monoprotic, diprotic and triprotic acids, one can consider the total buffer capacity β equal to the sum of the buffer capacities β_i of the individual buffering components. The general equation for the buffer

capacity of a sample with l monoprotic, m diprotic, and n triprotic weak acids can be written as equation (3.2) (Van Vooren et al., 2001):

$$\beta = 2.303[H^+](1 + \frac{K_w}{[H^+]^2} + \sum_{i=1}^{l} \frac{[HB_i]K_a^i}{([H^+] + K_a^i)^2} + \sum_{i=1}^{m} \frac{[H_2B_i^{'}]K_{a1}^i([H^+]^2 + 4K_{a2}^i[H^+] + K_{a1}^iK_{a2}^i)}{([H^+]^2 + K_{a1}^i[H^+] + K_{a1}^iK_{a2}^i)^2} + \sum_{i=1}^{n} \frac{[H_3B_i^{''}]K_{a1}^i([H^+]^4 + 4K_{a2}^i[H^+]^3 + (K_{a1}^i + 9K_{a3}^i)K_{a2}^i[H^+]^2 + (4[H^+] + K_{a2}^i)K_{a1}^iK_{a2}^iK_{a3}^i)}{([H^+]^3 + 4K_{a1}^i[H^+]^2 + K_{a1}^iK_{a2}^iK_{a3}^i)^2}) \tag{3.2}$$

where:

β: buffer capacity ($eqL^{-1}pH^{-1}$)
$[H^+]$: hydrogen ion concentration (mol/L), equals 10^{-pH}
$[HB][H_2B^{'}][H_3B^{''}]$: concentration of respectively a mono-protic, diprotic, triprotic weak acid (mol/L)
K_a: acidity constant

By minimizing the sum of squared errors (SSE) between the calculated buffer capacity curve and the experimental buffer capacity curve, the acidity constant values and the acid concentrations can be estimated. This model was implemented in an MS-Excel file and a solver function using the nonlinear optimization algorithm, Generalized Reduced Gradient (GRG2) (Fylstra et al., 1998), was implemented. Once the solver runs, the acid (buffer) concentrations and the acidity constant (K_a) values are changed to minimize the SSE.

In Table 3.3, the buffers considered in this thesis are listed and their chemical equations and default pK_a values are given. The estimated pK_a values by the model may vary from sample to sample since the acidity constant is influenced by ionic strength (Van Hulle et al., 2009).

Table 3.3: List of the considered buffers, their chemical equations and acidity constants at 25 $^{\circ}C$

Buffer	Chemical Equation	pK_a1	pK_a2	pK_a3
TAN	$NH_4^+ + H_2O \leftrightarrow NH_3 + H_3O^+$	9.24		
TNO_2	$HNO_2 + H_2O \leftrightarrow NO_2^- + H_3O^+$	3.29		
TP	$H_3PO_4 + H_2O \leftrightarrow H_2PO_4^- + H_3O^+$	2.12		
	$H_2PO_4^- + H_2O \leftrightarrow HPO_4^{2-} + H_3O^+$		7.21	
	$HPO_4^{2-} + H_2O \leftrightarrow PO_4^{3-} + H_3O^+$			12.32
TIC	$H_2CO_3 + H_2O \leftrightarrow HCO_3^- + H_3O^+$	6.37		
	$HCO_3^- + H_2O \leftrightarrow CO_3^{2-} + H_3O^+$		10.5	
VFA	$CH_3COOH + H_2O \leftrightarrow CH_3COO^- + H_3O^+$	4.76		
H_2O	$H_2O + H_2O \leftrightarrow H_3O^+ + OH^-$	14		

The modelled buffer symbols listed in the table represent the following compounds:

- TAN (Total Ammoniacal Nitrogen) expressed as NH_3/NH_4^+,
- TNO_2 (Total Nitrite) expressed as $HNO_2 + NO_2^-$,
- TP (Total Phosphate) expressed as $H_2PO4^- + HPO4^{2-}$,
- TIC (Total Inorganic Carbon), which is the sum of all inorganic carbon species including: carbon dioxide, carbonic acid, bicarbonate, and carbonate species. It is expressed as the sum of bicarbonate (H_2CO_3/HCO_3^-) and carbonate (HCO_3^-/CO_3^{2-} buffers,
- VFA (Volatile Fatty Acids) expressed as $CH_3COOH)/CH_3COO^-$), and
- H_2O (water).

The mathematical model is implemented in an Excel file composed of five sheets. In the "Legende" sheet, the titration data are given as an input to the model. Then, in the "Titrage" sheet, the titration curve is plotted. The model also takes dilution effects and dosage of chemicals into account in the "Echantillion" sheet.

The "Calculation" sheet, as the name implies, is where the buffer capacity is calculated for each considered buffer. Moreover, the calculated buffer capacity, which is determined as the theoretical buffer capacity curve in the model, and the experimental curve are plotted in this sheet. The default acidity constants (K_a) and the concentration values for the buffers in the model are also presented in this sheet, and one can see the changes in these parameters after running the solver.

The solver only functions in the last sheet, "Résumé", where the concentration values and the pK_a values can be initialized and modified. By running the solver, the minimized SSE will change, following the curve fitting. As an example, in Figure 3.6, the down-titration of a primary effluent sample with weak sulfuric acid (0.05 N) is presented. The result sheet (Résumé) for this titration is presented in Figure 3.7.

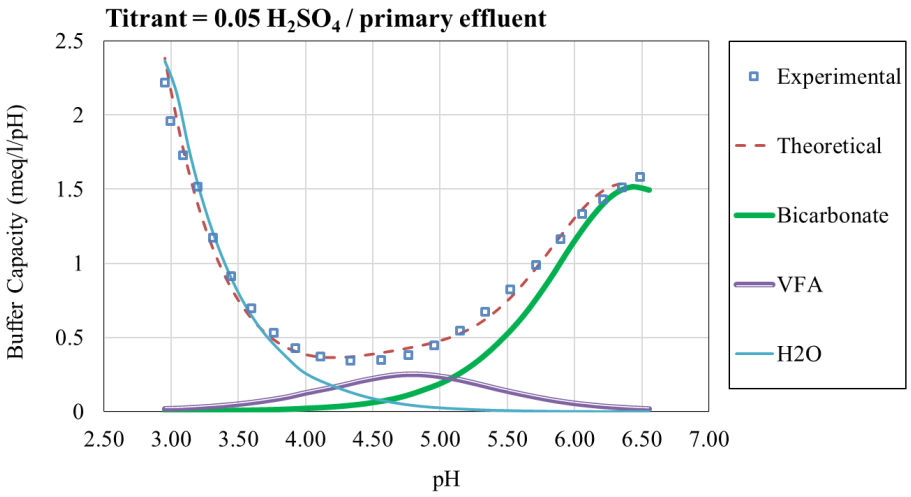

Figure 3.6: Typical buffer capacity curves resulting from down-titration of a primary effluent sample

The results of the model are validated with chemical laboratory analysis which will be further discussed in Section 3.5. Comparing the estimated concentration of the modelled buffers with the results of the laboratory analysis obtained, one can evaluate the quality of the titration-based measurements. However, one must take into account that the used buffer capacity model is not taking into account all components of a typical wastewater system, and deviations may thus occur.

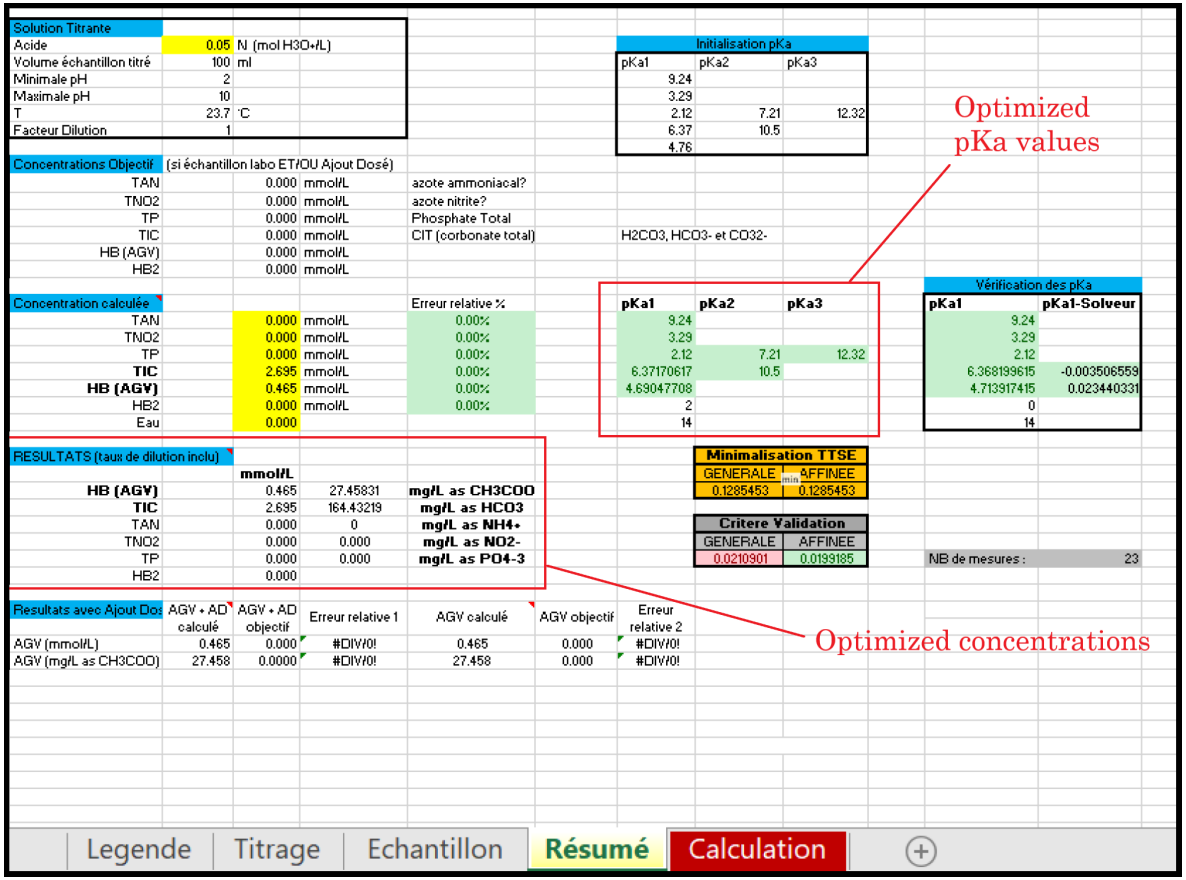

Figure 3.7: The result sheet (Résumé) of the titration shown in Figure 3.6, after model optimization

3.4 PHREEQC

To have a more complete description of the equilibrium reactions of the chemical system under study, an advanced modelling tool is needed to solve the non-linear equilibrium equations for calculating the species concentrations and to also consider potential precipitation reactions in the model. One of the modelling tools that has been used recently by water and wastewater specialists is PHREEQC. It is a public domain software and containing a designated thermodynamic database which is elaborated more in detail below.

3.4.1 Introduction

Various approaches have been studied in literature to model chemical equilibria. Since the linear method as implemented in the buffer capacity model can only handle simple acid-base chemical equilibria, a more complex approach is essential to carry out non-linear calculations and to incorporate more parameters for better model estimation. Thus, for the purpose of this work, PHREEQC version 3 was chosen.

PHREEQC version 3 is a computer program written in the C^{++} language and provides a wide variety of aqueous chemical calculations (Parkhurst and Appelo, 2013). Its development started and continued at the United states Geological Survey (USGS) in 1980 (de Moel et al., 2015). Besides its free accessibility which contributed significantly to its success, it has been modified and extended by users and adapted to new scientific methodologies and knowledge.

Despite its high potential in water treatment applications, PHREEQC has mainly been known for geohydrology and geochemical applications. At the Delft University of Technology (TU Delft) (Delft, The Netherlands) in 2013, P.J. de Moel and his colleagues started to provide a self-study course on PHREEQC for modelling water quality and water treatment entitled "Aquatic Chemistry for Engineers" (de Moel et al., 2015). In the course, they justified the unpopularity of the software in the domain of water and wastewater by explaining that the water chemistry knowledge employed in the program is above the average skills in water chemistry of water professionals. All relevant chemical equilibria in water and wastewater systems such as acid-base reactions, precipitation and dissociation reactions and reduction-oxidation (redox) reactions are incorporated in the PHREEQC (de Moel et al., 2015).

Moreover, the scientific literature on water treatment in PHREEQC is limited. For instance, in the Ph.D. work of Vaneeckhaute (2015), PHREEQC was used and developed as an external software tool for speciation calculations. In her work, that focused on nutrient recovery from bio-digestion waste, she coupled PHREEQC with another programming software for optimizing resource recovery treatment trains.

In this section, first, the basic concept of PHREEQC and the theory behind its calculations are briefly explained, then, the application of Excel as a container of PHREEQC (PHREEQXCEL) is introduced, and, finally, the implementation of the titration model in PHREEQXCEL is given.

3.4.2 Basic concept of PHREEQC

PHREEQC is based on an ion-association model for aqueous solutions and is capable of speciation calculations and batch reaction calculations. Moreover, it is designed to perform one-dimensional (1D) transport calculations including reversible reactions (such as ion-exchange equilibria), irreversible reactions (including specified mole transfers of reactants, kinetically controlled reactions, mixing of solutions, and reactions with changes in temperature), and inverse modeling (which is related to mineral and gas mole transfer between the waters due to the differences in their compositions).

PHREEQC uses different initial constraints as input, including the sample's composition, measurement units, dissolved gas, temperature, pH and redox potential. The sample's composition is determined using chemical analyses. The model is working based on the conversions of the units in which the concentrations are measured to moles of components per kg of water. A set of non-linear algebraic equations derived from chemical reactions, charge balances, and mass balance equations are then instantaneously solved to define the activities of the species in a specified system. To enable the model to solve the matrix of non-linear equations, a charge balance is needed. The model can calculate pH, redox potential, aqueous speciation, gas and mineral equilibrium, kinetic and surface reactions, and redox reactions.

The non-linear algebraic equations are solved using the Newton-Raphson method (Parkhurst and Appelo, 2013). All equations to be solved are derived from a database containing equations in standard chemical mass action forms. The chemical interactions between the two sides of a reaction are represented in the form of these equations. The reactions are assumed to reach equilibrium; the aqueous phases are assumed to be in thermodynamic equilibrium, but the redox elements can have disequilibrium in their valance state (Parkhurst and Appelo, 2013). When considering kinetic reactions that lead to concentration variations in time, chemical reactions will reach the equilibrium at different specified rates. The equilibrium constant (K) and its negative log (pK), which determines the ratio of reactants consumed over the ratio of products produced, is used for the mathematical calculations. The rate laws used in the model are varied for different reactions, though they all include the simple first-order law.

One of the model calculations is the speciation calculation where the distribution of the aqueous species for each element or component included in the database is calculated. The speciation models calculate the activities, distribution of species, mineral saturation indices

(SI), gas fugacity, and ion ratios in a determined pH and redox potential condition (Thyne, 2007).

The model solves the matrix of equations considering the minimum number of master equations that in PHREEQC are defined as SOLUTION_MASTER_SPECIES located under the database tab. These species, including all solutes, gases, and solids, are the vital species for modelling a system that is thermodynamically balanced. In the input tab, all information on the initial solution can be given including the temperature, pH, pE (negative log of the activity of the electron), and the density of the system. All new components added to the system should be listed under the SOLUTION_MASTER_SPECIES heading. All the concentrations used by the model are in molal (mol/kg) units, although the concentrations are given in other units. Therefore, an assumption of having one kilogram (1 kg) of water is automatically considered.

The batch reaction models, also known as mass transfer models, use the speciation calculations in the beginning and develop the model along with changes in temperature, pressure, pH, and addition of a new reactant to the system. These changes in the reaction path are measured by applying incremental steps with stepwise dosing or removing of mass (Thyne, 2007). Dissociation and precipitation reactions are modelled using the same procedure.

In conclusion, the input file is created given the initial data available of the system under study, then the calculations which are defined as "Simulations" in the input file, are performed by each "Run". The calculations in each run are performed using all equations and the chemical definitions collected in the database library. Multiple simulations can be executed in a single run and for each run, an output file is created.

The limitations and uncertainties of the program have been acknowledged and evaluated to date and some improvements have been made over time. For instance, a more inclusive database such as the LLNL database is provided. It has fewer uncertainties in the data and covers a wider range of chemical definitions for the elements or species in the systems under study. Furthermore, after many years of updates and modifications, the batch version of PHREEQC is now available on different platforms including Windows, Linux, and MacOS. It is also equipped to be called from different software applications. For instance, IPhreeqcCOM is the module manipulated in Microsoft Windows which allows incorporation of PHREEQC in different programming languages (Visual Basic, Python, etc.) and in different applications (e.g. Excel and Matlab) (de Moel et al., 2015).

3.4.3 Using PHREEQXCEL as PHREEQC's container

PHREEQXCEL is one of the applications built around the IPreeqcCOM module which allows PHREEQC to perform all PHREEQC calculations in Microsoft Excel. PHREEQXCEL, is an open-source Excel-based interface introduced and designed by de Moel et al. (2015) and his

team. It displays all files of a PHREEQC run in different sheets of a single Excel file. The Excel file is macro-enabled (.xlsm file) and is composed of 6 sheets (Run_Control, Input, Database, phreeqc.out, Output, and Messages) and four generic VBA (Visual Basic for Application) subroutines (Figure 3.8). The Excel sheet names and the four VBA subroutines in addition to their functions are listed in Table 3.4

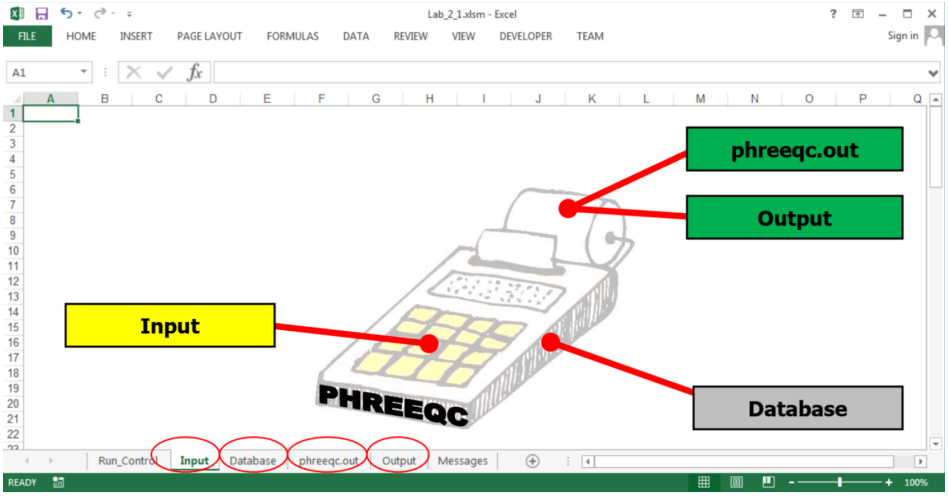

Figure 3.8: PHREEQXCEL, a container for PHREEQC calculations (de Moel et al., 2015)

Table 3.4: Summary of PHREEQXCEL's composition (de Moel et al., 2015)

Sheet name	Function
Run_Control	Run settings and start button
Input	PHREEQC input code
Database	Chemical database for PHREEQC
Phreeqc.out	Lined output (PRINT)
Output	Tabulated output (SELECTED_OUTPUT)
Messages	PHREEQC warnings errors
VBA subroutines	
RunPhreeqc()	Generic VBA program code for PHREEQXCEL applications
Button1_Click()	Macro to start RunPhreeqc()
Button2_Click()	Macro to select an external input file
Button3_Click()	Macro to select an external Database file

In the Input sheet, the simulations to be run can be defined. The required equations and chemical definitions needed for each run are defined under the "Database" sheet. Once the calculations are performed, the results will be presented in an output file. PHREEQXCEL presents the two types of output of PHREEQC, lined output and tabulated output, in two different sheets "phreeqc.out" and "Output", respectively. The lined output in PHREEQXCEL presents a full report on the calculations while the tabulated output can be used for data processing and enables extending the graphical applications in Excel. "Raw Water" and

"Water treatment" are other sheets added to extend PHREEQXCEL for its application for water and wastewater systems.

3.5 Laboratory tests: Chemical Analyses

Online measurements can contribute significantly to monitor and characterize the quality of water systems. However, the new measurement technology is suffering from inherent problems of non-identified bias, which can cause non-optimal control decisions or serious safety issues (Thomann et al., 2002). Obtaining good quality data relies on the application of quality assessment and quality control practices (Alferes and Vanrolleghem, 2016). Besides its time consumption, manual laboratory analyses are still considered a valid data assessment process. Yet, the sheer size of the data sets to be dealt with makes the data assessment process crucial for an effective monitoring strategy (Alferes and Vanrolleghem, 2016).

As Rieger and Vanrolleghem (2008) discussed while developing the mon*EAU* system, data quality assessment is essential and is based on different information sources including reference samples to validate the sensor data, and time-series information to be used for univariate or multivariate statistical analysis. In this framework, Alferes et al. (2013) presented the procedure of water quality assessment presented in Figure 3.9.

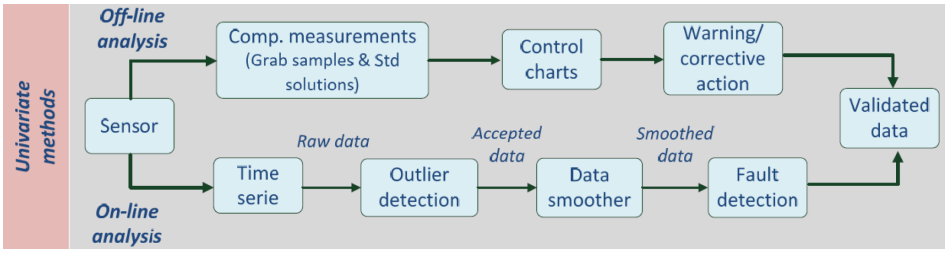

Figure 3.9: Univariate methods for data quality assurance of water quality data (Alferes et al., 2013)

In this thesis, only the off-line univariate methods have been applied to control and validate the collected data. In the off-line analyses, the sensor values are being compared with the values obtained from the corresponding grab samples. The samples are measured with a reference method (ISO, 2003), enabling further systematic or gross error detection in control charts.

In the laboratory of the civil and water engineering department of Université Laval, a DR5000 Hach Spectrophotometer (Loveland, Colorado, US) is installed for analysing chemical analysis kits. The DR 5000 is a complete scanning UV/VIS spectrophotometer with a wavelength range of 190 to 1100 nm (HACH, 2008). Depending on the component to be measured, different methods with different lab procedures are provided. In the frame of this work,

the Hach chemical kits for soluble and particulate COD (Method 8000), ammonia nitrogen ($NH_3 - N$) (Method 10031), and total phosphorus ($PO_4 - P$) (Method 8190) were used.

Chapter 4

Results and analyses

4.1 Improvements of the lab procedures

The buffer system composed of inorganic carbon buffers including bicarbonate (H_2CO_3/HCO_3^-) and carbonate (HCO_3^-/CO_3^{2-}) buffers, VFA (CH_3COOH/CH_3COO^-), ammonium (NH_3/NH_4^+), phosphate ($H_2PO_4^-/HPO_4^{2-}$), and nitrite (HNO_2/NO_2^-) were analysed with the titrimetric set-up. The concentrations of these buffers were measured using the buffer capacity model and PHREEQC software. Colorimetric methods were further applied to validate the model calculations for the ammonium, phosphate and nitrite buffers.

The titration method varied depending on the components of the measurement and their pKa values. Down- and up-titration were the two methods applied and relevant modifications to the lab procedures were carried out to improve the quality of the analyses.

Among the buffer systems mentioned above, the ammonium and phosphate buffers can only be estimated from the up-titration test according to the basic range of their pKa values, whereas all other buffers can be obtained from the down-titration test. However, the pKa value is not the only parameter that a measurement method can be affected by. For instance, the VFA buffer has a pKa value of 4.76 at $25°C$ which indicates that both measurement methods can be used for the determination of this buffer. However, as the study of Van Hulle et al. (2009) has shown, the VFA buffer may be subject to volatilization when applying up-titration. This volatilization of the VFA was also observed in this study when comparing the VFA concentration estimated from the up-titration to the concentration obtained from the down-titration test; the VFA buffer measured in the up-titration is usually underestimated. Therefore, it was decided to only use down-titration for the determination of the VFA concentration.

The concentration of the bicarbonate buffer can also be different depending on the titration method selected. As shown in Table 3.3, the pK_a of the bicarbonate is 6.37 at $25°C$. Since the samples of this study are wastewater samples, the initial pH is normally between

6.5-7.5 depending on the location where the samples are taken (influent or effluent of the pilEAUte plant). Therefore, the bicarbonate buffer should be measurable when the sample is down-titrated to pH 3, or when the acidified sample is up-titrated to pH 11. When the sample is down-titrated with diluted acid (H_2SO_4, 0.05 N), due to volatilization of CO_2, an increase in pH occurs in between acid dosages and therefore more acid needs to be dosed to compensate for this loss. Thus, the bicarbonate concentration will be overestimated. To avoid this, the sample is only mixed slowly during the down-titration to allow the model to provide a reliable estimation of the concentration of the bicarbonate buffer.

Once the sample is acidified, it is up-titrated to pH 11 using a diluted base ($NaOH$, 0.05 N). However, before and during the up-titration, the sample may be absorbing CO_2 from the atmosphere and the acidity concentration is increasing. As such the pH is decreasing. To compensate for this, the volume of base dosed into the sample has to be increased. As a result, the bicarbonate's buffer capacity is overestimated. Besides, when the sample contains other buffering components such as ammonium and phosphate, which can only be estimated from the up-titration test, the overlaps of the pK_a values can cause errors in the calculations. The pK_a values of bicarbonate and phosphate buffers overlap, and so do the carbonate and ammonium buffers. This overlap of the buffers as demonstrated in Figure 1.6, suggests the benefit of eliminating the presence of inorganic carbon buffering systems to enable better estimation of ammonium and phosphate buffers during the up-titration.

Because of the continuous absorption of carbon dioxide, the bicarbonate's buffer capacity increases over time during an up-titration. This leads to the obscured asymmetric shape of the buffer capacity curve for the bicarbonate buffer. To better understand this phenomenon, one may imagine to take multiple samples over time (at different pH values) from the titrated batch and being analyzed for the buffer capacity curves (Figure 4.1). Assuming that these samples are in equilibrium with the atmosphere, they would contain different amounts of CO_2 at different times since they have absorbed carbon dioxide over time. Thus, the buffer capacity of each sample would be different and therefore, the estimation of the bicarbonate buffer. In other words, for each sample, the obtained titration curve and the calculated buffer capacity curve would be different.

In Figure 4.2, the theoretical buffer capacity curves of the individual samples in equilibrium with the atmosphere at different pH are shown (the dots on each curve represent the corresponding pH and buffer capacity at the time when the samples are grabbed). For each of these curves, one assumes that the amount of carbon does not change over time and leads to a certain buffer capacity curve. In real life, however, the sample has time to come to equilibrium with the atmosphere at each pH increase. Thus, the resulting experimental titration curve shifts from one instantaneous buffer capacity curve to the other as the pH increases. Figure 4.3 presents the increase in the bicarbonate buffer capacity in the sample titrated over time.

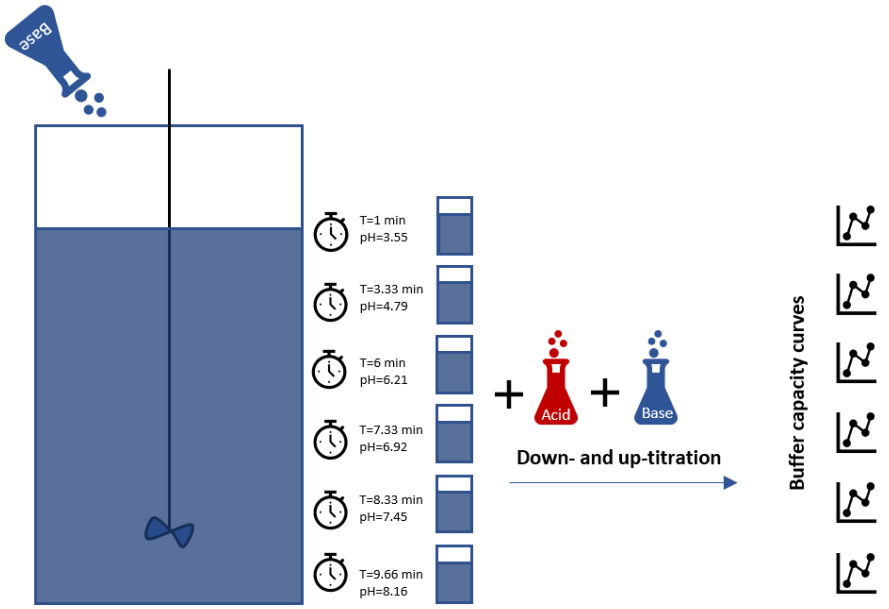

Figure 4.1: Schematic view of the hypothetical titration experiment

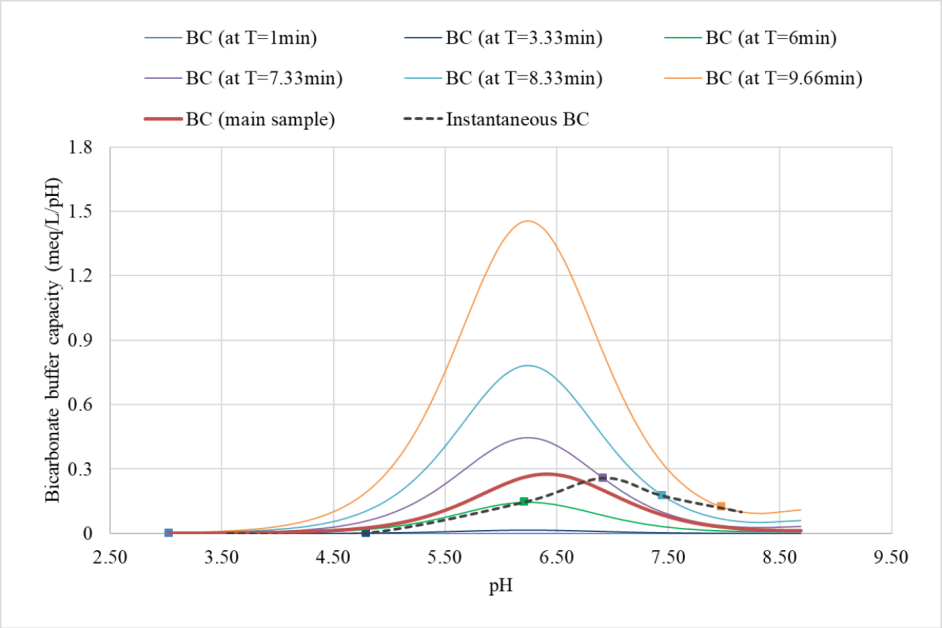

Figure 4.2: i) The dotted line (instantaneous buffer capacity BC) shows the observable buffer capacity of the sample at the time it is grabbed. ii) Each BC curve represents the complete theoretical buffer capacity curve of a solution at equilibrium with atmospheric CO_2 at a given pH. iii) The dots show from which theoretical BC curve the observed BC comes, as the sample absorbs more and more CO_2 as time goes on and pH increases.

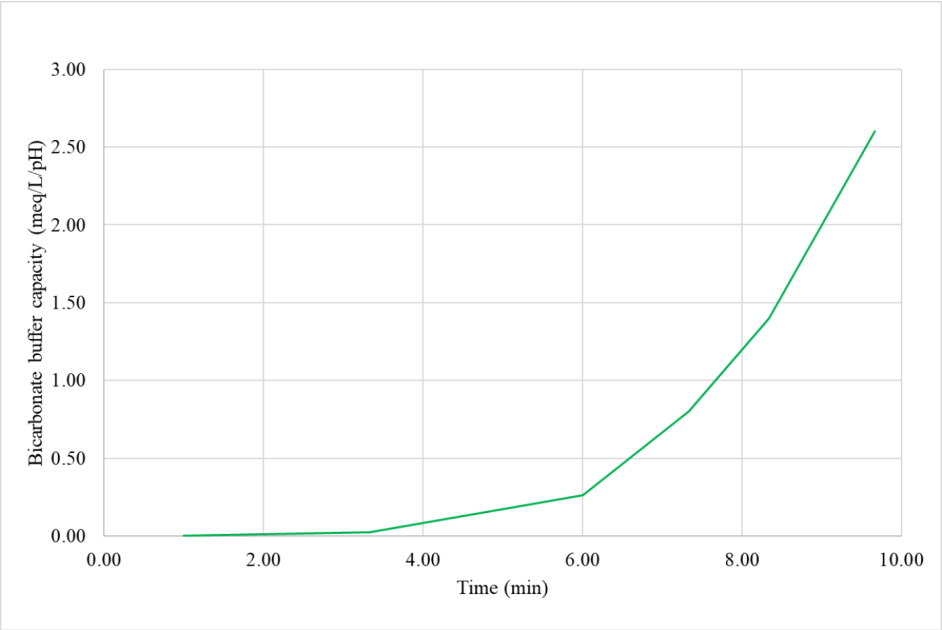

Figure 4.3: Bicarbonate buffer capacity over time during up-titration

To compensate for this increase in the bicarbonate buffer capacity with time, all other buffers with pK_a values overlapping with the bicarbonate buffer (e.g.: VFA, phosphate and ammonium buffers), may experience an overestimation in their concentration values. To overcome this drawback, one must prevent the CO_2 absorption before and during the up-titration test. To this end, the following modifications to the laboratory procedures were made to improve the measurements: CO_2 *stripping* and *nitrogen blanketing*.

In the following sections, the implementation of the two modifications is explained. Then, their influence on the results of the titration and the model calculations are discussed.

4.1.1 CO_2 stripping

Once the sample is down-titrated to pH 3, an additional stripping step can be applied to eliminate all CO_2 from the sample. For this, the sample is mixed with a high-speed mixer. Three minutes of mixing was selected after trying five minutes of mixing and observing the same effect of stripping. As such, it is expected that the CO_2 in the sample is fully stripped.

To see the effect of stripping, two different samples with approximately the same concentration of bicarbonate alkalinity (as evidenced by the down-titration test) were compared. For the May 18^{th} sample; as listed in Table 4.1, the CO_2 was not stripped before the up-titration, while the June 4 th sample was subjected to stripping.

The titration data of the two samples were interpreted by the buffer capacity model. To prevent the interfering effect of the water buffer on the model calculations, only the titration

Table 4.1: Effect of CO_2 stripping on the bicarbonate alkalinity measurements

Sample	Stripping	Bicarbonate (HCO_3^-)		Ammonium (NH_4^+)	
		Down-titration	Up-titration	Up-titration	Hach kit
May 18^{th}	✗	2.69 mmol/L	1.51 mmol/L	39.30 mg/L	26.55 mg/L
June 4^{th}	✓	2.69 mmol/L	0.19 mmol/L	25.31 mg/L	21.70 mg/L

data for pH below 10 were used. The resulting buffer capacity curves are presented in Figure 4.4.

It can be seen that the bicarbonate concentration decreases by approximately 87 % after stripping the CO_2 in the June 4^{th} sample. To validate the titration results, the ammonium content of the samples was measured with the Hach chemical kit tests. Comparing the titration and Hach kit ammonium concentration values for the May 18^{th} sample, one can see that without stripping the CO_2 content, the titration-based ammonium is significantly higher than the one obtained from chemical Hach kit tests. However, for the June 4^{th} sample, the two measured values are close, and the Hach kit ammonium can validate the titration-based ammonium concentration. This is due to the low concentration of bicarbonate and thus, the smaller interference with the ammonium buffer. As such, the accuracy of the model for calculating the ammonium buffer increases for the stripped sample.

4.1.2 Nitrogen blanketing

Even when the CO_2 is stripped before a titration, it may still be absorbed from the air during the titration. To impede this absorption, a blanket of N_2 is put on the top of the sample by applying a gas to the vapour space of a container or a vessel to control its composition (Yanisko et al., 2011).

Nitrogen is the most common inert gas which is easily accessible and relatively inexpensive. Therefore, nitrogen blanketing has been widely applied in chemical, pharmaceutical, and food processing industries to protect sensitive products being degraded by contact with oxygen or other gaseous contaminants.

System design

In this work, nitrogen blanketing is used to protect the samples against the infiltration of carbon dioxide in the air, by flowing the nitrogen gas on the vapour space of the container. For this, a nitrogen gas cylinder followed by a two-gauge pressure regulator which provides a reading of the dispensing pressure (in psi units) and an indicator for the gas cylinder pressure (Figure 4.5).

The pressure is reduced to 20 psi to provide a slightly positive pressure blowing on top of the sample container. The gas then flows through a plastic tube to the titration devices. The

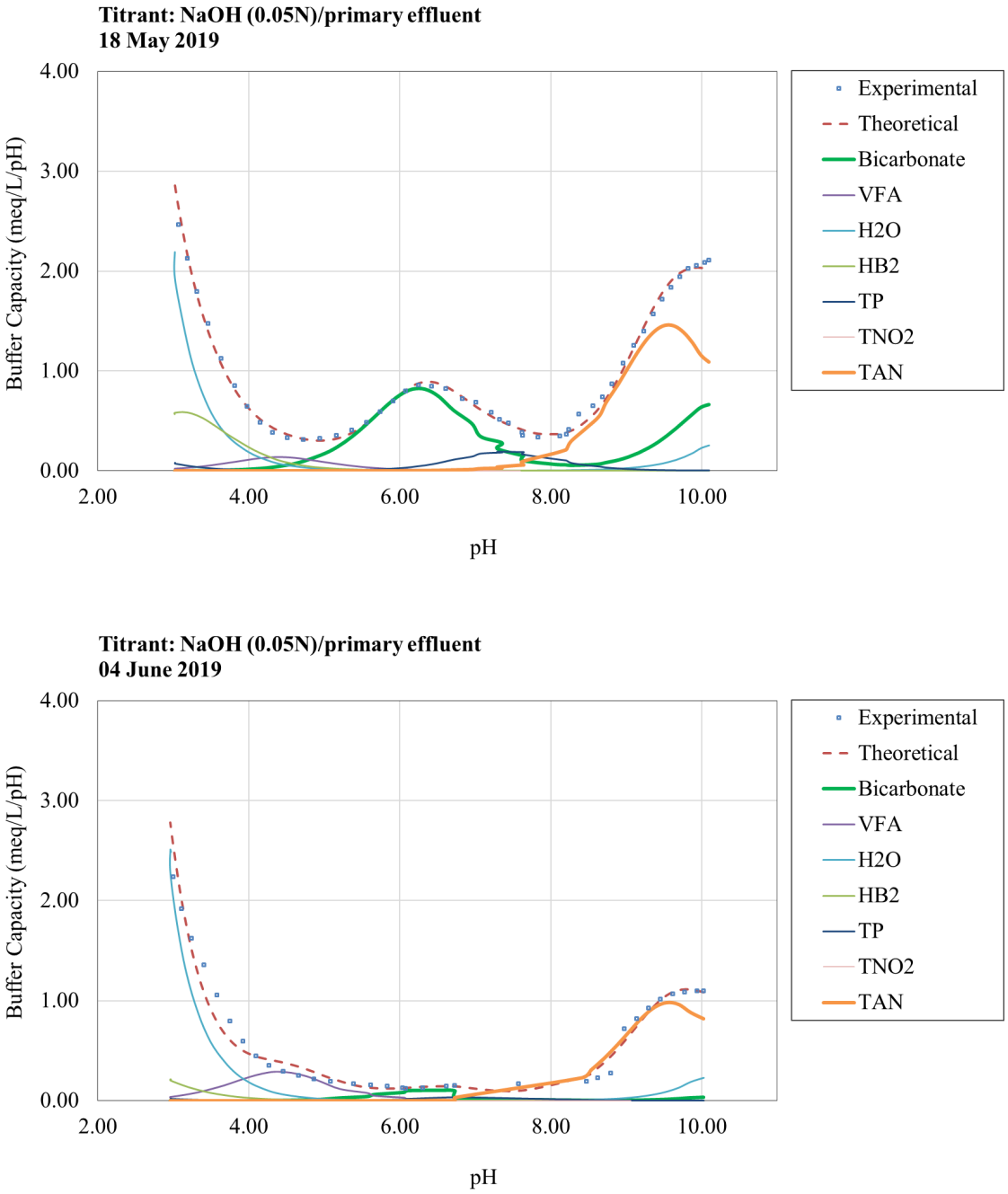

Figure 4.4: Comparing the effect of CO_2 stripping on two up-titration tests: (Top) Buffer capacity curve for the May 18^{th} influent sample up-titrated without stripping step, (Bottom) Buffer capacity curve for the June 4^{th} influent sample up-titrated with stripping step

location of the tube installed on the head of the sample processor is presented in Figure 4.6. Moreover, the stripping step performed using the magnetic mixer is presented in the left picture.

Figure 4.5: Nitrogen gas cylinder and its two-gauge regulator

Figure 4.6: From left to right: sample mixing with a magnetic mixer, sample processor from the front with the yellow gas tube installed on its head, sample processor from the top view

Data interpretation

To evaluate the nitrogen blanketing effect, two different primary effluent samples were chosen as summarized in Table 4.2. Both samples were down-titrated and mixed for three minutes for CO_2 stripping. It can be seen that the two samples contain similar bicarbonate buffer concentrations, as measured by the down-titration. However, the measured buffer concentration after blanketing with nitrogen gas, reduced it by 84 %. Although it was expected to see an improvement in the estimation of the ammonium buffer after nitrogen

blanketing, but when comparing the simulation results with the Hach chemical kits, this conclusion cannot be made.

Table 4.2: Effect of nitrogen blanketing on the bicarbonate alkalinity measurements

Sample	Stripping	N_2 gas	Bicarbonate (HCO_3^-)		Ammonium (NH_4^+)	
			Down-titration	Up-titration	Up-titration	Hach kit
June 1^{st}	✓	✗	3.18 mmol/L	0.41 mmol/L	35.33 mg/L	30.45 mg/L
June 30^{th}	✓	✓	3.19 mmol/L	0.06 mmol/L	21.79 mg/L	13.90 mg/L

The titration curves of the two samples are compared in one graph in Figure 4.7. One can see that around the pK_a of bicarbonate, the sample which is covered by the nitrogen gas (red thick line) has a sharp increment in its pH value for a very small addition of base (less than 1 mL). According to the titration data, this sample consumes 29 % less base compared to the sample without a nitrogen blanket. The low resistance of the sample of June 30^{th} against pH-change upon addition of base around the pK_a value of the bicarbonate buffer, indicates the absence of this buffer in the system. The corresponding buffer capacity curves of the two titrations are presented in Figure 4.8 and Figure 4.9.

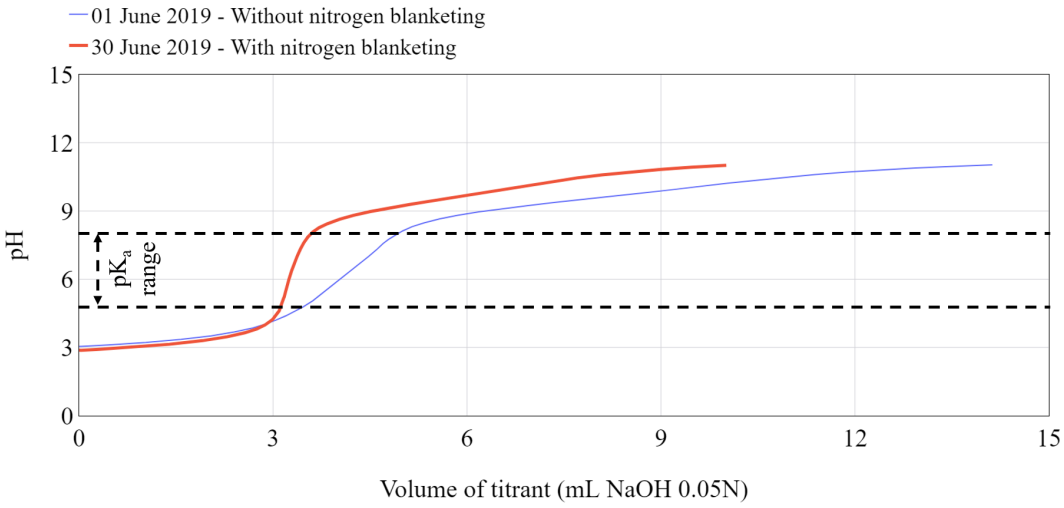

Figure 4.7: Comparing the difference between two titration curves regarding the nitrogen blanketing effect

During the simulation, it has been observed that the estimation algorithm fails to measure the phosphate and bicarbonate buffer for the June 1^{st} sample since their pKa values overlap. Therefore, to enable measuring the bicarbonate buffer present in the system and later comparing this value with the one with nitrogen blanketing, the phosphate buffer was removed from the estimation algorithm and thus, from the buffer capacity curve shown in Figure 4.8. However, after blanketing with nitrogen gas, since the bicarbonate buffer in the

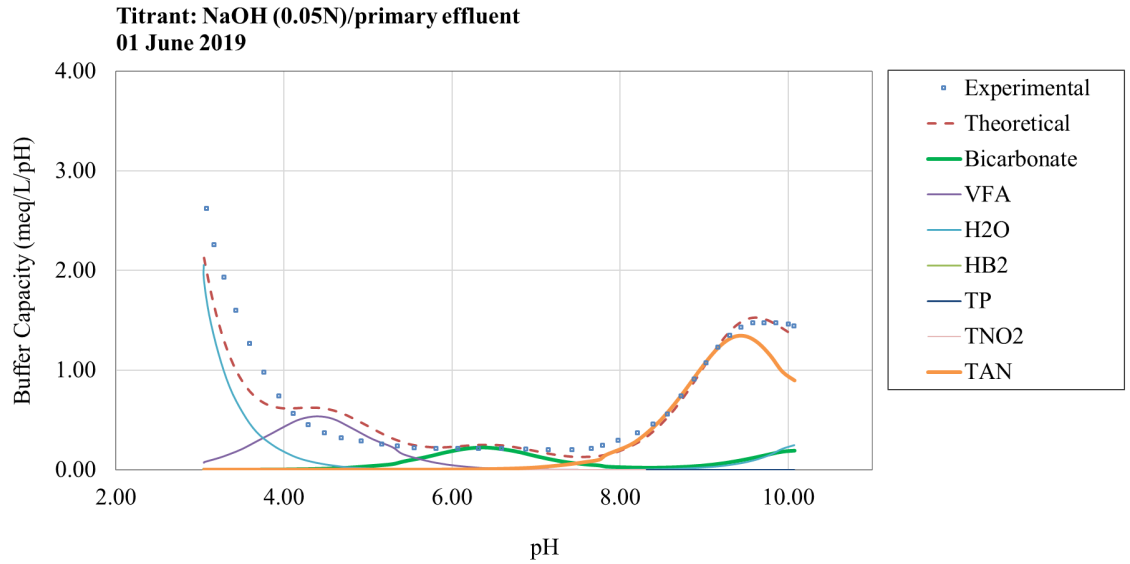

Figure 4.8: Buffer capacity curve of the June 1^{st} primary effluent sample without nitrogen blanketing

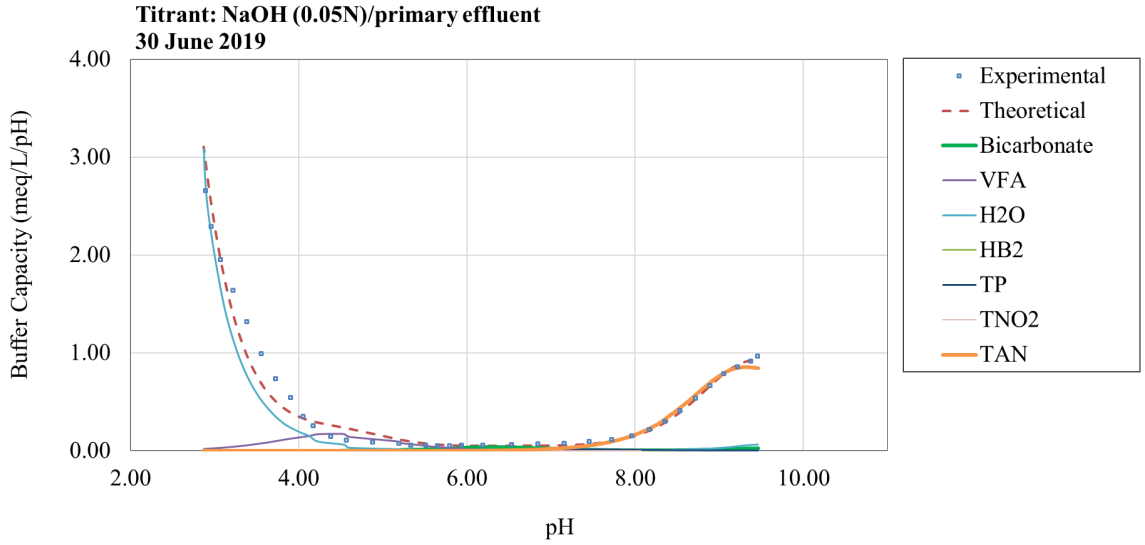

Figure 4.9: Buffer capacity curve of the June 30^{th} primary effluent sample with nitrogen blanketing

system is reduced, the estimation algorithm can distinguish the two buffers and calculate their concentrations (Figure 4.9).

Moreover, as can be seen in Figure 4.8, the theoretical buffer capacity curve can hardly fit the experimental curve at lower pH values. Although the curve fitting seems to have a better performance for the June 30^{th} sample with nitrogen blanketing (Figure 4.9), the estimation algorithm still suffers for the lower pH values. One can see from the two figures that the main buffer present at the lower pH ranges is the water buffer. This is studied below.

The water buffer

The main buffer present at low pH values (below pH 4) is the water buffer which fits the two experimental and theoretical buffer capacity curves. At the beginning of the up-titration, since the acidified sample has a low pH value (around pH 3 in this experiment) and the pH probe is rinsed with Nano water (and therefore has a neutral pH), the probe has difficulties to reach an equilibrium with the acidified sample. As such, the water buffer is the only buffer that can accommodate for the effect of the equilibrium.

In some cases, the water buffer fails to perform good curve fitting at the lower pH values in the area where buffers of interest are present and thus, overlap. To fix the model estimation for the overlapping buffers, one may limit the ranges of the pKa values in the solver and limit their peak locations to minimize the interferences between the buffers. However, the problem of interferences of buffers with the water buffer at the lower pH values remains unsolved. For instance, the VFA buffer can overlap with the water buffer (see Figure 4.8) affect curve fitting.

To overcome this, similar to the work of Van Vooren (2000), a blind buffer (HB_2) is introduced at the lower pH values. The blind buffer is a monoprotic buffer with an unknown pK_a and concentration value. Since it is introduced to reduce the effect of the erroneous water buffer in the model, its pK_a value is forced to be below pH 3. The model calculations for the samples of June 1^{st} and June 30^{th} were repeated with the addition of the blind buffer, and the new buffer capacity curves are presented in Figure 4.10 and Figure 4.11.

To evaluate the effect of the addition of the blind buffer on the VFA buffer concentration estimate, the VFA concentration values with and without the addition of the blind buffer (HB_2) are compared with the value estimated from the down-titration test in Table 4.3 and Table 4.4. The estimated VFA concentrations for the two samples are higher than the values estimated by the down-titration test. It can be seen that both samples are more than 50 % overestimated. However, as mentioned earlier in this chapter, the VFA buffer estimated by the up-titration has usually lower values than the values estimated by the down-titration test due to volatilization of VFA during the up-titration. Therefore, what can be deduced from this is that the VFA buffer estimated before the addition of the blind buffer is not reliable. This even can be visually confirmed from the buffer capacity curve of the June 1^{st} sample (Figure 4.8).

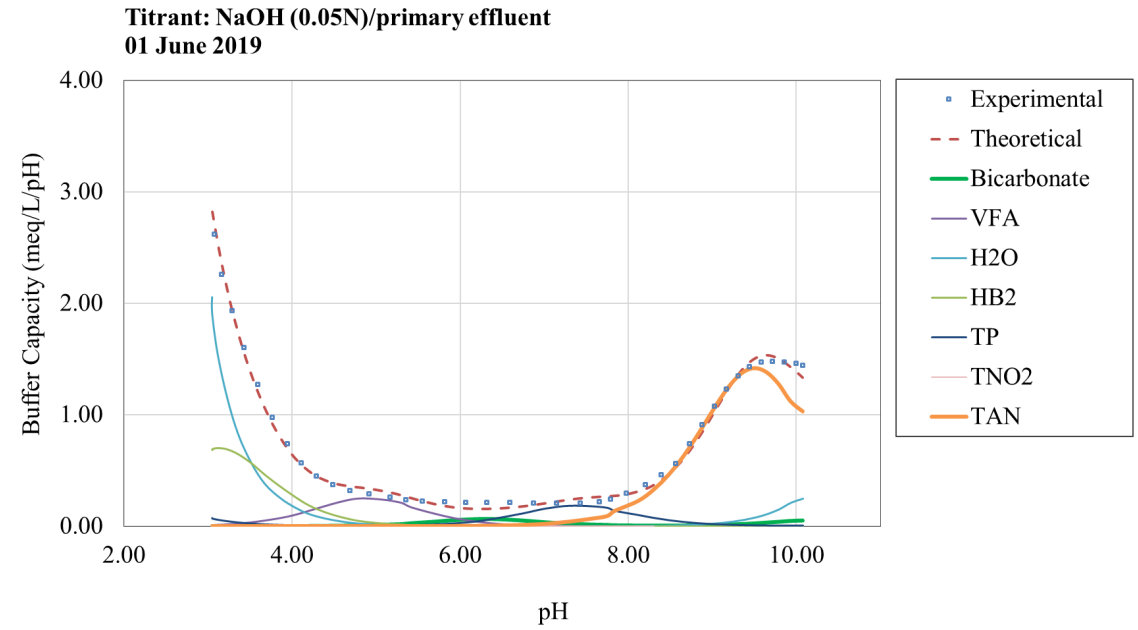

Figure 4.10: Buffer capacity curve of the June 1^{st} primary effluent sample without nitrogen blanketing and with addition of the blind buffer to the buffer capacity model

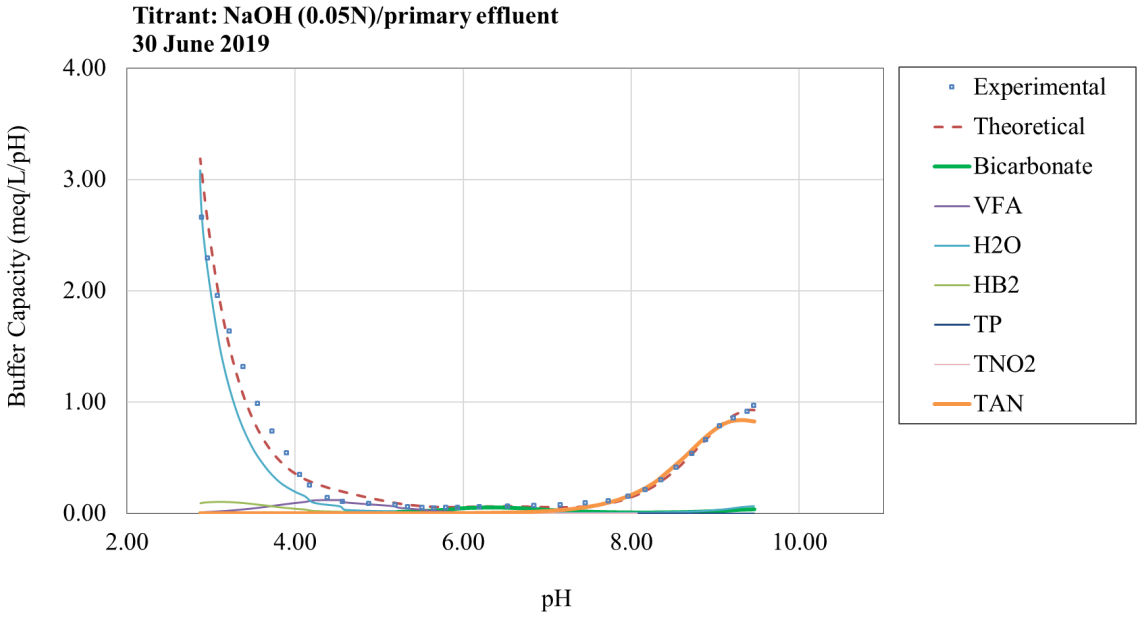

Figure 4.11: Buffer capacity curve of the June 30^{th} primary effluent sample with nitrogen blanketing and with addition of the blind buffer to the buffer capacity model

Table 4.3: The model estimation for the VFA concentrations before the addition of the blind buffer in the estimation algorithm

Sample	VFA (CH_3COO^-)	
	Down-titration	Up-titration (without HB_2 addition)
June 1^{st}	0.56 mmol/L	0.92 mmol/L
June 30^{th}	0.20 mmol/L	0.31 mmol/L

Table 4.4: The model estimation for the VFA concentrations after the addition of the blind buffer in the estimation algorithm

Sample	VFA (CH_3COO^-)		Blind buffer (HB_2)	
	Down-titration	Up-titration (with HB_2 addition)	Up-titration	pK_a
June 1^{st}	0.56 mmol/L	0.22 mmol/L	1.22 mmol/L	3.34
June 30^{th}	0.20 mmol/L	0.18 mmol/L	0.22 mmol/L	3.30

The estimation of the VFA buffer improves by addition of the blind buffer in the algorithm (Table 4.4). First, for both samples, the estimated values are smaller than the ones of the down-titration. Besides, the estimated VFA concentration for the June 30^{th} sample is very close to the measured value from the down-titration test (10 % lower) which indicates an improvement in the model estimation.

However, this improvement in the VFA estimation is not observed for the June 1^{st} sample in which nitrogen blanketing was not performed. The VFA concentration value is reduced to 60 % compared to its corresponding down-titration value. Given the model estimation for the blind buffer (Table 4.4), one can see that the concentration of the HB_2 buffer in this sample is higher than the June 30^{th} sample, even though the estimated pK_a values are relatively close. In other words, the model raises the concentration of the blind buffer to compensate for the water buffer effect rather than for correcting the VFA estimation. It should be noted that since these interpretations are not for a set of data but only for single experiments, there might be uncertainty in the model results. Thus, the aforementioned are the observations made, and more statistical tests and a larger number of experiments are needed to come to a firm conclusion.

When comparing Figure 4.8 and Figure 4.10, one observes that the phosphate buffer changes significantly. By including the blind buffer, it thus became possible to estimate both the bicarbonate and phosphate buffers adequately.

4.1.3 Changing of pH probe

The Aquatrode+ pH probe used for performing titration tests was in use since 2012. As a probe performance factor, the calibration time can define the accuracy and reliability of the electrode. While a consistently good performance pH probe requires less than 30 seconds of

calibration time, it was experienced that more than one minute was needed for the current pH probe. This probe also seemed no longer reliable since it picked up noise during titration, leading to bumps in the titration curve and resulting in inaccurate buffer capacity model results. Note that once bumps were observed in the titration curve, the probe was no longer used for any titration experiments. Thus, the titration results presented along this MSc are not affected by the poor performance of the probe.

To deal with this issue, a new Aquatrode+ electrode was purchased from Metrohm Co. To compare the performance of the new probe with the old one, a down-titration test was performed on two identical copilot effluent samples.

The two probes were first calibrated with two standard solutions of pH of 4 and 7. The average calibration time recorded for the old probe was 1.40 minutes, while this value was around 24 seconds for the new probe.

In Figure 4.12, the two titration curves obtained by the two sensors are provided. The new probe produces a smoother curve with fewer outliers compared to the old one. The volume of acid dosed per step decreases gradually as the pH decreases with the new electrode, whereas the old electrode has erratic changes in the volume dosed into the samples. Therefore, to have accurate measurements and as a result produce reliable data, the sensor should not be in use for long periods.

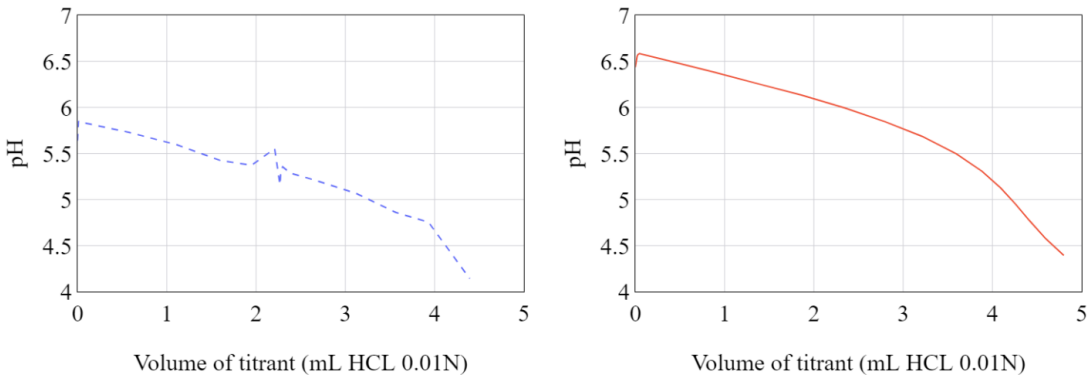

Figure 4.12: Titration curves obtained from the two pH probes for the same sample (Old pH probe: left; New pH probe: right)

4.1.4 Removing sensor washing step for better equilibrium

As mentioned before, during the up-titration the pH probe is more noisy in the low pH ranges. One may assume that the disequilibrium between the probe and the acidic solution could be the cause of this sensor problem. In fact, after each titration, the probe is automatically washed using Nano water. As predefined in the sample processor's program, the Nano water

is pumped from its separate storage tank through a plastic tube and washes the probe after each titration.

When the sample is down-titrated to pH 3, the pH probe is in equilibrium with the acidified sample. This equilibrium is disrupted by the washing step between the two titrations. In other words, the pH probe suffers to again reach the equilibrium from neutral pH to the acidic pH.

To improve this, one may consider removing the washing step and increasing the contact time between the acidified sample and the pH probe. For this, four different conditions were tried out:

Use of Nano water: Nano water is the reference washing solution in the titration process. This water is pumped through a plastic tube connected to the sample processor to rinse the pH probe in the automation mode.

Use of tap water: To better understand the effect of the washing step, tap water was used as an alternative washing solution.

3 minutes resting with the solution: The probe was not rinsed after the titration but was kept in the sample after the CO_2 stripping for 3 minutes. As such, it was expected there would be fewer oscillations in the signal since the pH probe is preadapted to the initial pH range.

15 minutes resting with the solution: This condition has been tried out on a different sample (taken on May 13^{th}) as the sample tested in the three aforementioned conditions (taken on May 5^{th}). By resting the probe with the solution for a longer time, the efficiency of this condition was evaluated. Since the sample used for this condition was taken at a different day, its composition differs with the May 5^{th} sample. However, the estimated bicarbonate concentration from the down-titration test was similar (2.880 mmol/L HCO_3^- estimated for the May 13^{th} sample and 2.719 mmol/L HCO_3^- estimated for the May 5^{th} sample).

In all mentioned conditions, the samples were first down-titrated to pH 3, followed by an up-titration test. However, for the May 13^{th} sample, the CO_2 in the sample was first stripped by stirring for 3 minutes. Then the probe was put inside the sample to rest for 15 minutes with the solution. Along with the up-titration, nitrogen blanketing was performed to prevent carbon dioxide absorption.

Applying these sensor washing conditions, the effect of washing the probe and resting the probe with the solution for different equilibrium time lengths on the titration curves and the model calculations can be compared. In Figure 4.13, the buffer capacity curves of the tested conditions are provided.

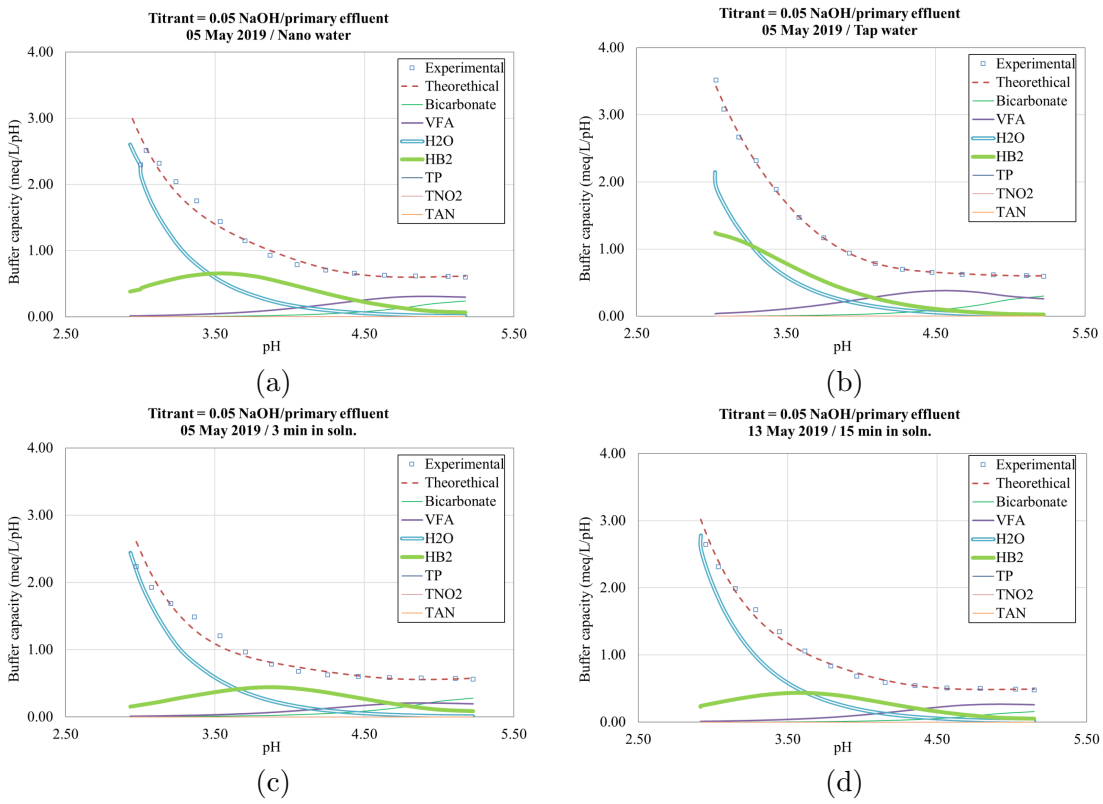

Figure 4.13: Comparing different washing steps effect on the buffers behavior

For the three samples of May 5^{th}, variation in the peak locations (pK_a) of the water buffer, the blind buffer (HB_2), and the VFA buffer are observed. As explained before, with the water buffer alone it is impossible to perform the curve fitting at lower pH's with the defined stop criteria for the model components. Thus, the blind buffer was determined to compensate for this problem.

When the pH probe is washed with tap water, the water buffer alone cannot fit the model to the experimental curve. This could be deduced from the big gap between the water buffer curve and the two fitted curves. To compensate for this, the HB_2 concentration rises with a smaller pK_a value, thus shifting this buffer's peak location to the left. Consequently, also the peak location of the other buffers, including VFA, shift to the left. Although the model fitting presents a reliable model calculation, both VFA and HB_2 buffers are overestimated.

Nano water as the reference washing step has a better quality of data compared to tap water. It can be seen in the Figure 4.13 that the gap between the water buffer and the two curves for Nano water decreases and the HB_2 buffer shifts more to the right and is lower in concentration. However, for tap water, the blind buffer is compensating for this gap by shifting more to the left and a higher buffer capacity. This shifting in peak location of the HB_2 buffer leads to better estimation of the VFA buffer since the algorithm is able to estimate the VFA buffer

closer to its real pK_a peak location compared to Nano water washing. The higher buffer capacity of the HB_2 can even be seen from the estimated values summarized in Table 4.5. The HB_2 buffer estimated for the tap water washing condition is larger than the one of Nano water. Even though this leads to a smaller SSE and thus, better curve fitting, it makes the tap water washing condition less reliable than the Nano water.

The estimation of the blind buffer when the probe stayed in the solution for 3 minutes decreases compared to the two other aforementioned conditions. However, the estimated SSE and the curve fitting need to be improved. Given the bicarbonate concentration estimated for the May 5^{th} sample, one can see that applying 3 minutes of resting time leads to an increase in the bicarbonate concentration. As such, it was decided to repeat this experiment with the addition of CO_2 stripping and nitrogen blanketing. Therefore, the estimated bicarbonate concentration for the May 13^{th} sample decreases, even after applying 15 minutes of resting time.

Given the SSE results obtained (Table 4.5), it can be concluded that the more accurate model estimation can be provided in a low bicarbonate alkalinity sample and a longer equilibrating time for the pH probe resting in the titrated sample.

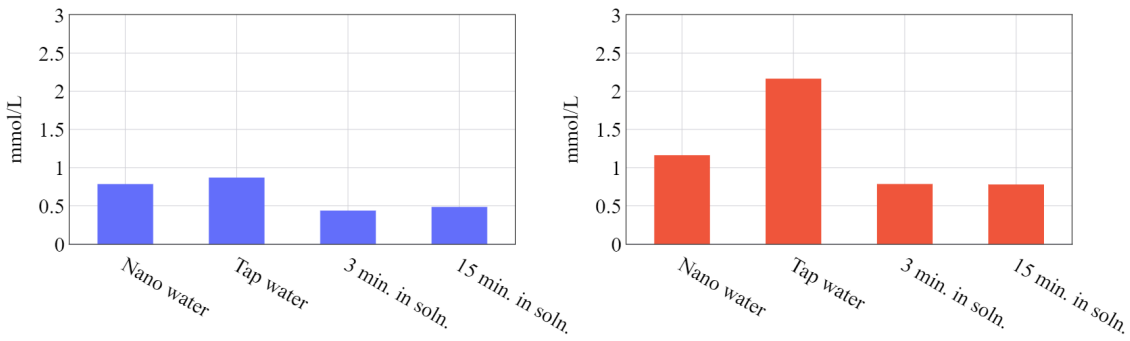

Figure 4.14: Sensor washing step effects (VFA: left; HB_2: right)

Table 4.5: Buffer capacity model results for the sensor washing step experiment

Solution	Bicarbonate	VFA	Additional buffer	SSE
Washing step	meq/L as HCO_3^-	meq/L as CH_3COO^-	meq/L as HB_2	
Nano water	0.949	0.785	1.163	0.255
Tap water	1.119	0.870	2.165	0.020
3 minutes resting	2.302	0.438	0.786	0.252
15 minutes resting	0.666	0.486	0.780	0.067

4.2 Improvements of the PHREEQC interpretation

4.2.1 Developing a lab simulation as an input file for titration tests

Titration is a mixing process of a titrant and an analyte where acid-base chemical reactions are taking place after each dosing step until an endpoint where the new solution reaches chemical equilibrium. PHREEQC contains three basic methods for dosing chemicals into a solution, using the following keywords (de Moel et al., 2015):

1. **REACTION**: is used for adding moles of any chemical to a solution.
2. **MIX**: is used for mixing a chemical solution with a sample (sample could be any solution, e.g.: water or wastewater).
3. **EQUILIBRIUM_PHASE**: is used for adding a chemical solution until equilibrium is reached.

Using these keywords and defining the sample as a PHREEQC solution using the keyword SOLUTION, one can proceed with the simulation. PHREEQC also uses 1 Kg of "Pure water" as a default solution with a density of 1 kg/L, a temperature of $25°C$, a pressure of 1 atm, a proton activity of 10^{-7} (pH = 7) and an electron activity of 10^{-4} (pE = 4) (de Moel et al., 2015). The default values are then used for the conversion of the parameter's units (mmol/kgw) and redox (pE).

To determine the composition of the sample, two calculation steps are required: (I) Initial solution calculation where the amount of substance per element is defined, (II) Final solution calculations where the single values for the master variables (pH and pE) are defined. The amount of substance for an element in a solution is calculated based on its molal concentration (mol/kgw) and the mass of water (1 kg as default) since PHREEQC considers the mass of water as a quantity of solvent. The speciation calculation is performed using the values of the master variables pH and pE, where the pE value is defined based on a specific redox couple. The redox couple $O(-2)/O(0)$ is used for drinking water and wastewater solutions since they contain a minimum amount of dissolved oxygen (de Moel et al., 2015).

Excel can assist in transforming the chemical data into input codes for PHREEQC. Extended by an additional sheet "Raw water" (see Figure 4.15), PHREEQXCEL enables the user to add the input values which are linked to the PHREEQC code on the "Input" sheet where the numeric values are converted into text strings. The calculations are started by pressing on "Run PHREEQC".

Dosing of a chemical to a solution by applying the three methods described earlier, a simulation lab file was implemented by de Moel et al. (2015). This was further developed in this MSc study by the addition of the titration data to the input file. As shown in Figure 4.16,

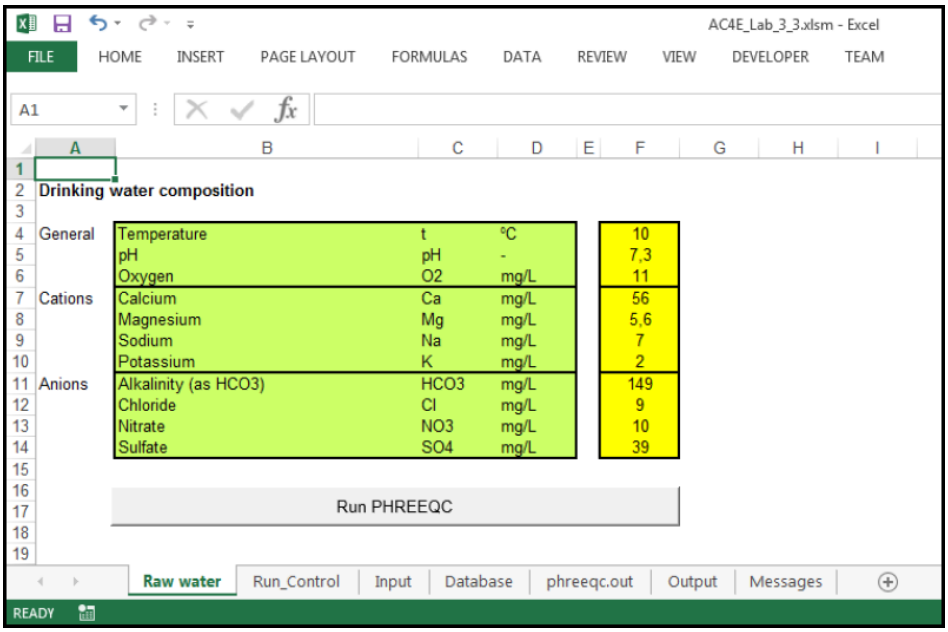

Figure 4.15: PHREEQXCEL input for the example drinking water (de Moel et al., 2015)

the wastewater sample is to be mixed with a dosed acid (H_2SO_4) and the final solution (Solution 3) is to be calculated.

The amount of acid to be dosed in each step was considered to be equal and the number of dosing steps is defined by the user. However, with the modifications, the volume of acid per step (or base, depending on the titration test) can be set as a variable. This allows the model to predict the number of dosing steps based on the number of titration data points and further, the number of simulations performed.

The experimental curve is plotted using the titration data points for the pH as a function of the added volume of the acid. Once the model runs, the PHREEQC simulation curve is plotted on the same graph (red), with the same data of dosed acid but with the simulated pH values.

The model outputs a set of results for each simulation. The latter can be summarized into three types:

Simulation 1: As it is the beginning of the process, this simulation carries on the speciation calculation of the initial solution ("Solution 1") and further performs the calculation of the batch reaction between Solution 1 and 1 kg of water introduced by PHREEQC as the default solution for electron balancing.

Simulation 2: First, a solution of pure water with default parameters (named "Solution 2") is set to equilibrium with O_2. Then, its charge balance is calculated. The total amount of the acid dosed is calculated in mmoles and is then allowed to react with the pure water using

the “Reaction” keyword. The new solution after the batch reaction is now named “Solution 2” and the simulation is ended after the speciation calculation for this solution.

Simulation 3,4,5...,n: In Simulation 3, 1 mole of “Solution 1” is mixed with the dosed amount of “Solution 2” given by the corresponding titration data point. Then, the batch reaction between the two solutions is calculated. The model then calculates the next solutions until the resulting pH reaches the last experimental pH data point.

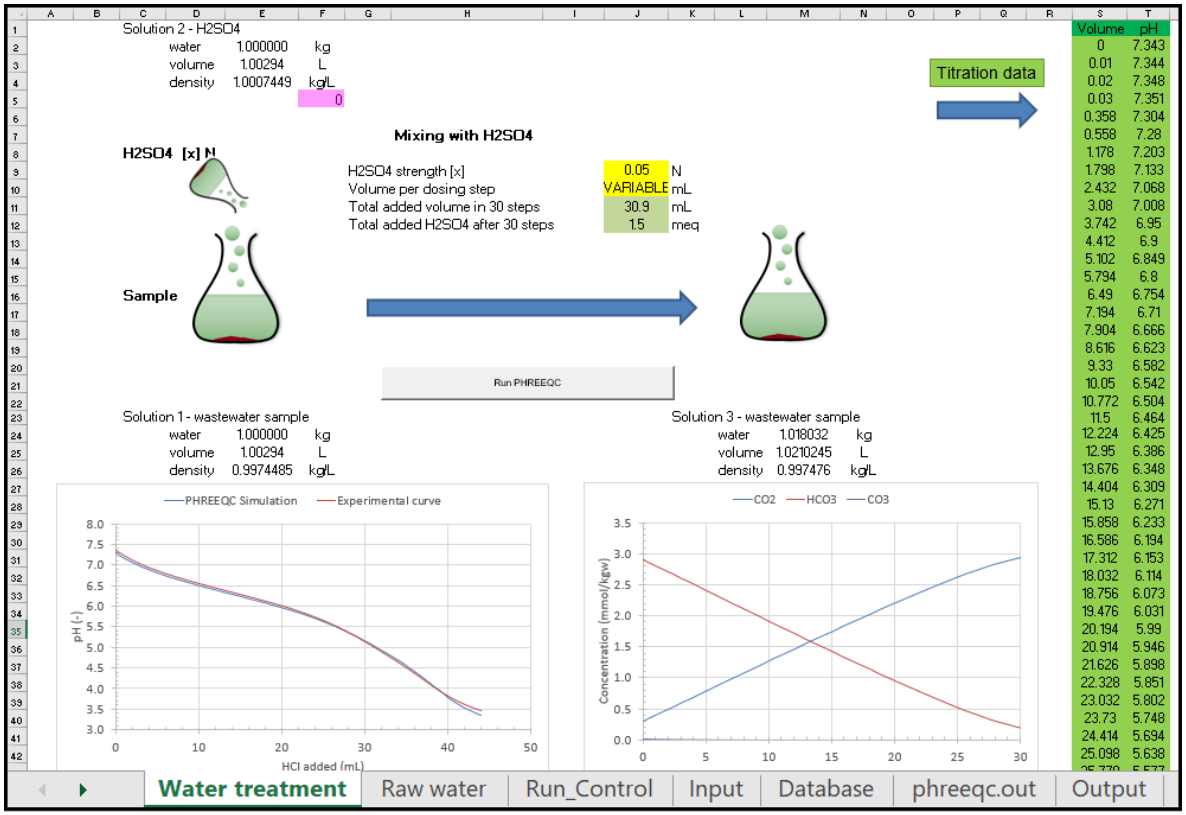

Figure 4.16: Titration test implemeneted in PHREEQXCEL's simulation lab file

4.2.2 Addition of OpenSolver

Using PHREEQC in Excel through the PHREEQXCEL interface is beneficial to the user in many ways. Working with Excel does not require programming skills. Besides, its tabulated output enables to perform model optimization in Excel through running a solver.

A graphical summary is presented in Figure 4.17 to summarize the performed processes in a simulation run in PHREEQXCEL. The processes can be divided into simulation steps and optimization steps. The simulation steps are manually implemented in PHREEQXCEL by adding the titration data and using the volume of the acid (base) in each step as a time series. Running PHREEQC and calling the chemical information stored in the database, a titration curve is simulated.

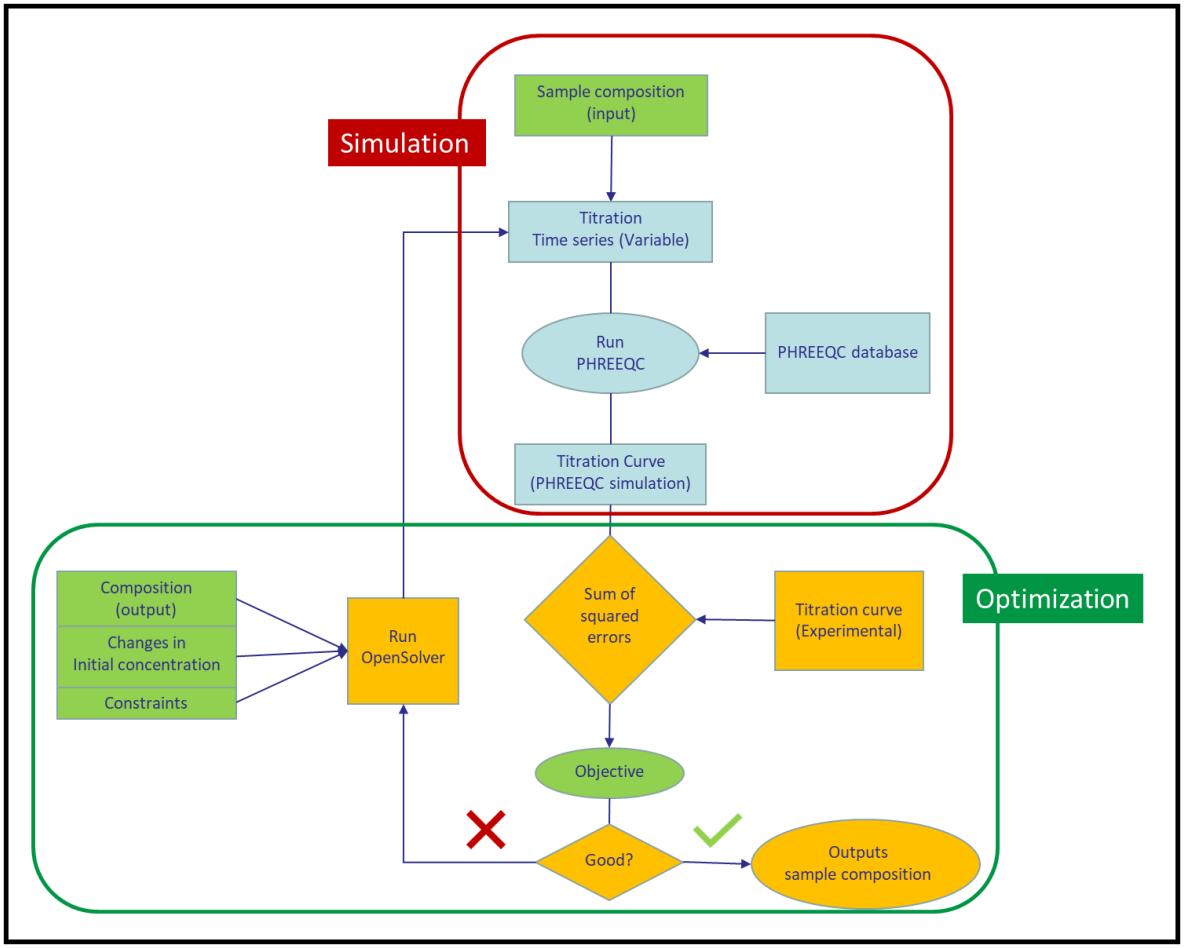

Figure 4.17: Schematic view of the processes performed in a simulation run in PHREEQXCEL

Given the titration data, the simulated and experimental pH can be compared. The sum of squared errors is manually formulated to compare the two data sets and evaluate the model fit. To optimize the model fit, a solver is needed to change the variables until the simulation

reaches the minimum of the sum of squared errors. The variables that can be adjusted are the concentration values of the buffers defined in the input of the model. In contrast to the buffer capacity model, the variables to be adjusted in PHREEQC are only the concentration values of the components and not their pK_a values. To change these concentrations, one must know that the model requires to run the simulation again. As such, the solver must be able to perform a simulation process for each iteration. Once the solver reaches the minimum value, the model outputs the results and plots the best PHREEQC simulation curve fitted to the experimental curve.

The mathematical procedure used in the PHREEQC model computation is an iterative method, which uses an initial guess to generate a sequence of improving approximate solutions for a class of problems, and each approximation is derived from the previous ones. This iterative method built in the algorithm has termination criteria and can be called convergent if the corresponding sequence converges for given approximations (Amritkar et al., 2015). Therefore, the convergence rate together with the size of the data (that determines the time it takes to simulate each titration curve) can affect the speed of the optimization process.

To be more flexible compared to the Excel built-in solver and to improve the convergence rate, PHREEQXCEL was extended with OpenSolver. It is an open-source Excel add-in for Microsoft Windows that uses the COIN-OR (Computational Infrastructure for OR) CBC optimizer capable of solving large linear and integer programs (Mason, 2012).

The OpenSolver is compatible with the built-in Excel solver and has no restriction for solving large models. Moreover, compared to the built-in solver, OpenSolver can perform the optimization process faster and can visualize the constructed model on-sheet by highlighting the variables and the objective cell to be minimized in colours. One of the advanced features of this optimizer is that it can interact via the command line. Thus, a command line is added in the Raw water spreadsheet, to start the OpenSolver after running the Button1_Click which is a macro to start RunPhreeqc().

4.2.3 Using the Stimela.dat library to avoid the redox equilibrium between N-species

Oxidation states of nitrogen

Nitrogen can have four oxidation states in the natural environment: N(5), N(3), N(0), and N(-3). In wastewater, nitrate (NO_3^-) with oxidation state of N(5) and dissolved nitrogen gas N(0) are present. Under anoxic conditions, nitrate may be reduced to nitrogen gas, which volatilizes, by a biological process called denitrification. Nitrogen gas can reduce to ammonia (as shown in the reaction path in the middle-left in Figure 4.18) only through special chemical or biological reactions. In a chemical process called the Haber-Bosch process, atmospheric nitrogen (N_2) converts to ammonia (NH_3) by a reaction with hydrogen (H_2) using a metal

catalyst under high temperatures and pressures (Appl, 1982). The Haber process is an artificial nitrogen fixation process which is mainly used to produce fertilizer today. Through biological nitrogen fixation (BNF), discovered by Beijerinck in 1901, specialized group of prokaryotes utilize the nitrogenase enzyme to catalyze the conversion of atmospheric nitrogen to ammonia (Wagner, 2011).

In theory, the oxidation of NH_4^+ should follow the reversed reaction path as the reduction path of nitrate (the reaction path in the leftmost part of Figure 4.18). However, due to kinetic constraints, this is not the case. In practice, oxidation of NH_4^+ follows the reaction path shown in the right part of the Figure and results in the formation of NO_2^- and NO_3^-, respectively.

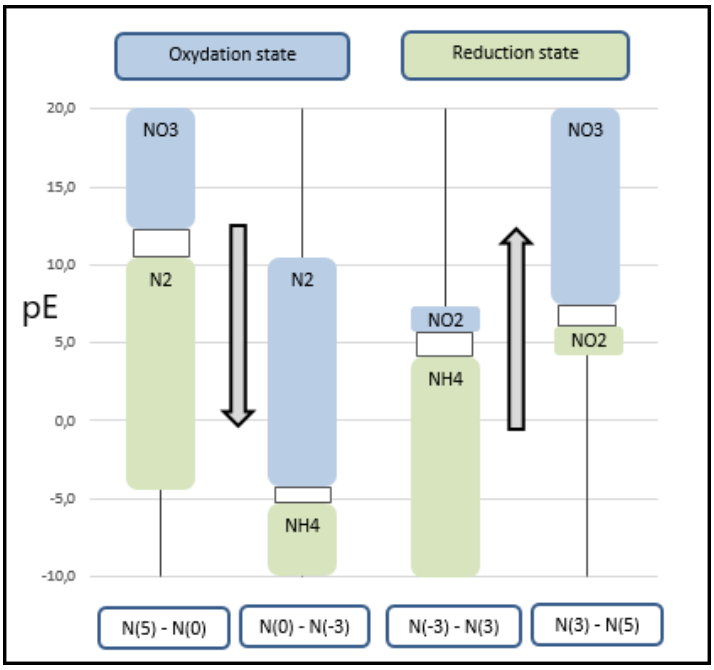

Figure 4.18: Nitrogen oxidation states and pE in reduction of NO_3^- and oxidation of NH_4^+ at a temperature of 10-25°C and pH 7.2-8.2 (de Moel et al., 2015)

Redox reactions in PHREEQC

In PHREEQC, to determine the speciation of a water sample, the hydrogen activity (pH) and the electron activity (pE) play an important role. The pH value is changing along with a titration test and therefore, it is to be adjusted to maintain the charge balance. If the charge is specified for pH, it may not be specified for any other element. The pE value, or the conventional negative log of the activity of electrons, can be adjusted to achieve a redox equilibrium. Redox reactions are a type of chemical reaction in which the oxidation states of atoms are varied and are characterized by the transfer of electrons between chemical species. Most often one species undergoes oxidation while another species undergoes reduction. The

redox indicates the definition of a redox couple that is used to calculate the pE. For instance, a sample being titrated is in equilibrium with the atmosphere, therefore, the redox couple that determines the pE value is oxygen in which its oxidation state alternates between O(-2)/O(0) in the PHREEQC simulation.

The original concept of redox reaction calculations in PHREEQC is based on considering single equilibrium constants for the conversion from one oxidation state into another, and calculating electron balancing over all elements with different oxidation states. However, as demonstrated by the oxidation states of nitrogen in Figure 4.18, such electron balancing calculation for a component with multiple oxidation states may involve unrealistic reactions. The aforementioned unrealistic redox reaction path for nitrogen has led to developments in the PHREEQC database. For instance an additional PHREEQC database, amm.dat, for groundwater flows was developed, in which NH_4^+ was introduced as an inert, or redox-uncoupled element Amm. With this database the oxidation of NH_4^+ can controlled, in this way preventing NH_4^+ from participating in kinetically impossible oxidation or reduction reactions. The redox-uncoupled species are now introduced for all gases including nitrogen in PHREEQC version 3 (de Moel et al., 2015).

For practical applications in water and wastewater, the PHREEQC database Stimela.dat was developed by Peter de Moel and his colleagues within the Stimela platform of TU Delft University of Technology (Delft, Netherlands) (de Moel et al., 2013). This database is an extension of the chemical database phreeqc.dat, which is in compliance with standard methods and allows major groundwater species to be modelled as redox-uncoupled elements for water and wastewater systems. The redox reactions used in Stimela.dat for nitrogen species are given in Table 4.6. In *Redox-uncoupled elements* column, the definition of the redox-uncoupled elements used in the Stimela.dat are presenetd. Note that *Ntg* refers to redox-uncoupled nitrogen gas N(0) and *Amm* refers to redox-uncoupled ammonium [N-3].

Table 4.6: Redox reactions for nitrogen elements used in the Stimela.dat database for PHREEQC

Elements	Species	Formation reactions	Redox-uncoupled elements
N	NO_3^-	-	
N(5)	NO_3^-	NO_3^-	
N(3)	NO_2^-	$NO_3^- + 2H^+ + 2e^- = NO_2^- + H_2O$	[N+3]
N(0)	N_2	$2NO_3^- + 12H^+ + 10e^- = N_2 + 6H_2O$	Ntg
N(-3)	NH_4^+	$NO_3^- + 10H^+ + 8e^- = NH_4^+ + 3H_2O$	Amm [N-3]

The formation reactions in Table 4.6 show that redox reactions do not just include electron (e^-) transfers. They may also contain hydrogen ions (H^+) either as part of the reaction or as part of the oxygen reduction reaction O(-2)/O(0). This means that redox reactions not only lead to changes in pE but can also alter pH. Thus, for a titration simulation that changes

hydrogen ions, and consequently pH, and only depends on the addition of an acid or a base, it is necessary to eliminate the redox-coupled species because it would affect pH and therefore the simulation results.

In the frame of this MSc study, it is observed that modelling up-titration tests with redox-coupled N-species results in unrealistic redox reactions, and related pH changes since the titrant used (NaOH) and the sample itself contain oxygen. Stimela.dat is capable of measuring the concentrations of N-species buffering systems such as ammonia and nitrite, without interfering through their possible redox reactions. It includes inert/redox-uncoupled NH_4^+ as [N-3]H4+ and NO_2^- as [N+3]O2-. Thus, the model outputs separate speciation calculations for each oxidation state of the nitrogen component. Further, the oxygen concentration remains almost constant during the simulation.

4.2.4 Modifying the database for the component of interest: HNO_2 and NO_2^-

The Stimela.dat database enables the model to estimate different nitrogen species with respect to their different oxidation states. Although the redox reactions are provided for the redox-uncoupled elements, some of the chemical information of these elements is missing. To engage the additional components in the model, one must add the chemical association reactions, the related Log K and the reaction enthalpy as well as the analytical expression relating log K to T.

As the chemical information is essential for the speciation calculation of the buffer, these additions are attached under Solution_Species keywords in the input of the up-titration simulation file (see Figure 4.19). The missing chemical information was mainly related to NO_2^- and its acid form HNO_2. For both redox-coupled (expressed as N(3)) and redox-uncoupled (expressed as [N+3]) elements, the formation reactions and the aforementioned kinetic and thermodynamic parameters were added. In addition to NO_2^-, the chemical information of NO_3^- and HNO_3 was added to the input file. These modifications were later approved by Peter de Moel through personal communication.

The simulated model was not only suffering from the incomplete database and considering N-species as redox-coupled elements. The solution was not charge-balanced and due to a systematic error in the software, the partial pressure of oxygen was not readable. Therefore, the solution was not electrically balanced either. Consequently, by running the solver for optimizing the simulation results, several bumps appeared on the best-fitting PHREEQC curve around pH 5.5-6.2 and also around pH 8.0 as shown in Figure 4.20. A clear discrepancy with the experimental curves was the result and the sum of squared error for this simulation was estimated as 5.19.

```
Added/modified by Maryam Tohidi:
       1.0000 NO2- + 1.0000 H+  =  HNO2
              log_k           +3.2206
               -delta_H         -14.782            kJ/mol           # Calculated enthalpy of reaction           HNO2
       #       Enthalpy of formation:              -119.382 kJ/mol
              -analytic 1.9653e+000 -1.1603e-004 0.0000e+000 0.0000e+000 1.1569e+005                    # analytic overrules log_k and delta_H
       #      -Range:  0-200
               # gamma omitted means activity is default as Davies (so llnl_gamma is skipped)
               # dw omitted means not included in calculated conductivity,  HNO2 is uncharged so not relevant for conductivity
               # Vm omitted means not included in calculated density
       1.0000 [N+3]O2- + 1.0000 H+  =  H[N+3]O2
              log_k           +3.2206
               -delta_H         -14.782            kJ/mol           # Calculated enthalpy of reaction           HNO2
       #       Enthalpy of formation:              -119.382 kJ/mol
              -analytic 1.9653e+000 -1.1603e-004 0.0000e+000 0.0000e+000 1.1569e+005                    # analytic overrules log_k and delta_H
       #      -Range:  0-200
               # gamma omitted means activity is default as Davies (so llnl_gamma is skipped)
               # dw omitted means not included in calculated conductivity,  HNO2 is uncharged so not relevant for conductivity
               # Vm omitted means not included in calculated density
       1.0000 NO3- + 1.0000 H+  =  HNO3
              log_k           -1.3025
               -delta_H         16.8155            kJ/mol           # Calculated enthalpy of reaction           HNO3
       #       Enthalpy of formation:              -45.41 kcal/mol
              -analytic 9.9744e+001 3.4866e-002 -3.0975e+003 -4.0830e+001 -4.8363e+001                  # analytic overrules log_k and delta_H
       #      -Range:  0-300
               # gamma omitted means activity is default as Davies (so llnl_gamma is skipped)
               # dw omitted means not included in calculated conductivity,  HNO2 is uncharged so not relevant for conductivity
               # Vm omitted means not included in calculated density
```

Figure 4.19: Modifications and additions to the Stimela database in the input file of PHREEQC

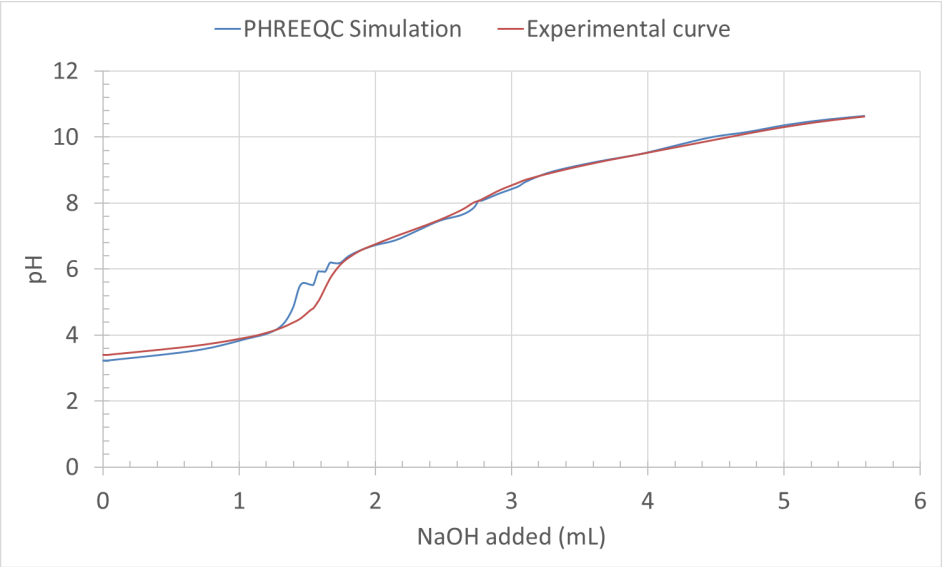

Figure 4.20: Best-fitting PHREEQC simulated curve for an up-titration test before model developments

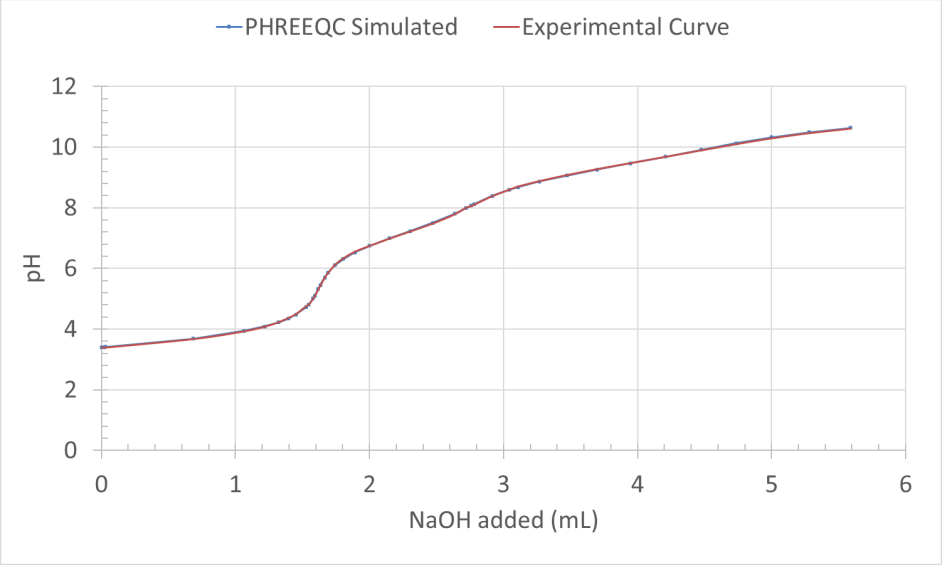

Figure 4.21: Best-fitting PHREEQC simulated curve with SSE of 0.011 for the up-titration test after model developments

Using the Stimela.dat database to prevent unrealistic redox-coupled reactions of nitrogen species, and modifying this database with the addition of new chemical components and their chemical information, the simulation results improved. However, the bumps were not yet removed completely after running the solver and the sum of squared error increased to 69.92 which clearly shows that the algorithm failed. To deal with this, it was necessary to increase the accuracy of the dosed titrant in the input file by increasing the number of digits from 4 to 6. Moreover, nitrate had to be used as a charge balance component to make the

solution charge-balanced. Running the OpenSolver, the SSE now reached 0.011 (improved by 99 % compared to the estimated SSE of 5.19 before the modifications), and the curve fitting improved significantly (see Figure 4.21).

4.3 Reactive settler case study

4.3.1 Introduction

A primary clarifier aims to remove the settleable solids, including both inorganic and organic particles, from wastewater. Optimizing the performance of the primary clarifier results in higher organic particle removal which then can lead to low carbon availability for the denitrifiers in the downstream biological nitrogen removal processes. On the other hand, the removal of inorganic particles is essential, since low solids removal performance leads to an increase of the inorganic portion of the sludge in the biological reactors that has to be removed and thus, reduces the SRT. This endangers the proper functioning of the biological processes. This challenge of simultaneously removing the particles and preserving the readily biodegradable organic matter has led to manipulations of chemical processes such as supplying an external carbon source to provide the necessary carbon for denitrification, and the addition of the coagulants to increase the efficiency of the solids removal (Ponzelli, 2019).

In recent years, several physical and chemical processes in the primary clarifier have been studied. However, less attention has been drawn to the biological reactions that can occur in this system. An example of a biological reaction is hydrolysis, in which complex organic matter is converted into rbCOD. Since these reactions have a low rate, an elevated concentration of sludge is essential. Therefore, thanks to the sedimentation of the particles to the bottom of the clarifier, a sludge blanket can be formed, providing the required conditions for the biological reactions.

To create an enhanced concentration of rbCOD in the clarifier's effluent, an elutriation process can also be applied. Elutriation is a process for separating different types of particles by a stream of gas or liquid flowing usually in the opposite direction to the sedimentation. Within this process, the lighter or smaller particles rise to the top, since their sedimentation velocities are lower than the rising fluid. As a result of applying this process, the amount of concentrated rbCOD present at the top of the primary clarifier, and thus, ready to be consumed by the denitrifiers in the downstream, is increased.

Anaerobic digestion (AD) is a biological process in which organic waste is converted into readily biodegradable organics such as VFAs, a valuable substrate for biological nitrogen and phosphorus removal. The reactions involved in the anaerobic digestion process are both biological and chemical, as presented in Figure 4.22. As a first step, the complex organics present in the primary sludge breaks into monomers such as amino acids, sugars and fatty

acids through hydrolysis. Then, these monomers are converted into VFAs that mostly exist in the form of acetic acid (CH_3COOH) through acidogenesis.

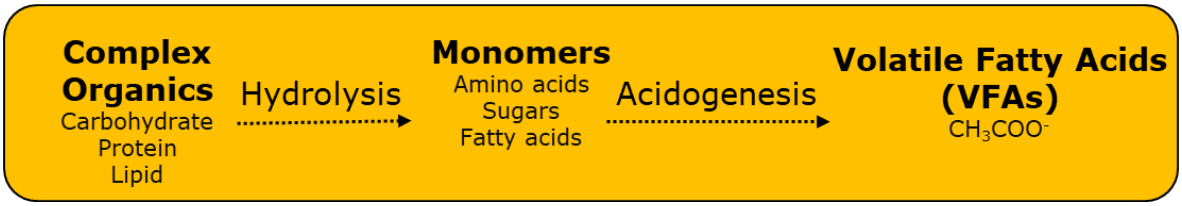

Figure 4.22: Biochemical reactions involved in the anaerobic digestion of primary sludge

Hydrolysis is the rate-limiting step in the fermentation process and it can affect the VFA production. Literature (Lee et al., 2014) states that the parameters such as operational pH, temperature, hydraulic retention time (HRT), SRT, organic loading rate, recirculation rate, and additives influence the concentration and the yield of the VFA produced. These operational parameters have been tested in a real treatment system, and thus studied in the MSc project of Ponzelli (2019), where he developed reactive primary clarification processes at the pilEAUte, as a mainline fermenter.

A reactive primary clarifier is a physico-biochemical reactor that not only aims to remove the settleable solids, but also promotes the biochemical reactions within it (Ponzelli, 2019). To maximize the rates of the biological and chemical reactions in the primary clarifier, a high concentration of solids is needed. As mentioned earlier, a high sludge blanket and elutriation processes can provide the required conditions. The elutriation is performed through an internal recirculation line, where the settled sludge at the bottom of the clarifier is pumped back to a certain height above the bottom. As a result, the produced VFA in the sludge blanket is transferred to the top of the clarifier. One must note that elutriation is not increasing the VFA concentration at the bottom of the clarifier. Another effect of elutration is that, because of the recycle that is needed to perform elutriation, the sludge concentration at the bottom of the clarifier reduces. Thus, for a same waste flowrate, less sludge is wasted.

4.3.2 Design and implementation

The modified primary clarifier (PC) set up in the pilEAUte is shown schematically in Figure 4.23. This clarifier has a volume is 2.1 m^3, its free surface covers 1 m^2 and its typical overflow rate is 1.1 m/h. The inlet of the PC is fed from the outlet of the storage tank and the outlet from the PC is represented by two flows: effluent (Q_E) and waste (Q_W). An internal return line and a manual back-valve were installed. The recycle flowrate (Q_R) can be adjusted by the back-valve manually to make it proportional to the clarifier inflow rate (Q_{IN}). Using a pump this flow is recirculating through the line to the sludge blanket at a

Table 4.7: Summary of the configurations, function of the operational parameters, for the eight experimental stages studied (Ponzelli, 2019)

Stage	Flow rates			HRT	SRT		Chemical Dosages	
	Q_{IN}	Q_R	Q_W	HRT_{EFF}	$SRT_{DESIRED}$	SRT_{ACTUAL}	$NaHCO_3$	$FeCl_3$
#	m^3/d	$\%Q_{IN}$	m^3/d	h	d	d	$mgHCO_3/L$	mg/L
1	26.4	0%	0.096	2.0	1	0.74	0	0
2	38.4	0%	0.04	1.4	1	1.51	0	0
3	16.8	50%	0.04	2.1	1	1.51	0	0
4	16.8	50%	0.02	2.1	3	1.83	0	0
5	16.8	14%	0.02	2.8	3	0.80	0	0
6	16.8	14%	0.02	2.8	3	0.74	100	0
7	16.8	14%	0.02	2.8	3	1.16	0	20
8	16.8	14%	0.02	2.8	3	1.00	100	20

fixed height of 0.5 m from the tank's bottom. The wastage is still done by an automatic valve opening for a fixed period of time (Ponzelli, 2019).

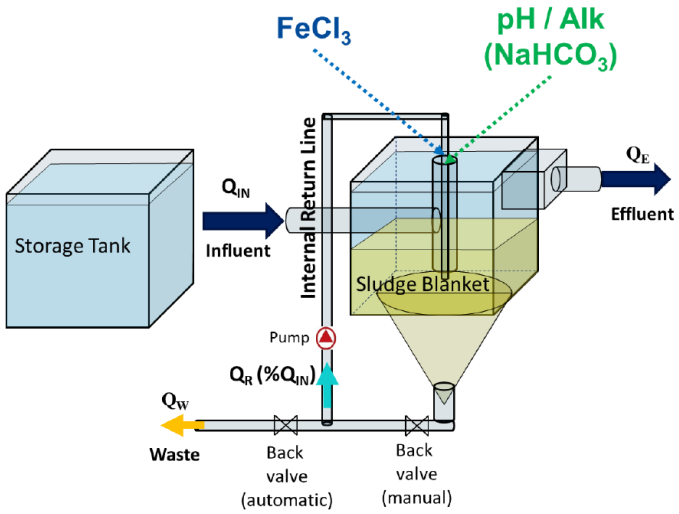

Figure 4.23: Schematic view of the modified primary clarifier (Ponzelli, 2019)

To quantify the main process parameters that affect the solubilization process within hydrolysis, several experimental configurations have been tried out. The main parameters studied are the SRT, the internal recirculation flow rate (Q_R), alkalinity dosage, flocculant addition ($FeCl_3$), pH, and temperature. The resulting eight experimental stages are summarized in Table 4.7.

During the sampling campaigns that have been carried out, both composite and grab samples have been taken. As illustrated in Figure 4.24, the inlet and outlet of the primary clarifier and the waste line were the three sampling locations in this study where composite samples were taken by a refrigerated autosampler.

At each 0.20 m of the settler, samples were grabbed manually to examine the behaviour of the sludge blanket as function of its height and the TSS concentration. Analyzing the samples with the developed titrimetric method aimed to provide information on the VFA, alkalinity and pH at different sludge blanket heights.

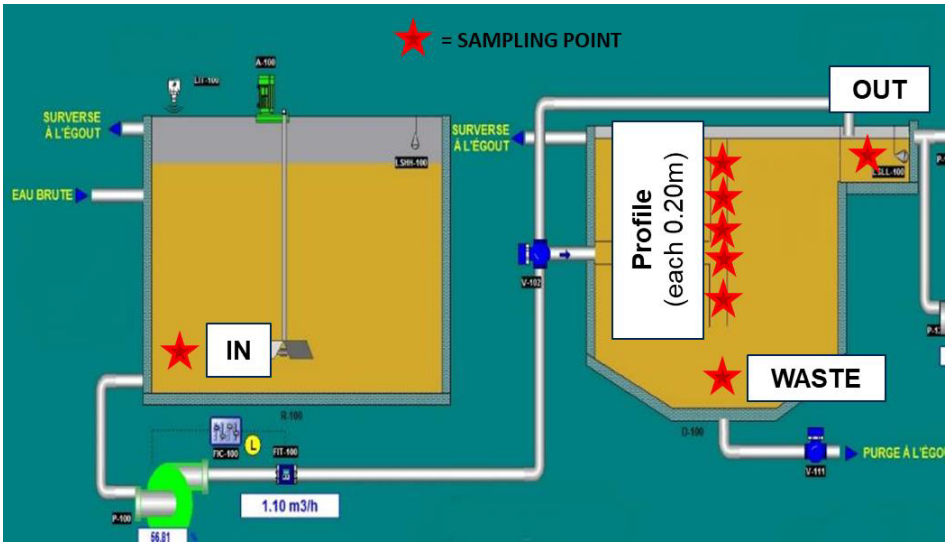

Figure 4.24: Sampling locations for the eight experimental stages, as indicated on the SCADA interface (Ponzelli, 2019)

As SRT cannot be measured directly, it was calculated using the flows entering and leaving the clarifier, along with the TSS measurements taken along the depth of the sludge blanket. The calculation performed is shown in Equation (4.1).

$$SRT = \frac{V_1 X_1 + \Sigma V_i X_i}{Q_W X_W + (Q_{IN} - Q_W) X_E} \tag{4.1}$$

V_1 and X_1 are the volume and TSS concentration of the supernatant. V_1 is calculated by subtracting the volume of the sludge blanket from the total volume of the primary clarifier. The volume of the sludge blanket, in turn, is determined by the location of the sharp increase in the concentration profile of the TSS. Q_{IN} is the influent flowrate, Q_W is the waste flowrate, X_W is the waste TSS concentration, and X_E is the TSS concentration of the effluent leaving the clarifier (considered equivalent to the supernatant TSS concentration).

The term $\Sigma V_i X_i$ represents the mass of sludge stored in the sludge blanket. To determine this mass, since the sludge blanket varies in concentration along the vertical dimension, the clarifier

volume was broken down into segments which were assumed to have a uniform concentration equal to the average concentration of its top and bottom TSS measurements. Given the conical shape of the bottom of the clarifier, the volume segments containing the sludge blanket were in the shape of truncated cones. The volume of the slices was thus calculated according to Equation (4.2).

$$V = \frac{1}{3} * \pi * H * (r^2 + r * R + R^2) \tag{4.2}$$

Where R and r represent the upper and lower base radii, respectively and H represents the height of the cone slice.

4.3.3 Effect of alkalinity

In this case study different scenarios were tested on the primary clarifier to evaluate the fermentation process and to understand the conditions optimizing the VFA production rate. In parallel with the experiments conducted by Ponzelli (2019) above, the author of this MSc has investigated the effect of alkalinity addition using titration tests. Throughout 72 hours, the dynamics in bicarbonate alkalinity and VFA concentrations in the inlet and outlet of the primary clarifier were tracked, as shown in Figure 4.25 and Figure 4.26. Note that the filled marked data are the measured data, and the open symbols are predicted based on the real measurements using the same relative change as in the periods where both in and out were measured (see more details regarding the performed calculations in Ponzelli (2019)).

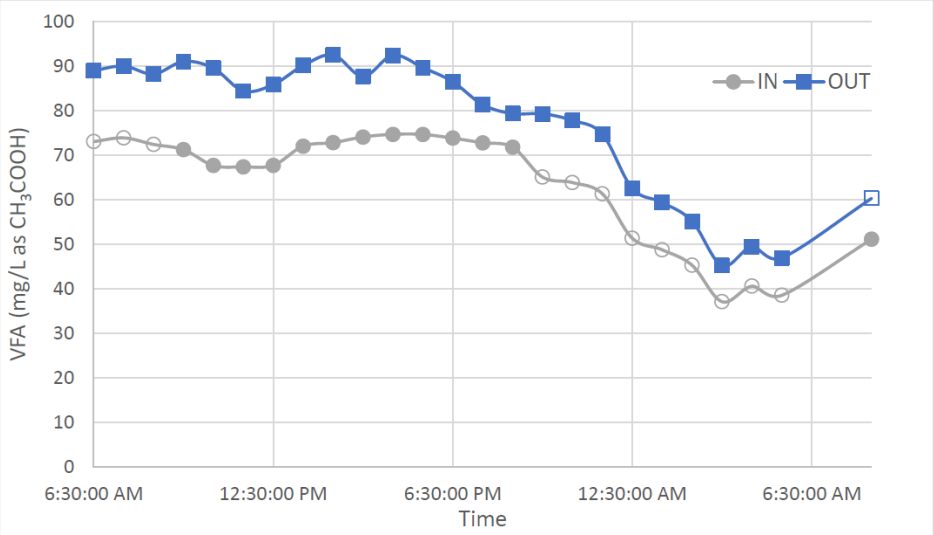

Figure 4.25: VFA concentration profile in the inlet and outlet of the primary clarifier on July 25^{th} and 26^{th} (Ponzelli, 2019)

One can see that the bicarbonate alkalinity drops by typically 5-30 mgHCO_3/L to a minimum of 100 mgHCO_3/L around 6 am (Figure 4.26). However, an overall VFA production of 8-20 mgCH_3COOH/L is observed in Figure 4.25.

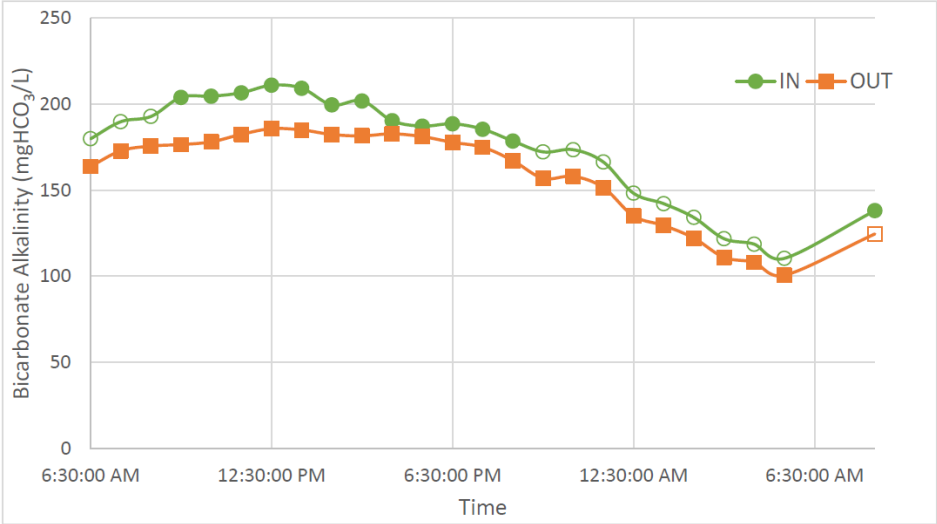

Figure 4.26: Bicarbonate alkalinity concentration profile in the inlet and outlet of the primary clarifier on July 25^{th} and 26^{th} (Ponzelli, 2019)

The required alkalinity indicated by Metcalf & Eddy (2014) for ensuring the nitrification process is 200 mg$CaCO_3$/L. To compensate for the potential lack, a basin of 50 L volume filled with a saturated concentration of sodium bicarbonate ($NaHCO_3$) was installed as shown in Figure 4.27. As such, the required alkalinity in the primary effluent could be guaranteed. To suggest this, a sampling campaign was performed on day 4 and day 5 of the dosing period (see the results in Figure 4.28 and Figure 4.29). One can see that the bicarbonate alkalinity concentration only started to improve on day 5 since a stirrer was only installed in the dosing basin on that day. This increasing pattern remained until the next days. On day 6 and day 7 of the measurement campaign, samples were grabbed at the dosing location in the primary clarifier (see the dosing location in Figure 4.27), titrated and analyzed. The measured bicarbonate concentrations for these samples were 52.4 gHCO_3/L on day 6 and 71.1 gHCO_3/L on day 7. The bicarbonate concentrations measured at the outlet of the primary clarifier thus increased to 342 mgHCO_3/L and 346 mgHCO_3/L in the composite samples of day 6 and 7 respectively. These measured concentration values for the bicarbonate alkalinity, as well as pH and VFA values for day 1 (before the addition of the stirrer), day 6 and day 7 (after the addition of the stirrer) are summarized in Table 4.8.

In the measurement campaign of the 6^{th} experimental scenario (see stage 6 in Table 4.7), the desired SRT in the sludge blanket was three days. To achieve this, the internal recirculation flowrate was set to 14 % of Q_{IN}, and the waste flowrate was reduced to 0.02 m^3/d. Besides, 100 mgHCO_3^-/L was dosed as sodium bicarbonate. In Figure 4.30, the TSS concentration measured along the sludge blanket height is shown for two consecutive days (day 7 and 8). These TSS concentration values are used for each conical segment to calculate the mass of the sludge stored in the clarifier. This information is then used to calculate the actual SRT of the

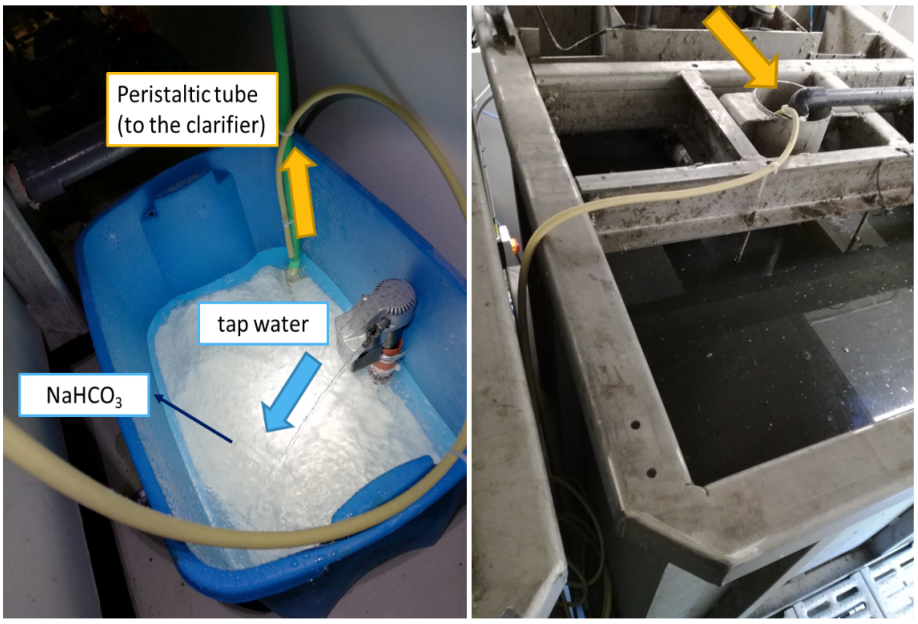

Figure 4.27: Alkalinity dosing set-up at the pilEAUte using a saturated sodium bicarbonate solution. Left: the dosing basin, right: dosing location on the primary clarifier

Table 4.8: pH, VFA and bicarbonate alkalinity values during the dosage of sodium bicarbonate ($NaHCO_3$) (Ponzelli, 2019)

Day	Primary inlet (storage tank)			Primary outlet			Added $NaHCO_3$ solution		
	pH	VFA (mg/L as CH_3COOH)	Alkalinity (mg/L as HCO_3)	pH	VFA (mg/L as CH_3COOH)	Alkalinity (mg/L as HCO_3)	pH	VFA (mg/L as CH_3COOH)	Alkalinity (mg/L as HCO_3)
Day1	7.31	77	252	7.34	82	234	7.86	0	823
Day6	6.96	64	174	7.16	79	342	8.67	0	52,403
Day7	6.97	60	154	7.21	91	346	8.76	0	71,127

clarifier during the experiment. This calculation produced an actual SRT of 1.18 days which is much shorter than the desired SRT of 3 days. This may be because the sludge wasting was decreased to increase SRT; however, the selected Q_W was not sufficient to increase SRT due to the presence of the recirculation flow, which increased the TSS concentration in the supernatant, leading to sludge loss in the effluent. Moreover, the floating sludge present at the surface during the experiment led to a further unplanned increase in effluent TSS concentration.

The profile measurements carried out for VFA, bicarbonate alkalinity, and pH for the same days are presented in Figure 4.31.

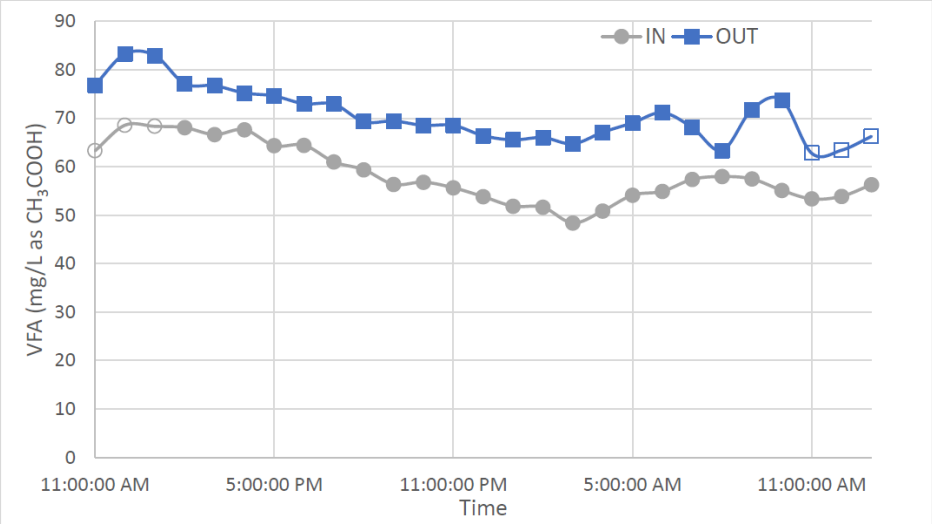

Figure 4.28: VFA concentration profile in the inlet and outlet of the primary clarifier on day 4 and 5 (Ponzelli, 2019)

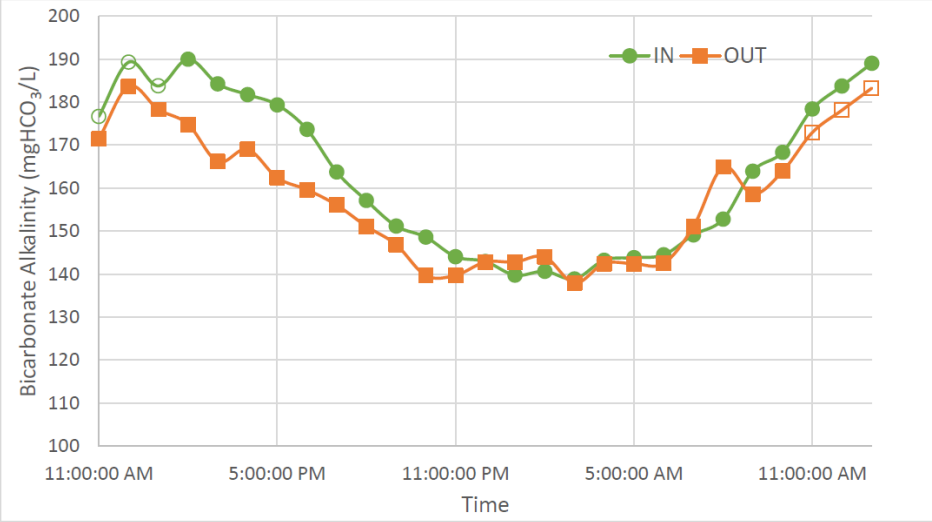

Figure 4.29: Bicarbonate alkalinity concentration profile in the inlet and outlet of the primary clarifier on day 4 and 5 (Ponzelli, 2019)

It can be seen that the VFA concentrations measured in the sludge blanket of 0.3 m for day 7 is higher than for day 8. This can be explained by the higher TSS values observed on this day (see Figure 4.30). Thus, a higher fermentation rate can be expected. This increase in the VFA concentration coincides with the pH drop below 6 on day 7.

The bicarbonate concentration measured along the sludge blanket on these two days is different. For instance, between the immersion height of 0.5 m to 0.3 m, the bicarbonate decreases with a larger gradient for day 7 than for day 8. One can also see that the VFA

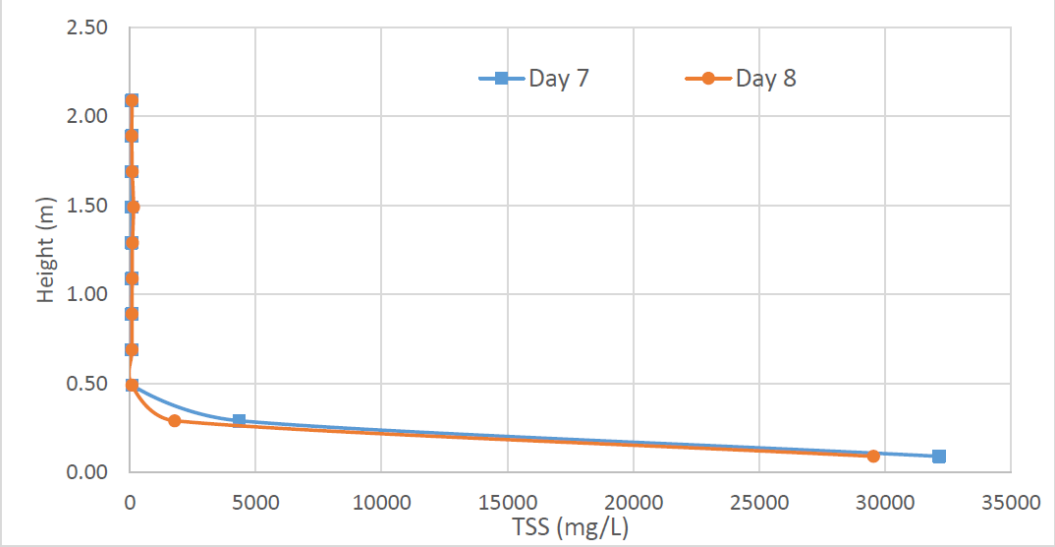

Figure 4.30: TSS concentration profile along the sludge blanket height in the pil*EAU*te's primary clarifier (experimental stage 6) (Ponzelli, 2019)

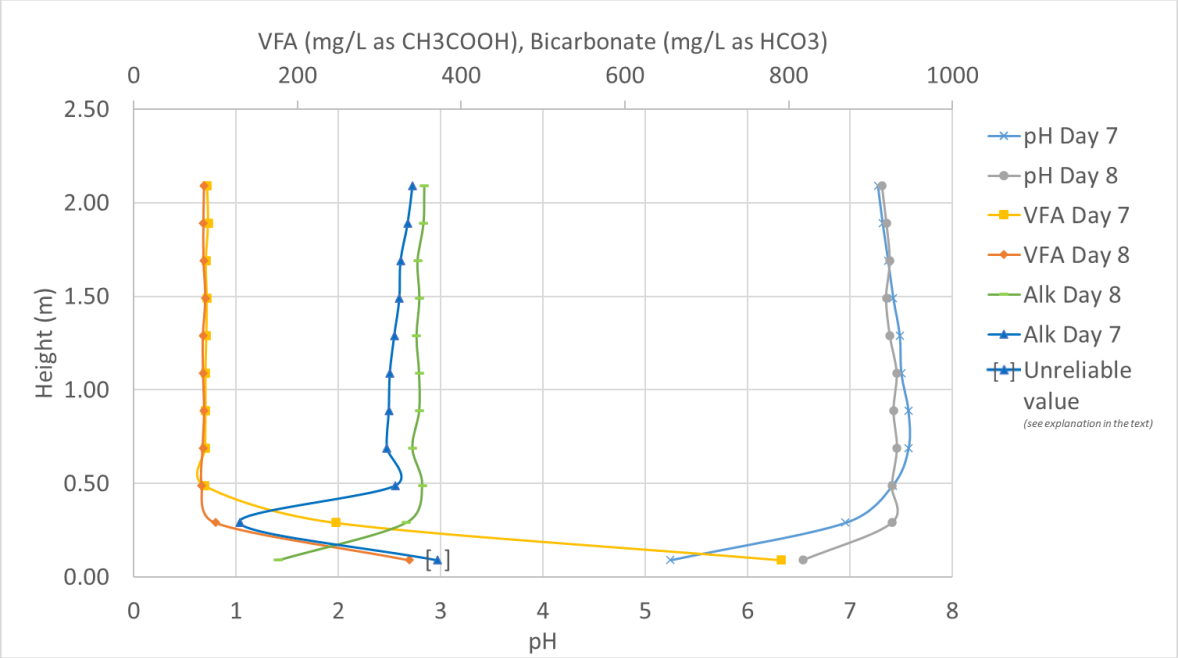

Figure 4.31: Bicarbonate, VFA, and pH profiles along the sludge blanket height in the pil*EAU*te's primary clarifier (experimental stage 6) (Ponzelli, 2019)

measured at an immersion height of 0.5 m is similar for the two sampling days. However, at 0.3 m the VFA measured for day 7 is approximately two times larger than the measured value for day 8. Consequently, the pH value drops with a larger gradient for day 7 than for day 8.

The VFA concentration rises further along the sludge blanket and reaches almost 800 mgCH_3COOH/L at the immersion height of 0.1 m for day 7. As a result, the pH drops sharply to almost pH 5. However, an unexpected increase is observed in the bicarbonate concentration at this height for day 7 (shown as the unreliable value in square brackets in Figure 4.31). In fact, the bicarbonate at this height is destroyed by the VFA produced, which explains the extreme reduction in pH. Because the titration experiment only started at a pH around 5 (more than 1 unit below the bicarbonate pK_a), no titration data were collected that contain information regarding the bicarbonate presence. Hence, the estimated concentration for bicarbonate in this sample is not reliable.

Although the pH drops as well for day 8 at the immersion height of 0.1 m with the production of VFA, it remains higher than on day 7, i.e. it stays in the neutral range (pH 6.5 at immersion height of 0.1 m). Thus, the bicarbonate buffer is still present in this sample. Therefore, the algorithm can estimate the bicarbonate concentration at this height.

4.4 AvN project case study

4.4.1 What is AvN?

In the previous section, the importance of sufficient organic carbon supply for efficient nitrogen removal through nitrification and denitrification was outlined. In addition, the application of the reactive primary settler as a mainline fermenter was introduced as an efficient method to enhance the bioavailability of organic carbon. In this section, the application of the nitrite shunt is discussed.

Achieving the nitrite shunt (ammonia to nitrite oxidation and nitrite denitrification) as an alternative to full conventional nitrification/denitrification over nitrate aims at reducing the needed aeration energy for partial nitrification, increasing the efficiency of COD use for denitrification while producing an effluent which is treatable through anaerobic ammonia oxidation (anammox) (Klaus, 2019).

The nitrite shunt can be achieved through the combination of partial nitritation and anaerobic ammonia oxidation (anammox, also known as deammonification). In the partial nitritation/anammox (PNA), reactions occur in two steps. In the first step, ammonia is partially oxidized to nitrite by ammonia-oxidizing bacteria (AOB), and nitrite oxidation to nitrate by nitrite-oxidizing bacteria (NOB) is avoided. In the second step, the remaining ammonia and the produced nitrite are converted to nitrogen gas and small amounts of nitrate by anaerobic ammonium oxidizing bacteria (AMX). To avoid the conversion of nitrite to nitrate in the first step, the NOB should be outselected, while maintaining high AOB growth rates. However, the outselection of NOB is hard to achieve in the main treatment stream since it requires either a high free ammonia (FA) concentration or a high temperature. Thus,

even though the PNA process is economical due to decreased aeration energy required and the avoided need for external carbon and alkalinity, in practice the NOB cannot be fully outselected in the mainstream treatment (Klaus, 2019).

However, nitrite can also be generated through partial denitrification of nitrate back to nitrite. This of course leads to consuming more aeration energy for the nitrite conversion to nitrate and then consuming carbon for generating nitrite by partial denitrification of nitrate followed by anammox (PDNA). Partial denitrification can be achieved using internally stored carbon (such as fermented VFA) or by the addition of supplemental carbon. This means that performing PDNA offers less aeration energy and external carbon savings than PNA, however PDNA has the advantage of not requiring the problematic outselection of NOB.

The partial denitrification and the anammox process can take place in a single reactor. For instance, in the work of Klaus (2019), these processes took place in an MBBR reactor which was installed in the A/B pilot located at the Hampton Roads Sanitation District (HRSD) Chesapeake-Elizabeth Plant located in Virginia Beach, VA (Figure 4.32). In this A/B pilot, the effluent from the A-stage clarifier fed the B-stage nitrogen removal reactor which consists of 5 tanks in series: one anaerobic selector and 4 intermittently aerated CSTRs, followed by a secondary clarifier. The effluent of the B-stage is then fed to an anoxic anammox MBBR which was fed glycerol to promote the partial denitrification combined with the anammox process in which the residual ammonia and the remaining nitrite are removed in a polishing step.

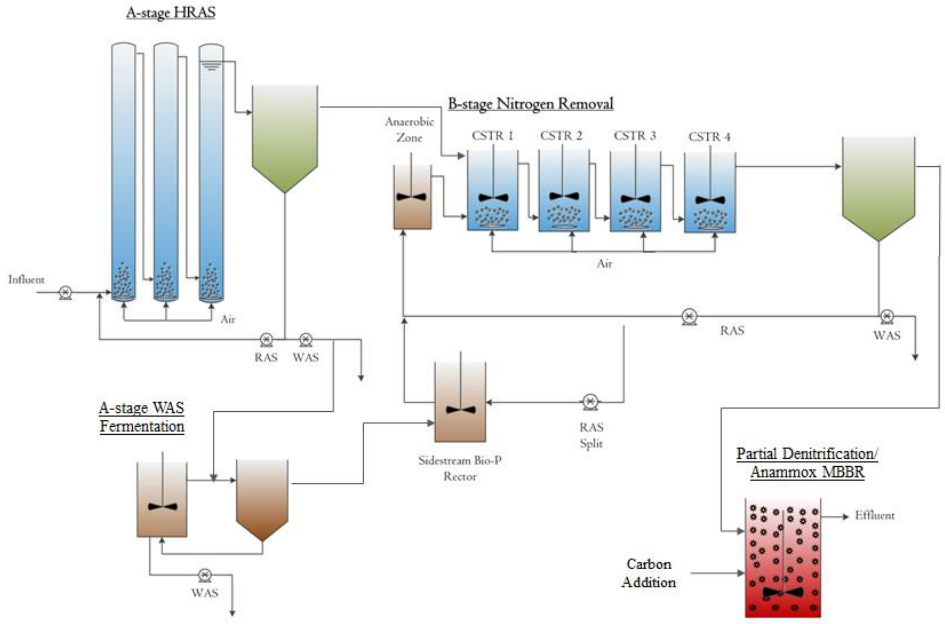

Figure 4.32: A/B pilot configuration

Several strategies have been developed to outselect NOB over AOB in mainstream biological removal processes relying on the nitrite shunt, including: maintaining a sufficiently high ammonia residual in the effluent, imposing transient anoxia, high DO concentrations (during alternating aeration), low DO concentrations (during continuous aeration), and aerobic solids retention time control (Regmi et al., 2014) (Klaus, 2019).

The Ammonia vs. NO_x (AvN) control strategy was developed by DC Water (Washington D.C., USA) and HRSD (Virginia, USA) to operationally achieve the nitrite shunt by adapting some fundamental concepts into an operational control algorithm (Regmi et al., 2014). In this strategy, the fraction of time during which the reactors are under aerobic conditions is controlled to obtain an effluent composition with an $NH_4 - N$ to $NO_x - N$ ($NO_2^- - N + NO_3^- - N$) ratio of approximately 1:1. Besides controlling the transient anoxia, the controller uses a non-limiting DO concentration, aerobic SRT control, and high residual ammonia concentrations to outselect NOB and promote AOB growth.

Equipped with two parallel N-removal activated sludge plants, the pil*EAU*te is particularly suited for comparing the performance of two versions of the AvN controller:

1. Standard AvN-controller based on the aerobic fraction of an intermittent aeration operation (alternating aeration), and
2. Modified AvN-controller based on varying (low) DO setpoints (continuous aeration).

The implementation of both AvN control strategies in the pil*EAU*te setup aims at learning about i) the feasibility of achieving partial nitritation in the biological nitrogen removal reactors, using the continuous aeration AvN control at lower SRT than typically required, and ii) improving the system capacity by decreasing the SRT and changing the AvN ratio set-point under the alternating aeration AvN controller. The two aeration control strategies and their perspectives are explained in the following section.

4.4.2 Implementation of AvN controllers in pil*EAU*te

As explained before in the Methodology chapter Section 3.1, the pil*EAU*te N-removing WRRF is running two identical process lanes ("pilot" and "copilot", see Figure 3.2) which are fed with the same wastewater. As one can see in Figure 4.33, originally the two lanes were working with two anoxic tanks (from the left, 1.08 m^3 and 1.46 m^3) and three aerobic tanks (1.08 m^3, 1.08 m^3, and 1.94 m^3) with a total volume of 6.64 m^3.

The AvN project is being evaluated on both pilot and co-pilot systems with similar sludge age and biomass concentration. The volume of the two lanes was reduced to 4.1 m^3 and the originally third basin was converted into the new anoxic tank, while the fourth and fifth basins remained as aerobic (Figure 4.34). As shown in Figure 4.35, the influent wastewater

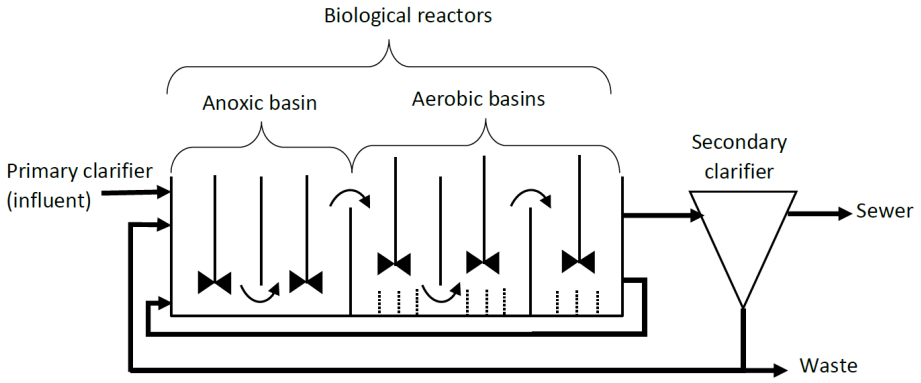

Figure 4.33: Original pilEAUte configuration

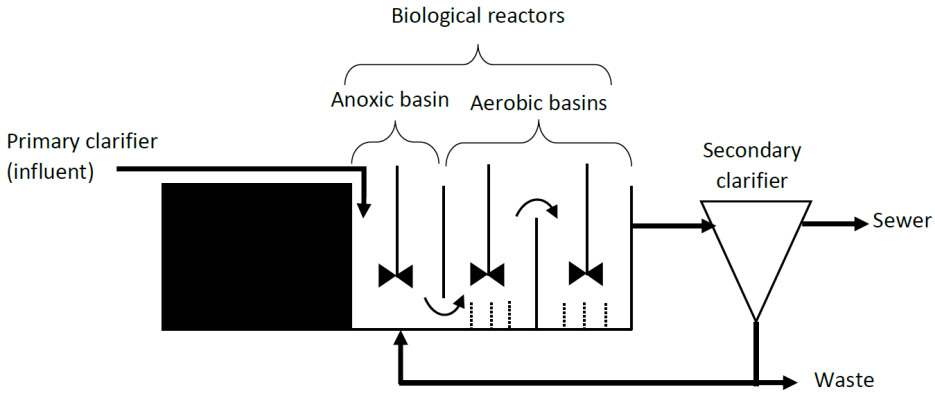

Figure 4.34: Modified pilEAUte plant for the AvN project

was by-passed directly to the third basin. Moreover, a new recycle line was installed to transfer the recycled sludge to the third basin. Sludge wasting was done discontinuously in the pilEAUte WRRF through a script in the SCADA computer.

The DO sensors are also monitored through the SCADA system. As mentioned earlier, the AvN controllers are based on two different aeration approaches, continuous and alternating. In the continuous aeration, the oxidation of ammonia to NO_x through nitrification is limited by low DO setpoints, thus pushing the system to an AvN ratio of 1. By lowering the DO setpoint, nitrification is increasingly limited leading to higher $NH_4 - N$ and lower $NO_x - N$ concentrations.

On the other hand, in the alternating aeration approach, the concentration of DO is changing via alternating aeration cycles. During the aerobic period of each cycle, the oxygen level provided allows oxidation of ammonia and thus nitrification. The aerobic period is then followed by an anoxic period where oxidation of ammonia is stopped, denitrification occurs, therefore changing the AvN ratio.

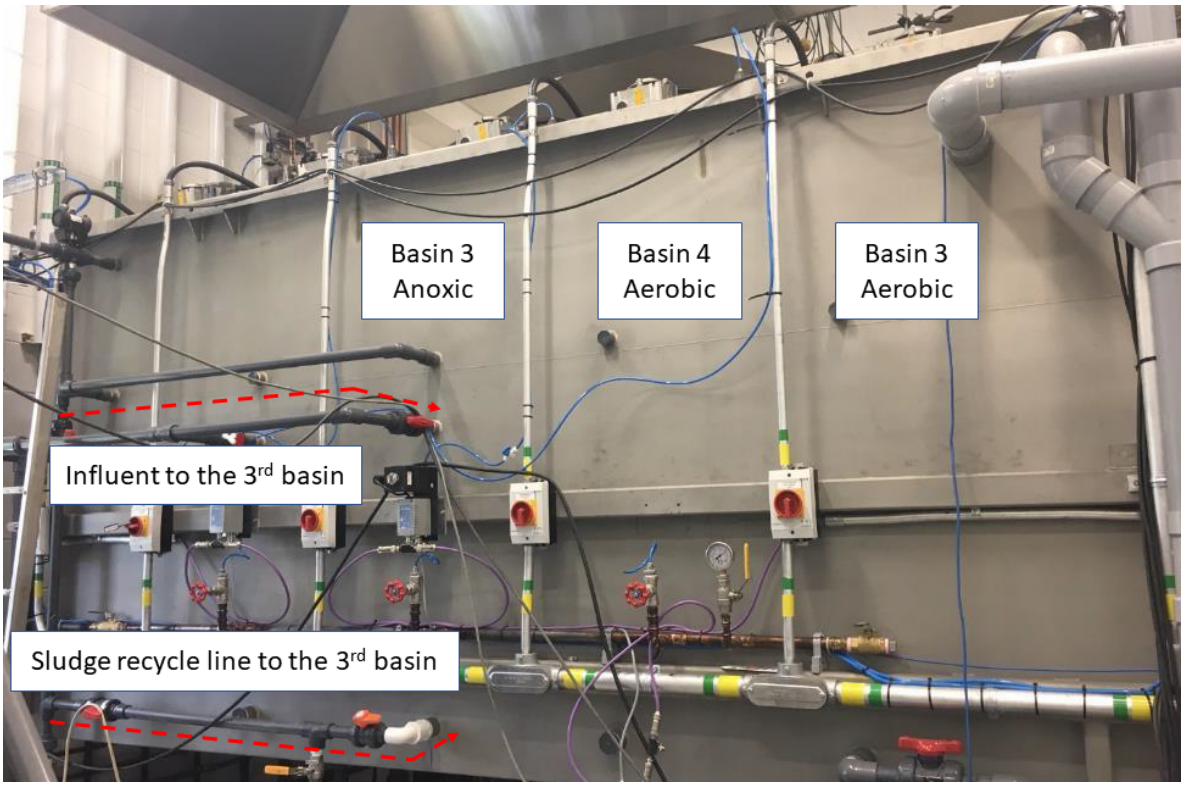

Figure 4.35: pil*EAU*te plant's new configuration: the influent feeding and the new installed sludge recycle line

The length of each cycle is fixed, but the aerated period and the remaining anoxic period in the cycle are regulated according to the AvN ratio obtained based on the online measurements of the $NH_4 - N$ and $NO_x - N$ concentrations. For this, the controllers first are fed with the relative sensor data of ammonia and nitrate at the effluent. Then, the controllers regulate the DO controllers by changing the aerobic cycle length in the alternating aeration. Figure 4.36 illustrates the implementation of the pil*EAU*te AvN controllers as modelled in the WEST modelling software (DHI, Denmark).

The continuous aeration control has been implemented in the co-pilot train providing low fixed dissolved oxygen concentration. The performance of the AvN controllers with respect to the dynamics in the online measurements of $NH_4 - N$ and $NO_3 - N$ for a period of four days is shown in Figure 4.37.

One can see that even relatively small changes in the airflow rate causing relatively small changes in the DO concentration, are strongly affecting the conversion of ammonia to nitrate and thus, the AvN ratio. Till then, on October 13^{th}, the DO concentration profile has fewer dynamics, and thus, the AvN ratio is getting very close to the AvN setpoint of one (in black with dash line). Note also that the dynamics in the influent ammonia after noon of October

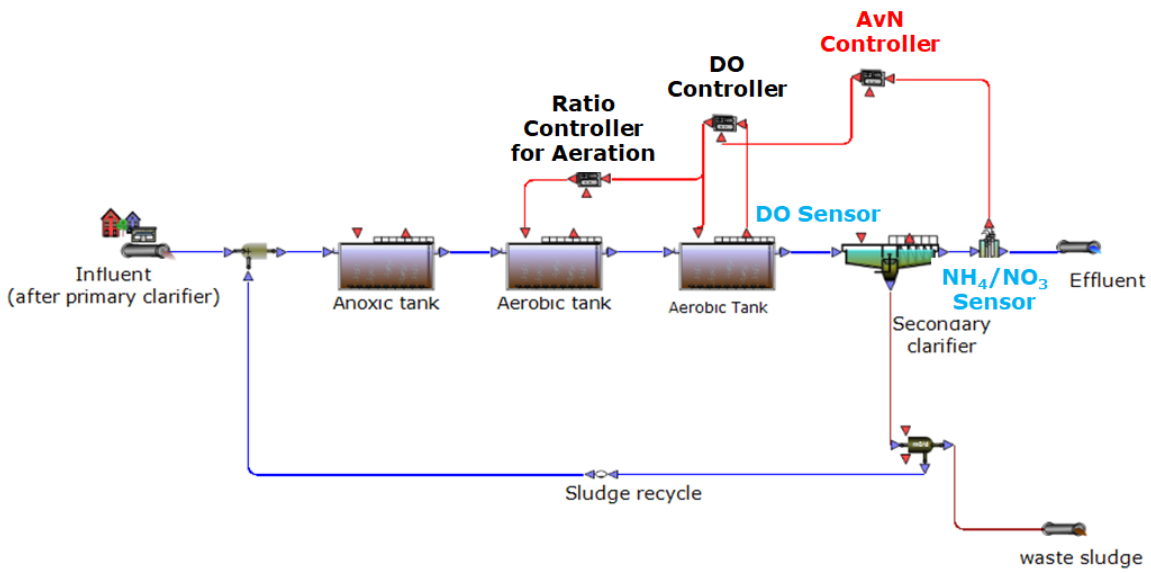

Figure 4.36: AvN, NH_4/NO_3-based aeration control implemented in pilEAUte, modelled in WEST (Kirim et al., 2019)

13^{th} challenges the AvN controller as can be seen in the effluent $NH_4 - N$, DO rise and imposed airflow to correct for the AvN deviation.

The alternating aeration control has been implemented in the pilot train. A lot of efforts went into tuning the controllers to avoid instability by adjusting the aeration fractions and validating/calibrating sensors. Comparing the AvN ratio graph with the Aeration graph shown in Figure 4.38, one can see that the performance of AvN in the pilot is a function of the aeration fraction. For instance, on October 13^{th}, the aeration fraction is gradually rising from 20 minutes to 40 minutes and the anoxic period is proportionally decreasing. As a result, the AvN ratio approaches the AvN setpoint of 1. This good performance occurs when the ammonia concentration in the influent is relatively stable. Therefore, changing the effluent ammonia concentration is done through manipulations of the aeration by the AvN controller.

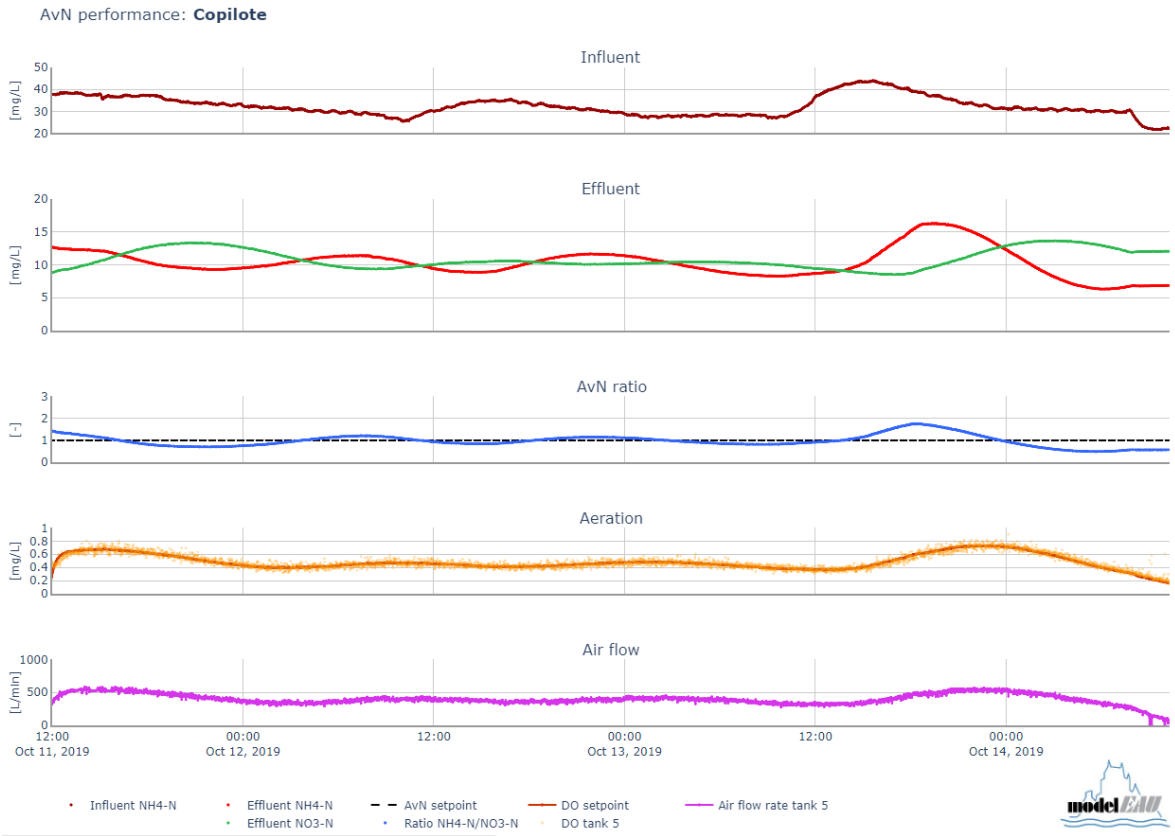

Figure 4.37: Continuous aeration AvN evaluation in the co-pilot train, DO setpoint adjustment

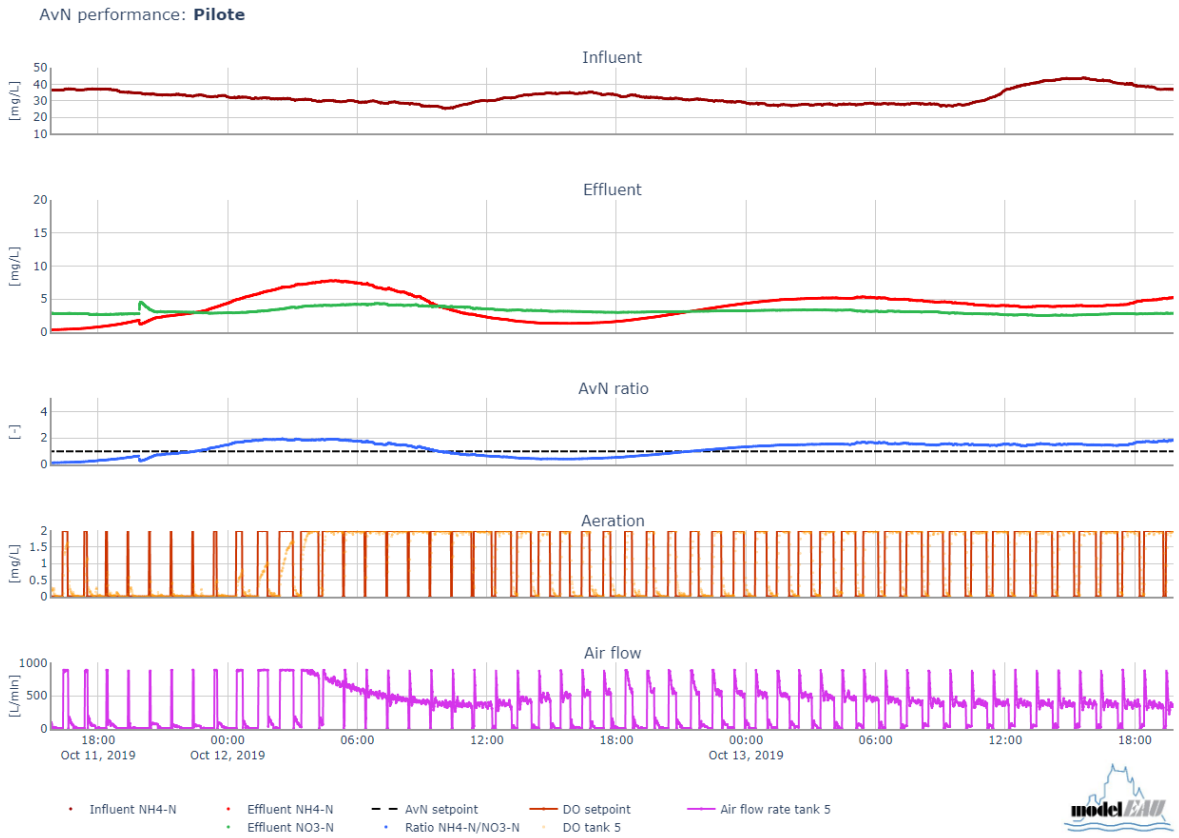

Figure 4.38: Alternating aeration AvN evaluation in the pilot train, aeration fraction adjustment

4.5 Application of titrimetric monitoring for influent and effluent characterization

So far, in this chapter, the purpose of the AvN control strategies and their implementation in pilEAUte have been discussed. Before running the controllers in the two trains, different operational conditions have been tried out, followed by an organized daily sampling campaign and offline measurements. During the sampling campaign that continued for about six months, composite samples from both inlet and outlets (from the two trains) were analyzed in the pilEAUte laboratory, using Hach chemical kits. In addition, titration analyses were performed to monitor the alkalinity and ammonia concentrations. In the next two sections, the results of the alkalinity monitoring upstream and downstream of the pilEAUte will be discussed. Moreover, the ammonia measured using titration analysis is compared with the chemical kits method.

4.5.1 Bicarbonate monitoring

Several operational conditions have been tried out before the installation of the controllers. Characterizing the inlet and outlet in terms of bicarbonate concentration contributes to the better understanding of the system and the ongoing biological processes. The samples for the bicarbonate monitoring were composite samples taken from the effluents of the primary and secondary clarifiers. The samples were down-titrated with H_2SO_4 (0.05 N), and the titration data were analyzed using the buffer capacity model. The bicarbonate and pH profiles obtained during four months of the measurement campaigns are presented in Figure 4.39 together with rainfall data (Environment Canada, 2019).

As shown in the figure, the average bicarbonate concentration in the influent is higher than 150 mgHCO_3/L, which is lower than the recommended bicarbonate alkalinity indicated by Metcalf & Eddy (2014) (244 mgHCO_3/L). Note that the concentration of bicarbonate does not represent bicarbonate alkalinity unless the pH of the solution is significantly higher than the pK_a value of bicarbonate (6.37 at $25°C$). The pH values recorded for the influent during the measurement campaign were higher than 7 (see the pH profile shown in Figure 4.39), and thus, the bicarbonate concentration measured with the buffer capacity model is relatively equivalent to the concentration of the bicarbonate alkalinity of the system. As such, the measured bicarbonate concentration in the influent can stand for its bicarbonate alkalinity. It was decided not to add any external source of alkalinity to the inlet, even though the amount present is lower than recommended, since the amount present is sufficient to cover the loss through nitrification. The daily rainfall data contribute to a better understanding of the influent bicarbonate alkalinity dynamics; for instance, on the days with intense rainfall, the bicarbonate concentration in the influent drops below 150 mg/L HCO_3^- because of dilution.

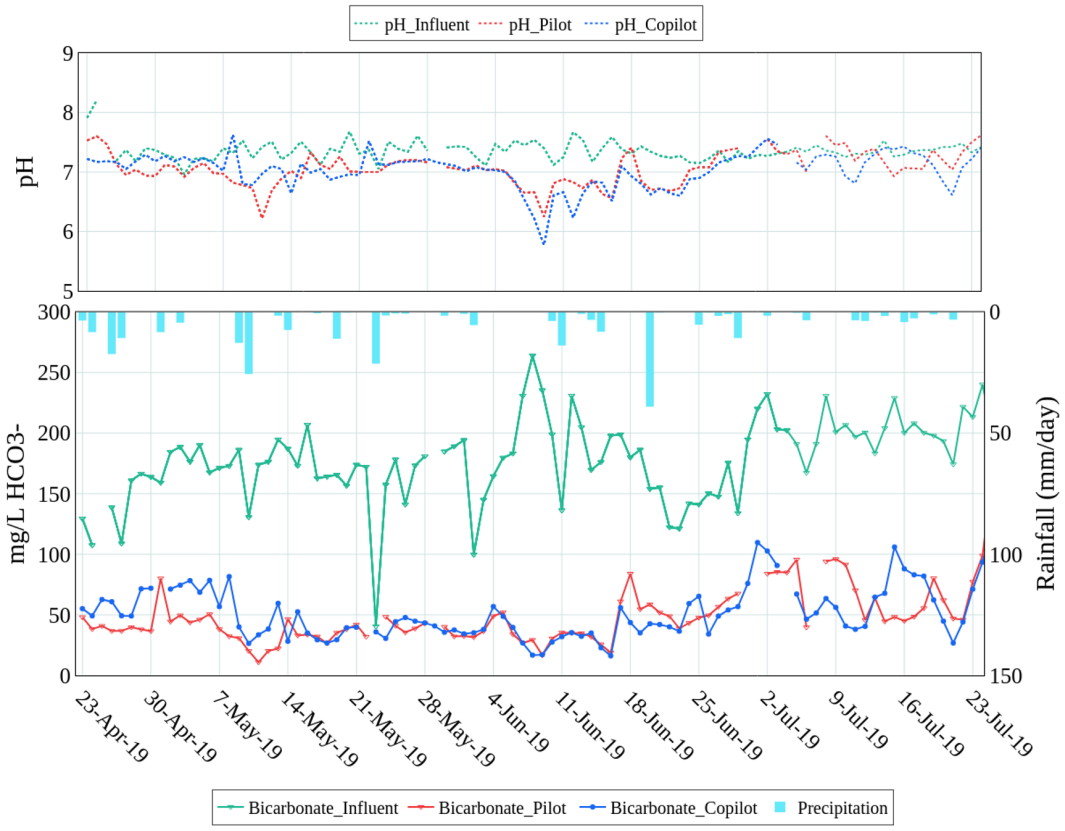

Figure 4.39: Primary and secondary effluent bicarbonate (bottom) and pH (top) profiles measured with titration along with daily rainfall data (bottom) (Environment Canada, 2019)

On the other hand, the bicarbonate concentration measured in the effluent of pilot and copilot varies between 50 to 100 mg/L HCO_3^-, which is almost half of the influent amount. As mentioned in the Literature Review (Section 1.3.2), the loss of two moles of alkalinity/mole of nitrogen during nitrification, is followed by one mole production of alkalinity/mole of nitrogen through denitrification. One mole overall loss of alkalinity thus results in the effluent. As such, the reduction of alkalinity in the effluent can be justified.

4.5.2 Ammonia monitoring

As shown in Figures 4.37 and 4.38, the influent ammonia concentration shows large dynamics. To evaluate the performances of the AvN controller in terms of nitrogen removal, it is important to validate the online influent $NH_4 - N$ concentration data. Also, since the AvN controller relies on online data captured in the effluent it is important to validate the online data collected in the effluent before adjusting the controllers.

The ammonia in the effluent of the primary clarifier is measured online by the ammo::lyser (see Section 3.1). In addition, Hach chemical kits are used to validate these online measurements on a regular basis. The ammonia concentration was also analyzed by up-titration tests followed

by data interpretation using the buffer capacity model to compare the results of this method with the chemical kits (hereafter termed lab ammonia) as shown in Figure 4.40.

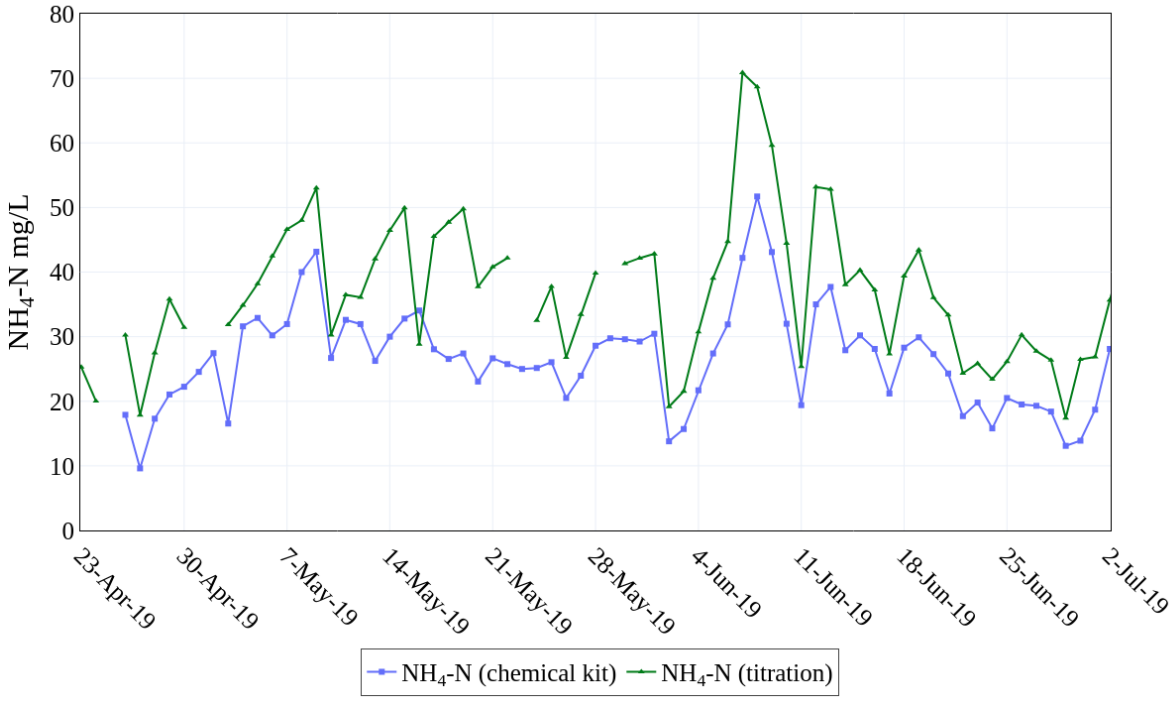

Figure 4.40: Influent ammonia concentrations measured by titration and chemical kit analyses

The two ammonia profiles exhibit very similar dynamics over time. However, the titration-based ammonia measurement always has a higher value than the lab ammonia concentration. The titration ammonia concentration differs from the lab data with an approximate ratio of 1.6. One explanation for this observation is that the titration data represent the sum of inorganic nitrogen (NH_3 + NH_4^+) and organic nitrogen, while the ammonia measured in the lab with the specific chemical kits only represents the inorganic nitrogen. Indeed, organic nitrogen may also exhibit a buffering capacity around a similar pK_a as NH_3/NH_4^+. An experiment was thus designed to validate this hypothesis as explained more in detail in the next section.

4.5.3 Glutamic acid experiment

Wastewater contains both organic and inorganic nitrogen. A portion of this organic nitrogen occurs in the form of amino acids since at least 20 standard amino acids are present in protein. These amino acids are used to synthesize proteins and are metabolized to urea which is then excreted with urine (Sakami and Harrington, 1963). The amino acids contain by definition amine (-NH_2) and carboxyl (-COOH) functional groups, along with a side chain (R group) specific to each amino acid (Figure 4.41).

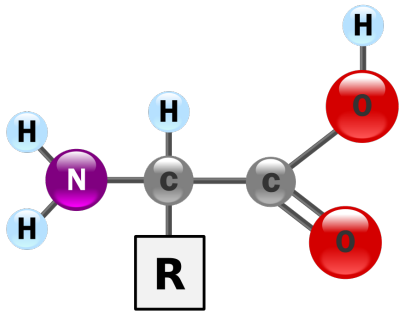

Figure 4.41: General structure of an amino acid (Mrabet, 2007)

Depending on the side chains (R), the amino acids can have different pK_a values. Glutamic acid, for instance, has three pK_a values of 2.16 (*alpha*-carboxylic acid group), 4.15 (*alpha*-carboxylic acid side chain group), and 9.58 (*alpha*-amino group) (Figure 4.42). The pK_a values of 9.58 and 4.15 which are related to the dissociation of the amine group and the side chain group, respectively, are very close to the pK_a values of ammonia (9.24) and VFA (4.76) buffers used in the buffer capacity model. As mentioned before, it may thus be that the buffer capacity model is considering both organic and inorganic nitrogen for calculating the concentrations of the ammonia buffer as reported in Figure 4.40. Thus, glutamic acid may be used as an example among the amino acids for validating this hypothesis.

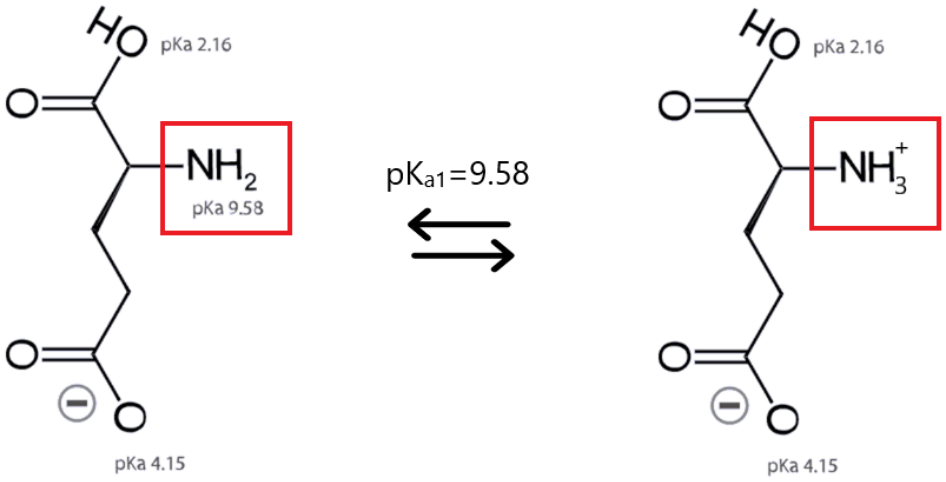

Figure 4.42: Glutamic acid chemical structure and its dissociation in water with regards to its amine group (Dancojocari, 2010)

The experiment designed to evaluate this hypothesis used two standard solutions, simulating the composition of the pil*EAU*te influent. Two standard solutions were prepared composed

of 1 mmol of ammonium, 0.5 mmol of VFA, and 3.5 mmol of bicarbonate. Further, for the purpose of the experiment, glutamic acid was introduced to only one of the standard solutions (Solution 2) in the same proportion as ammonium (1 mmol of N). NH_4Cl, $NaCH_3COOH$, $NaHCO_3$, and $C_5H_8NO_4Na$ were the salts used to represent respectively the ammonium, VFA, bicarbonate, and glutamic acid buffers. The concentration of these buffers in solution 1 and solution 2 is listed in Table 4.9.

Table 4.9: Composition of the two standard solutions made for the glutamic acid experiment

Composition	Solution concentrations		Unit
	Solution 1	Solution 2	
Ammonium (NH_4Cl)	0.957	0.958	mmol/L
Alkalinity ($NaHCO_3$)	3.452	3.535	mmol/L
VFA ($NaCH_3COOH$)	0.524	0.508	mmol/L
Glutamic acid ($C_5H_8NO_4Na$)	-	1.011	mmol/L

The two standard solutions were first down-titrated with H_2SO_4 (0.05 N), and then up-titrated with $NaOH$ (0.05 N) after being stripped from CO_2 and in presence of a nitrogen blanket during the up-titration. The titration data then were analyzed with the buffer capacity interpretation method and the estimated buffer concentrations are listed in Table 4.10. As shown in the table, the algorithm outputs the ammonium and/or glutamic acid as a TAN buffer. For instance, the TAN buffer modelled for solution 1 is only representing the ammonium buffer since the sample only contained ammonium initially. However, for solution 2 the modelled TAN buffer is the sum of ammonium and glutamic acid in the sample. In the same way, the VFA buffer modelled for solution 1 is only representing the VFA buffer, while in solution 2, the model estimation for the VFA buffer is due to both the VFA concentration and the dissociation of the *alpha*-carboxylic acid side chain group (pK_a=4.15). The bicarbonate buffer concentration presented in the Table 4.10 is estimated from the down-titration test, while the VFA and the TAN buffer result from the up-titration test.

Table 4.10: The results of the buffer capacity model for the glutamic acid experiment

Composition	BC model result solution concentrations		Unit
	Solution 1	Solution 2	
TAN (Ammonium + Glutamic acid)	1.117	2.005	mmol/L
Bicarbonate ($NaHCOO_3$)	3.492	3.036	mmol/L
VFA ($NaCH_3COOH$)	0.615	1.488	mmol/L

The bicarbonate concentrations reported in the Table 4.10 are obtained from down-titration tests (see the buffer capacity curves in Figure 4.43 and Figure 4.44). It can be seen that the model estimation for the bicarbonate concentration in solution 1 is very close to its actual concentration in the standard solution (3.452 mmol$NaHCO_3$/L). However, the estimated

bicarbonate concentration in solution 2 is lower than its concentration in the standard solution (3.535 mmol$NaHCO_3$/L). This may be explained by the presence of the glutamic acid, which is buffering around its pK_a of 4.15. Since more active buffers are present in solution 2, more acid is consumed to destroy these buffers and therefore, titration process takes longer. Since the sample is not covered with a nitrogen blanket during down-titration tests, CO_2 can volatilize during the titration. This possibility is even higher when the titration processing time is longer, and thus, a reduction in bicarbonate concentration can be observed.

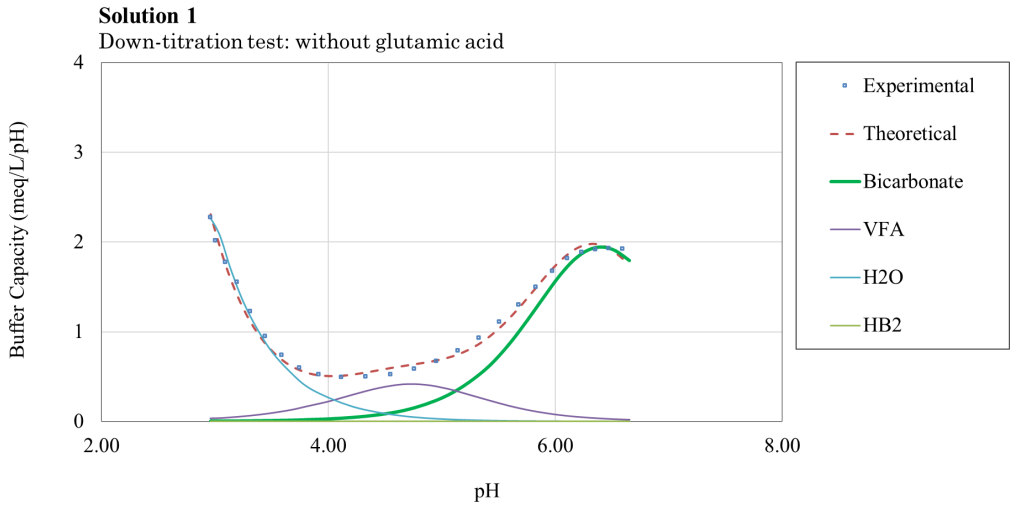

Figure 4.43: Down-titration buffer capacity curve for 1 L of an aqueous system (solution 1) comprised of 1 mmolNH_4Cl/L, 0.5 mmol$NaCH_3COOH$/L, 3.5 mmol$NaHCO_3$/L

As presented in the Table 4.10, the estimated TAN concentration in solution 2 has increased to 2.005 mmol/L and this increase can also be noticed when comparing the buffer capacity of TAN at its peak location on the two buffer capacity curves (Figure 4.45 and Figure 4.46). Moreover, the peak location estimated for the TAN buffer in solution 2 is shifted more to the right in Figure 4.46 (estimated pH=9.77), and thus, the pK_a corresponds to a higher value to cover for both ammonia and glutamic acid pK_a values. Consequently, the difference observed in the concentration of the TAN buffer corresponds to the 1 mmol glutamic acid added in solution 2.

As presented in the Table 4.10, the estimated TAN concentartion in solution 2 has increased to 2.005 mmol/L and this increase can be as well noticed comparing the buffer capacity of TAN at its peak location on the two buffer capacity curves (Figure 4.45 and Figure 4.46). Moreover, the peak location estimated for the "TAN buffer" in solution 2 is shifted more to the right in Figure 4.46 (pH=9.77), and thus, the pK_a corresponds to a higher value to cover for both ammonia and glutamic acid pK_a values. Consequently, the difference observed in the

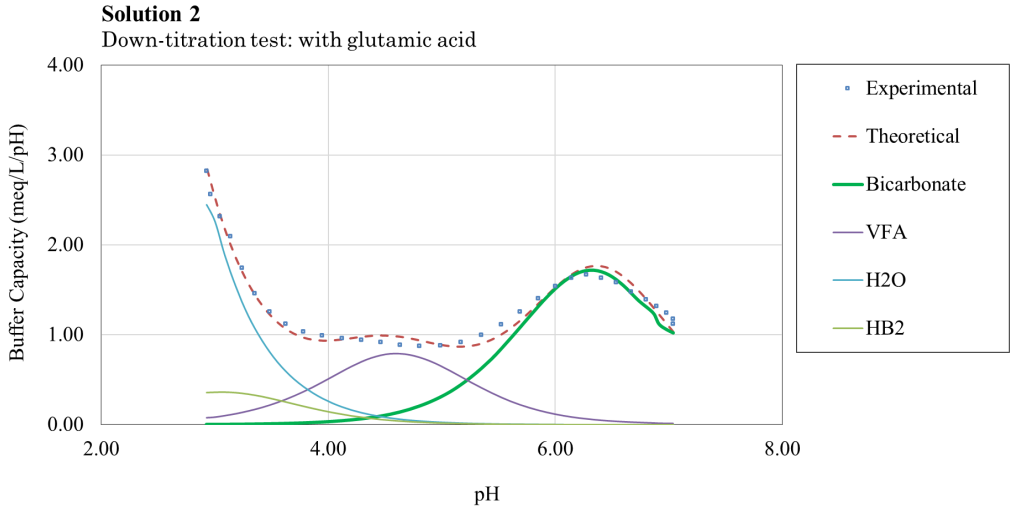

Figure 4.44: Down-titration buffer capacity curve for 1 L of an aqueous system (solution 2) comprised of 1 mmolNH_4Cl/L, 0.5 mmol$NaCH_3COOH$/L, 3.5 mmol$NaHCO_3$/L, and 1 mmol$C_5H_8NO_4Na$/L

concentration of the TAN buffer corresponds to the 1 mmol glutamic acid added in solution 2.

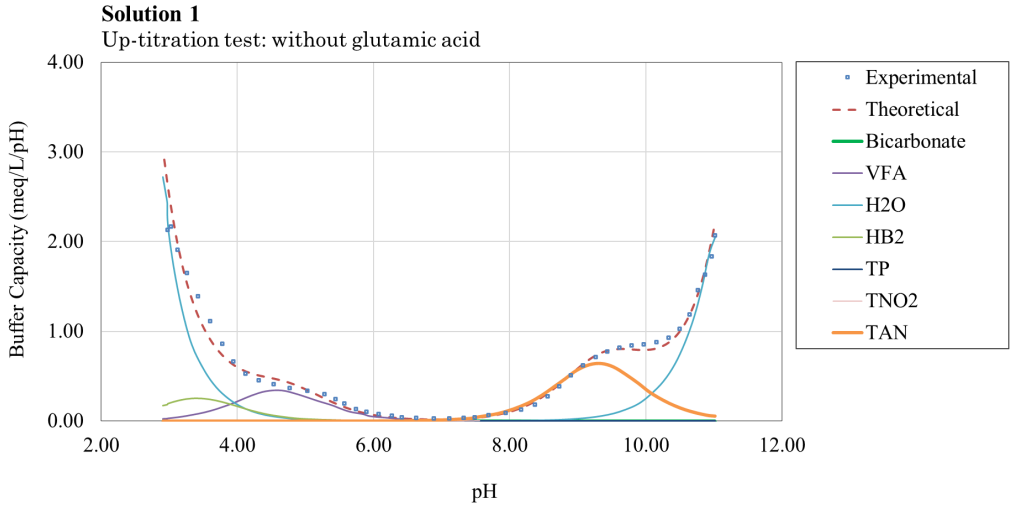

Figure 4.45: Up-titration buffer capacity curve for 1 L of an aqueous system (solution 1) comprised of 1 mmolNH_4Cl/L, 0.5 mmol$NaCH_3COOH$/L, 3.5 mmol$NaHCO_3$/L

Regarding VFA, it was found that the pKa value estimated for the VFA buffer in solution 2 is around 4.36, which is lower than the actual pKa of VFA (4.76). Also, the estimated VFA concentration in solution 2 is larger than the estimated value in solution 1. In fact

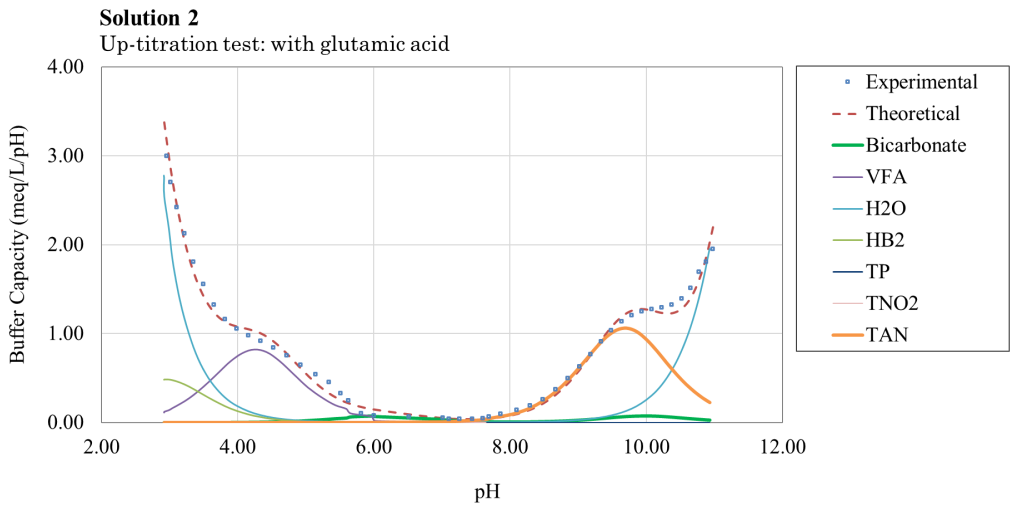

Figure 4.46: Up-titration buffer capacity curve for 1 L of an aqueous system (solution 2) comprised of 1 mmolNH_4Cl/L, 0.5 mmol$NaCH_3COOH$/L, 3.5 mmol$NaHCO_3$/L, and 1 mmol$C_5H_8NO_4Na$/L

the difference corresponds to the amount of glutamic acid added in solution 2. Thus, it can be concluded that the algorithm includes the acidic side chain of glutamic acid into the calculations, and treats it as VFA.

From this experiment and the results obtained, it can be concluded that both inorganic nitrogen and the organic nitrogen fraction, which will eventually be converted into ammoniacal nitrogen by hydrolysis and ammonification, are measurable using titrimetry.

Chapter 5

Conclusions and perspectives

In this MSc thesis, the pil*EAU*te plant's Titrino device was used for the purpose of chemical characterization of raw and treated wastewater. To fully take advantage of this device, multiple measurement methods were tested and mathematical tools were developed. With this in mind, in the current chapter, the achieved objectives are highlighted and conclusions are drawn from the findings. This will be followed by a discussion on further steps to improve and expand the application of the Titrino device.

5.1 Conclusions

The titrimetric analysis is comprised of two main steps: (i) performing the titration experiment in the pil*EAU*te's laboratory, and (ii) analyzing the titration data using mathematical models as computing tools. The buffer capacity model and PHREEQC were the two analysis tools applied in this study for estimating the wastewater composition, which together with the lab procedures, were developed in this study. Based on the results of this work, the following conclusions can be drawn

1. **Titrimetric monitoring was successfully performed under different operational conditions**: Titration tests were performed during different sampling campaigns performed on the pil*EAU*te, aimed at monitoring the influent and effluent wastewater compositions. Within these campaigns in which different operational conditions were tested, titration analyses helped to monitor the concentration of buffers such as bicarbonate alkalinity, VFA and ammonium. For instance, when the operational conditions were changed during the implementation of the AvN controllers in the pil*EAU*te, monitoring the alkalinity was crucial. For instance, in Figure 4.39, the influent and effluent bicarbonate alkalinity was monitored by titrimetric analysis. As demonstrated, the influent alkalinity was sufficient for successful denitrification in the biological reactors.

2. **An alkalinity dosage system designed and implemented in the pil*EAU*te, allows maintaining pH and reactions**: The bicarbonate alkalinity may vary in the influent stream together with variations in pH. During the implementation of the reactive primary settler, the bicarbonate alkalinity dropped due to the desired VFA production, and caused a significant decrease of the influent pH. Therefore, an external source of alkalinity was needed to ensure alkalinity destroying nitrification. To compensate for this potential lack, an alkalinity dosing system composed of a 50 L basin filled with sodium bicarbonate ($NaHCO_3$) to generate a saturated alkalinity solution, and a peristaltic tube pump was used to dose the prepared concentration of bicarbonate alkalinity to the inlet. Given the good performance of the dosage system, the required effluent alkalinity could be guaranteed.

3. **The buffer capacity model can reliably measure alkalinity, VFA and more**: The buffer capacity model, which is an Excel-based tool, was taken advantage of in this study. In this model, the capacity of each buffer is calculated using a set of linear algebraic equations. Besides, within this model, simple acid-base chemical equilibria are included and the concentration of different buffers can be estimated. Therefore, this study benefited from the simplicity of this method as it allowed to have a better understanding of the buffering systems in a short period of time. Within this thesis, the concentrations of bicarbonate alkalinity, VFA, and ammonium buffers were successfully calculated.

4. **A titration simulation model was successfully built in the PHREEQCXCEL software**: Application of PHREEQC as an advanced modelling tool permits solving the non-linear equilibrium equations for speciation calculations and, in general, to have a complete description of the equilibrium reactions of the chemical system under study. PHREEQC was used in Excel through the PHREEQXCEL interface, in which the acid-base reactions and the titration process were modelled. PHREEQXCEL was then successfully extended with an open-source solver (OpenSolver) which allows solving large models in a short processing time.

5. **Nitrogen blanketing and CO_2 stripping are necessary to perform reliable titration**: To improve the accuracy of the model in calculating the concentrations of the buffers, laboratory procedures had to be modified. Stripping the CO_2 content of acidified samples, and nitrogen blanketing the samples during subsequent up-titration, were the two modifications performed. Addition of the stripping step before up-titrating the samples was efficient in eliminating the bicarbonate alkalinity (a 87 % decrease was reported in 4.1). This elimination of the interfering bicarbonate buffer led to better model estimation for other buffers such as ammonium or VFA. To prevent further absorption of CO_2 during the up-titration, a blanket of nitrogen gas was applied to cover

the surface of the samples. The interference of bicarbonate buffer decreased significantly after applying the two-step modifications (4.2).

All these highlighted conclusions together tell a story of the successful application of titrimetric monitoring of the wastewater in the pil*EAU*te plant. Through this study, the experimental work could be improved significantly, allowing to make the model calculations more precise for estimating the wastewater composition from titration data. The methods were applied to two case studies with industrial potential and their efficiency in estimating wastewater composition reliably was evaluated and demonstrated to have increased substantially.

5.2 Paths for improvement

The experimental improvements and the two modelling tools developed contributed a lot to increasing the usefulness of the titrimetric analysis. However, there are further developments that could further increase the reliability of titration data and the modelling tools, and thus extend the application range of this cost-effective method. The following outlines some of these modifications:

1. **Automate the titration analysis**: Influent or effluent samples in this study were taken from the pil*EAU*te plant and titrated in the laboratory. The titration process was not performed in situ, and therefore the processing time was long. The titration data were produced as titration curves and further interpretation was needed to obtain the concentration of the buffers. As a result, it was not feasible to monitor the behaviour of the wastewater in terms of the buffers present and thus, performing any control actions was delayed or in some cases, no longer required.

   Automating the titration process might not seem to be a cost-effective alternative, but it can be important when necessary control actions are to be taken at critical times. The current measurement method used in this study can obtain the concentrations of bicarbonate alkalinity, VFA, ammonium, and, in principle, phosphate buffers. It can be beneficial to the modeller if these data can be collected in situ and within a short processing time after sampling. Therefore, designing an on-line titrimetric analyzer can be a path for improvement. At commercial scale, the AnaSense (De Neve and Lievens, 2004) is an example of an on-line titrimetric analyzer that was developed in collaboration with Ghent University in the former team of Vanrolleghem (Zaher et al., 2004), and designed specifically for monitoring anaerobic digesters. This analyzer has the potential of implementing the interpretation methods developed in this thesis, allowing for new control strategies under typical operating conditions. Such an analyzer, if applied at the pil*EAU*te plant, could reduce the experimental and modelling workload if it is extended with built-in analysis software.

2. **Using a titrimetric sensor's online data for a model-based control system**: The on-line data extracted from the titrimetric sensor could also be used as input to a model embedded in a control system, to calculate a control variable. For instance, bicarbonate alkalinity is a parameter that affects the nitrification reaction rate. If this parameter could be obtained on-line after a small processing time, the AvN control could be adjusted and thus, the aeration control system. Another model-based control system that could be designed in the pil*EAU*te, after being instrumented with an on-line titrimetric sensor, could be an automatic alkalinity dosage system. With the same procedure as described for the AvN control above, on-line bicarbonate alkalinity data could be used to regulate a pump to dose bicarbonate alkalinity to the inlet in case of insufficiency. In other words, the bicarbonate sensor data can be used in a control law that can output the amount of bicarbonate to be dosed as a control variable.

   The dosing model can also be extended to a chemical dosing model control system. For instance, dosing coagulants such as iron or other metal coagulants can contribute to the chemical removal of phosphorus. Given that on-line data of phosphorus can be obtained from the titrimetric sensor, a dosing chemical system can be developed to dose the coagulant aiming for precipitating the phosphorus components and enhancing the primary treatment to reduce suspended solids and organic loads from the primary clarifier.

   Modelling software like WEST (DHI, Hörsholm, Denmark) that has a library of complex models containing physical, biological, and chemical transformations, could be fed with the titrimetric on-line data as input to create a digital twin of the system. Such digital twin consists of a general model for the entire plant, coupled with real time streams of data coming from the plant itself. This model can then be used to predict the future state of the plant. These predictions can, in turn, be used to select relevant control actions. Thus, titrimetric sensor data such as bicarbonate alkalinity and VFA could be considered as new inputs and will thus affect the modelling results and control actions taken by the twin.

3. **Transfer data between PHREEQC and a modelling software such as WEST through model coupling**: Although data extracted from an on-line titrimetric analyzer is more relevant and can be produced faster, allowing for fast control action, off-line titration data could still be applicable in a model-based system. The speciation calculation output obtained by PHREEQC in this work can be transferred to WEST or other modelling software through model coupling. The coupling of the PHREEQC chemical speciation model to the models already implemented in WEST, could result in extending the WEST model library with new model variables and thus, can improve the simulation results. Transfer of data between PHREEQC and Tornado (the WEST back-end) through tight model coupling has already been tested by (Vaneeckhaute,

2015). In her PhD study, a digester chemical speciation model in PHREEQC was coupled to the kinetic mass balance model of the different components in Tornado, aiming for accurate chemical speciation at minimal computational effort.

Together, these improvements can make titrimetry a much more reliable measurement method, in addition to expanding its application and usefulness in characterizing and further monitoring wastewater systems. Regardless of whether these features are implemented, however, the work performed in this MSc study not only paves the way to including titrimetry to the pil*EAU*te's array of water quality measurements but also demonstrates that it is a reliable method to monitor key wastewater components in nitrogen and phosphorus removal.

Bibliography

Alferes, J., P. Poirier, C. Lamaire-Chad, A. K. Sharma, P. S. Mikkelsen, and P. A. Vanrolleghem (2013). Data quality assurance in monitoring of wastewater quality: Univariate on-line and off-line methods. In *Proceedings 11th IWA Conference on Instrumentation, Control and Automation*, Narbonne, France, pp. 4.

Alferes, J. and P. A. Vanrolleghem (2016). Efficient automated quality assessment: Dealing with faulty on-line water quality sensors. *AI Communications 29*(6), 701–709.

Amritkar, A., E. de Sturler, K. Świrydowicz, D. Tafti, and K. Ahuja (2015). Recycling Krylov subspaces for CFD applications and a new hybrid recycling solver. *Journal of Computational Physics 303*, 222–237.

Anderson, G. K. and G. Yang (1992). Determination of bicarbonate and total volatile acid concentration in anaerobic digesters using a simple titration. *Water Environment Research 64*(1), 53–59.

Appels, L., J. Baeyens, J. Degrève, and R. Dewil (2008). Principles and potential of the anaerobic digestion of waste-activated sludge. *Progress in Energy and Combustion Science 34*(6), 755–781.

Appl, M. (1982). The Haber–Bosch process and the development of chemical engineering. In W. F. Furter and A. C. Society (Eds.), *A Century of Chemical Engineering* (Illustrated ed.)., pp. 29–54. NY, USA: Plenum Press.

Bachis, G., T. Maruéjouls, S. Tik, Y. Amerlinck, H. Melcer, I. Nopens, P. Lessard, and P. A. Vanrolleghem (2015). Modelling and characterization of primary settlers in view of whole plant and resource recovery modelling. *Water Science and Technology 72*(12), 2251–2261.

Benefield, L. D., J. F. Judkins, and B. L. Weand (1982). *Process Chemistry for Water and Wastewater Treatment*. New Jersey, USA: Prentice-Hall.

Bouvier, J. C., J. P. Steyer, and J. P. Delgenès (2002). On-line titrimetric sensor for the control of VFA and/or alkalinity in anareobic digestion processes treating industrial vinasses. In *Proceedings IWA VII Latin American Workshop and Symposium on Anaerobic Digestion*, Institut National de la Recherche Agronomique, Narbonne, France.

Chapra, S. C. (2008). *Surface Water-Quality Modeling*. Long Grove, IL, USA: Waveland Press.

Charnier, C., E. Latrille, L. Lardon, J. Miroux, and J. P. Steyer (2016). Combining pH and electrical conductivity measurements to improve titrimetric methods to determine ammonia nitrogen, volatile fatty acids and inorganic carbon concentrations. *Water Research 95*, 268–279.

Dancojocari (2010). The 21 proteinogenic α-amino acids found in eukaryotes, grouped according to their side chains' pKa values and charges carried at physiological pH (7.4). https://en.wikipedia.org/wiki/Amino_acid#cite_ref-35. Accessed on 2020-01-17.

de Moel, P. J., A. W. C. Van der Helm, M. Van Rijn, J. C. Van Dijk, and W. G. J. Van der Meer (2013). Assessment of calculation methods for calcium carbonate saturation in drinking water for DIN 38404-10 compliance. *Drinking Water Engineering and Science 6*, 115–124.

de Moel, P. J., J. C. van Dijk, and W. G. J. van der Meer (2015). *Aquatic Chemistry for Engineers*, Volume 1. Delft, Netherlands: TU Delft Univeristy of Technology.

De Neve, K. and K. Lievens (2004). On-line analyser solves monitoring problem in bio-digester. *Water and Wastewater International 19*, 6.

Di Pinto, A. C., N. Limoni, R. Passino, A. Rozzi, and M. C. Tomei (1990). Anaerobic process control by automated bicarbonate monitoring. In R. Briggs (Ed.), *Instrumentation, Control and Automation of Water and Wastewater Treatment and Transport Systems*, pp. 51–58. Yokohama and Kyoto, Japan: Pergamon.

Environment Canada (2019). Historical Climate Data. https://climate.weather.gc.ca/historical_data/search_historic_data_e.html. Accessed on 2020-04-29.

Fylstra, D. H., L. S. Lasdon, J. Watson, and A. D. Waren (1998). Design and use of the Microsoft Excel Solver. *Interfaces 28*, 29–55.

Gernaey, K., P. A. Vanrolleghem, and P. Lessard (2001). Modeling of a reactive primary clarifier. *Water Science and Technology 43*(7), 73–81.

Google Inc. (2019). Université Laval Localization.

Guo, L., Z. Scott, E. Jang, J. Walton, E. Elbeshbishy, D. Santoro, and P. A. Vanrolleghem (2019). Using modelling and field testing to learn about bulk-biofilm interactions in reactive sewer systems. In *Proceedings 9th International Conference on Sewer Processes & Networks*, Aalborg, Denmark, pp. 11.

HACH (2008). DR5000 User Manual.

ISO (2003). ISO 15839:2003.

Jin, X., X. Li, N. Zhao, I. Angelidaki, and Y. Zhang (2017). Bio-electrolytic sensor for rapid monitoring of volatile fatty acids in anaerobic digestion process. *Water Research 111*, 74–80.

Kapp, H. (1984). Schlammfaulung mit hohem Feststoffgehalt. In *Stuttgarter Berichte zur Siedlungswasserwirtschaft*, Volume 86, pp. 300. OldenbourgVerlag, München, Germany: Kommissionsverlag Oldenbourg.

Kirim, G., R. Phillippe, and P. A. Vanrolleghem (2019). AvN Control Strategy Testing at Université Laval. Technical Report, Université Laval, Quebec, Canada.

Klaus, S. (2019). *Intensification of Biological Nutrient Removal Processes*. PhD thesis, Virginia Polytechnic Institute and State University, Blacksburg, Virginia.

Lee, W. S., A. S. M. Chua, H. K. Yeoh, and G. C. Ngoh (2014). A review of the production and applications of waste-derived volatile fatty acids. *Chemical Engineering Journal 235*, 83–99.

Lessard, P. and M. B. Beck (1988). Dynamic modeling of primary sedimentation. *Journal of Environmental Engineering 114*(4), 753–769.

Mason, A. J. (2012). OpenSolver - An Open source add-in to solve linear and integer progammes in Excel. In D. Klatte, H. J. Lüthi, and K. Schmedders (Eds.), *Operations Research Proceedings (GOR (Gesellschaft Für Operations Research e.V.))*, pp. 401–406. Berlin, Heidelberg, Germany: Springer.

Metcalf & Eddy (2014). *Wastewater Engineering: Treatment and Reuse*. NY, USA: McGraw Hill Education.

Metrohm (2002). 794 Basic Titrino (Instructions for Use).

Metrohm (2007). 789 Robotic Sample Processor XL 778 Sample Processor (Instructions for Use).

modelEAU (2012). Fractionnement des Acides Gras Volatils par Titrage à la Baisse. Standard Operation Prodedure (SOP) no. 38, Université Laval, Québec, Canada.

Moosbrugger, R. E., M. C. Wentzel, G. A. Ekama, and G. v. R. Marais (1993). A 5 pH point titration method for determining the carbonate and SCFA weak acid/bases in anaerobic systems. *Water Science and Technology 28*(2), 237–245.

Mrabet, Y. (2007). General structure of an amino acid. https://en.wikipedia.org/wiki/Amino_acid. Accessed on 2020-01-17.

Nopens, I., C. Capalozza, and P. A. Vanrolleghem (2001). Stability Analysis of a Synthetic Municipal Wastewater. Technical Report, Department of Applied Mathematics, Biometrics and Process Control, Ghent University, Ghent, Belgium.

Parkhurst, D. L. and C. A. J. Appelo (2013). Description of input and examples for PHREEQC version 3—A computer program for speciation, batch-reaction, one-dimensional transport, and inverse geochemical calculations. In *Modeling Techniques*, Volume 6-A43, pp. 497. Denver, Colorado, USA: U.S. Geological Survey Techniques and Methods.

Pedersen, K. M., M. Kummel, and H. Søeberg (1990). A real time measurement system for an activated sludge wastewater treatment plant. In R. Briggs (Ed.), *Instrumentation, Control and Automation of Water and Wastewater Treatment and Transport Systems*, pp. 171–178. Yokohama and Kyoto, Japan: Pergamon.

Pind, P. F., I. Angelidaki, and B. K. Ahring (2002). A novel in-situ sampling and VFA sensor technique for anaerobic systems. *Water Science and Technology 45*(10), 261–268.

Ponzelli, M. (2019). *Volatile Fatty Acids Recovery in a Reactive Primary Clarifier: A Pilot Case Study*. MSc Thesis, Ryerson University, Toronto, Canada.

Regmi, P., M. W. Miller, B. Holgate, R. Bunce, H. Park, K. Chandran, B. Wett, S. Murthy, and C. B. Bott (2014). Control of aeration, aerobic SRT and COD input for mainstream nitritation/denitritation. *Water Research 57*, 162–171.

Rieger, L. and P. A. Vanrolleghem (2008). monEAU: A platform for water quality monitoring networks. *Water Science and Technology 57*(7), 1079–1086.

Ruzicka, J. and E. H. Hansen (1975). Flow injection analyses: Part I. A new concept of fast continuous flow analysis. *Analytica Chimica Acta 78*(1), 145–157.

Sakami, W. and H. Harrington (1963). Amino Acid Metabolism. *Annual Review of Biochemistry 32*(1), 355–398.

Sawyer, C. N., P. L. McCarty, and G. F. Parkin (1994). *Chemistry for Environmental Engineering and Science*. New York, USA: McGraw-Hill.Inc.

Steyer, J. P., J. C. Bouvier, T. Conte, P. Gras, J. Harmand, and J. P. Delgenes (2002). On-line measurements of COD, TOC, VFA, total and partial alkalinity in anaerobic digestion processes using infra-red ectrometry. *Water Science and Technology 45*(10), 133–8.

Thomann, M., L. Rieger, S. Frommhold, H. Siegrist, and W. Gujer (2002). An efficient monitoring concept with control charts for on-line sensors. *Water Science and Technology 46*(4-5), 107–16.

Thyne, G. (2007). PHREEQC Modelling Short Course. Technical Report, Science Based Solutions LLC, Laramie, Wyoming, USA.

U.S. EPA (2013). Report on the 2013 U.S. Environmental Protection Agency (EPA) International Decontamination Research and Development Conference. Technical report, Research Triangle Park, NC.

Van De Steene, M., L. Van Vooren, J. P. Ottoy, and P. A. Vanrolleghem (2002). Automatic buffer capacity model building for advanced interpretation of titration curves. *Environmental Science & Technology 36*(4), 715–723.

Van Hulle, S. W., E. I. Volcke, J. L. Teruel, B. Donckels, M. C. van Loosdrecht, and P. A. Vanrolleghem (2007). Influence of temperature and pH on the kinetics of the Sharon nitritation process. *Journal of Chemical Technology & Biotechnology 82*(5), 471–480.

Van Hulle, S. W. H. (2005). *Modelling, Simulation and Optimization of Autotrophic Nitrogen Removal Processes*. PhD thesis, Ghent University, Ghent, Belgium.

Van Hulle, S. W. H., S. D. Meyer, T. J. L. Vermeiren, A. Vergote, J. Hogie, and P. Dejans (2009). Practical application and statistical analysis of titrimetric monitoring of water and sludge samples. *Water SA 35*(3), 329–333.

Van Hulle, S. W. H., U. Zaher, G. Schelstraete, and P. A. Vanrolleghem (2006). Titrimetric monitoring of a completely autotrophic nitrogen removal process. *Water Science and Technology 53*(4-5), 533–540.

Van Vooren, L. (2000). *Buffer Capacity Based Multipurpose Hard- and Software Sensor for Environmental Applications*. PhD thesis, Ghent University, Ghent, Beligium.

Van Vooren, L., P. Lessard, J. P. Ottoy, and P. A. Vanrolleghem (1999). pH buffer capacity based monitoring of algal wastewater treatment. *Environmental Technology 20*(6), 547–561.

Van Vooren, L., M. Van De Steene, J. P. Ottoy, and P. A. Vanrolleghem (2001). Automatic buffer capacity model building for the purpose of water quality monitoring. *Water Science and Technology 43*(7), 105–113.

Van Vooren, L., P. Willems, J. P. Ottoy, G. C. Vansteenkiste, and W. Verstraete (1996). Automatic buffer capacity based sensor for effluent quality monitoring. *Water Science and Technology 33*(1), 81–87.

Vaneeckhaute, C. (2015). *Nutrient Recovery from Bio-Digestion Waste: From Field Experimentation to Model-Based Optimization*. Joint PhD thesis, Faculty of Bioscience Engineering, Ghent University, Ghent, Belgium, and Faculté des Sciences et de Génie, Université Laval, Québec, Canada.

Vanrolleghem, P. A. and D. S. Lee (2003). On-line monitoring equipment for wastewater treatment processes: State of the art. *Water Science and Technology 47*(2), 1–34.

Von Sperling, M. (2007). *Wastewater Characteristics, Treatment and Disposal*, Volume 1. London, UK: IWA Publishing.

Wagner, S. C. (2011). Biological nitrogen fixation. In *Nature Education Knowledge*, Volume 3, pp. 10–15. Berlin, Germany: Nature Publishing Group.

Wikipedia (2020). Equivalent (chemistry).

Yanisko, P., S. Zheng, J. Dumoit, and B. Carlson (2011). Nitrogen: A Security Blanket for the Chemical Industry. *CEP (Chemical Engineering Process)*, 50–55.

Zaher, U. (2005). *Modelling and Monitoring the Anaerobic Digestion Process in View of Optimisation and Smooth Operation of WWTP's*. PhD thesis, Ghent University, Ghent, Belgium.

Zaher, U., J. Bouvier, J. Steyer, and P. A. Vanrolleghem (2004). Titrimetric monitoring of anaerobic digestion: VFA, alkalinities and more. In *Proceedings 10th World Congress on Anaerobic Digestion (AD10).*, pp. 7.

Appendix A

Dosage of Substrate Solutions to WRRF

A.1 Introduction and application area

There are two major sources of organic carbon utilized in wastewater treatment operations that originate from the influent wastewater entering the process or are added as external supplemental carbon source to the process. Carbon sources are termed external when the substrate is sourced from outside the wastewater treatment process. External substrate sources are brought into the wastewater treatment process usually as pure compounds or high strength waste materials.

One of the most common application areas of substrate addition is enhancing nitrogen removal in wastewater treatment systems. Indeed, the limiting factor for effective denitrification is often the absence of a readily biodegradable carbon source that can be used as an effective substrate by denitrifying bacteria during the denitrification process (U.S. EPA, 2013). Without the availability of a ready source of biodegradable carbon, denitrification will not occur, or will occur too slowly for sufficient nitrogen removal to occur. For that reason, substrate addition is generally done into anoxic reactors in the wastewater treatment systems since denitrification takes place in there. External substrate addition may also be added to improve phosphorus removal, due to its positive effect on the growth of polyphosphate accumulating organisms in enhanced biological phosphorus removal processes.

Substrate feeding or chemical addition to wastewater treatment systems can be done through dosage of solutions of a desired substrate or chemical. To obtain the required effect without overdosing, the required volume and concentration of the solution must be calculated for the specific system or unit process. This standard operation procedure (SOP) explains the calculations and preparation of a solution for substrate feeding to a reactive secondary settling tank (SST) and the biological reactor, and alkalinity dosage to influent.

Terminology: A solution is a homogeneous mixture prepared by dissolving one or more solutes in a solvent. A solute is the chemical that is present in the solution in a smaller amount than the solvent. Solutions with accurately known concentrations can be referred to as stock solutions. They typically have really high concentrations. These solutions can be bought directly from the manufacturer or formed by dissolving the desired amount of solute into a specific volume of solvent. Stock solutions are frequently diluted to solutions of lower concentration for experimental use.

To ensure the stability of the prepared solution, storage conditions are of major importance. By definition, substrate solutions may be subject to microbial growth, leading to a change in composition. As recommended by (Nopens et al., 2001), sterilization, refrigeration ($4°C$ or lower), and creating an alkaline (pH>11) or acid (pH<3) environment are conditions that are limiting microbial activity and thus, the stability of the solutions can be ensured.

A.2 Principle and theory

The solution can either be prepared from a solid or stock solution. Feeding of the solution can be done by using a peristaltic pump or diaphragm dosage (metering) pump. The suction tube is immersed in the solution storage container/bucket and the feeding tube is immersed into the reactor. It is suggested to practice the dosage process before the actual experiment to check the flowrate, calibrate the pump and see if the pump's wetted parts and tubes are compatible with the applied solution.

Calculations and preparation of a solution for substrate feeding to SST and alkalinity dosage to primary clarifier effluent are explained step by step in this section of the SOP.

A.2.1 Substrate dosage

An example of substrate dosage to the pilEAUte SST can be seen in Figure A.1.

An important point is to calculate the accurate concentration of the desired solution. This section explains the calculation steps to determine the concentration and quantity of a dosing solution and the crucial points that should be considered.

Substrate feeding into a secondary settling tank to enhance the denitrification which may take place in the sludge blanket, will be given as an example for each calculation step. Sodium acetate is suggested as substrate as it is a readily biodegradable COD source and will not influence the ammonia concentration in the reactor.

1. Determine current load: The first step is to determine the amount of chemical/substrate that is present in the influent of the system/reactor. It can be calculated by multiplying

Figure A.1: Substrate dosage into the pilEAUte SST

the incoming concentration with the flowrate of the system/reactor.

$$CurrentLoad = Concentration * Flowrate \tag{A.1}$$

Example: The soluble COD concentration at the inlet of the settling tank is measured as 18 mg/L and the influent flowrate is 0.5 m^3/h. Also, it is important to consider the sludge recycle flowrate to know the total inflow of settling tank which is 0.15 m^3/h in this example. So, the current substrate load is:

$$18(mg/L) * (0.5 + 0.15)(m^3/h) * 1(g)/10^3(mg) * 10^3(L)/1(m^3) = 11.7(g/h) \tag{A.2}$$

2. Determine the desired dosage load: The concentration of the solution can be calculated based on the desired load of the chemical into the system/reactor. The desired dosage load can be assumed by considering the current load (Step-a)

In case of substrate dosage to the SST, 2 or 3 times the current load can be accepted as dosage load to ensure that there will be sufficient organic material in the SST for biomass activity. The desired dosage load is accepted as:

$$11.7(g/h) * 2 = 23.4(g/h) \tag{A.3}$$

3. Determine the concentration of the solution: Depending on the aim and limiting factors of the substrate dosage, the following aspects should be considered to calculate the concentration of the substrate solution.

   The concentration of the substrate solution has to be lower than the maximum solubility of the chemical to ensure an applicable dosage concentration. It is better to consider

the solubility of substrate first and decide the concentration that will be dosed. Then, additional limiting factors should be considered, and dosage properties should be calculated.

It is important to choose the flowrate that will be fed to the reactor. The feed flowrate should be determined by considering the solubility of the chemical and the applicable flowrate range of the dosage pump. The applicable flowrate refers to the feeding flowrate that can be applied with the dosing pump. Peristaltic or diaphragm pumps can be used for dosing different chemicals into wastewater systems and they have a wide range for dosing solutions from mL/h to m3/h flowrates. Also, it is important to consider the feeding period which answers how long the solution can be dosed with a certain volume or how often the solution should be replaced.

The total volume of the solution that will be fed to the reactor can be calculated by considering the feeding period and decided feeding flowrate. It is important to consider the volume and availability of a storage tank (bucket/barrel) which will be used to store the total volume of the solution. In this step, the overall dosage flow should be checked by considering the calculated total volume of solution and feeding period.

In case of substrate dosage to the SST the first factor is the solubility of the chemical that will be used. It is not possible to prepare a solution with a higher concentration than its solubility in water and this should be considered in the calculations. It is known that the maximum solubility of acetate at $20°C$ ranges from 408.1 g/L to 762 g/L depending on the acetate salt chosen. First the dosage flowrate of the saturated solution can be calculated as follows:

$$\begin{aligned} Necessary\,dosage\,flowrate &= (Desired\,feeding\,load)/(Dosage\,concentration) \\ &= 23.4(g/h)/408.1(g/L) = 50(mL/h) \end{aligned} \tag{A.4}$$

However, it is not suggested to dose a highly saturated solution as it may be hard to prepare and dose in practise. For that reason, the calculation above gives an idea about the minimum feeding flowrate that can be applied.

The acetate solution concentration is chosen as 40 g/L (10 times lower than the maximum solubility).

$$\begin{aligned} Dosage\,flowrate &= (Desired\,feedingload)/(Chosen\,dosage\,concentration) \\ &= 23.4(g/h)/40(g/L) = 0.57(L/h) = 9.58(mL/min) \end{aligned} \tag{A.5}$$

Thus, in case of substrate dosage to the SST a flowrate of 10 mL/min is determined as dosage flowrate (which is higher than the 50 mL/h and the minimum applicable flowrate of the peristaltic pump). The feeding time period is assumed to be 18 h/day by considering the necessary solution amount, feeding flowrate and necessary substrate load for the system. The overall volume of solution needed for 18 h/day can be calculated as follows:

$$\begin{aligned} Dosage\,flowrate &= (Desired\,feedingload)/(Chosen\,dosage\,concentration) \\ &= 23.4(g/h)/40(g/L) = 0.57(L/h) = 9.58(mL/min) \end{aligned} \tag{A.6}$$

$$Daily\,volume\,of\,solution = 10(ml/min) * 18(h) = 10.8(L) \tag{A.7}$$

A bucket with 12 L volume is available and assumed to be used.

4. Determine the required chemical amount: The final step is to calculate the necessary chemical amount that will be used to prepare the solution. The total amount of chemical that will be used is calculated based on the concentration and the total volume of the solution as follows:

$$Daily\,amount\,of\,chemical = Concentration * Daily\,volume\,of\,the\,solution \tag{A.8}$$

To conclude the substrate feeding to SST example, the required acetate amount can be calculated as follows:

$$40(g/L) * 10(L) = 400(g) \tag{A.9}$$

Which means 400 g of sodium acetate should be dissolved in 10 L distilled water per day. It should be considered that 1 bottle of sodium acetate is 750 g and it may take a few weeks to order.

A.2.2 Alkalinity dosage

Dosing alkalinity to the primary settling tank (PST) of the pilEAUte could be another example of substrate dosing.

A.3 Solution preparation

To design an alkalinity dosage system, one needs to first precisely calculate the concentration of the desired solution. This section explains the calculation steps to determine the concentration and required quantity of the dosage solution.

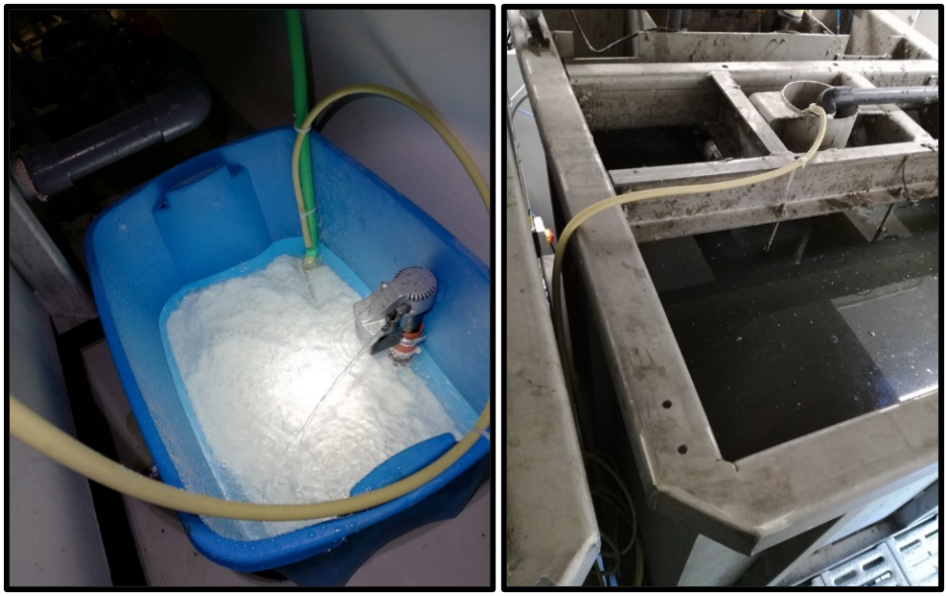

Figure A.2: Alkalinity dosage into the pilEAUte PST

Biological processes like nitrification and anaerobic digestion rely on alkalinity (Metcalf & Eddy, 2014). Without alkalinity, acids formed during these processes would drive the pH down to a point where the bacteria would be inhibited or could no longer survive. Influent wastewater that contains roughly 200 to 250 mg/L of alkalinity as $CaCO_3$ usually contains sufficient buffering capacity to prevent low pH values at the end of the treatment process. If the alkalinity present in the influent is not sufficient, chemical addition can help correct the deficiency (Metcalf & Eddy, 2014). Another reason to supplement the alkalinity of the influent is to keep the buffer capacity of the receiving water at a desired level. One of the common chemicals used for this purpose is sodium bicarbonate (baking soda) which is a soluble alternative of $CaCO_3$.

The amount of alkalinity present in the influent of the primary settling tank in the pilEAUte was measured with the Titrino set-up using titration curves. The average alkalinity measured with this method was 100 mg$CaCO_3$/L which is at least 100 mg/L short of the suggested alkalinity by Metcalf & Eddy (2014) (200 to 250 mg/L of alkalinity as $CaCO_3$). Therefore, the alkalinity needed to supplement the nitrification process is about 100 mg/L of $CaCO_3$. Since baking soda is the chosen substrate, all calculations should be adjusted for this component (modelEAU, 2012). By considering a saturated baking soda solution, the concentration of alkalinity to be dosed is assumed known, and the mass and volume of the baking soda solution needed to supplement this alkalinity can be calculated. Once the total volume of the baking soda aqueous solution is calculated, the volume of the tank needed to design the dosage system can be determined. These calculation steps are presented in the following sections.

1. Determine current load: As mentioned previously, the load of the substrate can be calculated by multiplication of the incoming concentration with the flowrate of the system.

   Knowing that the inlet flow rate to the PST is 0.7 m^3/h and the concentration of alkalinity in the inlet is 100 mg/L, the current load is:

   $$100(mg/L) * 0.7(m^3/h) * 1(g)/10^3(mg) * 10^3(L)/(m^3) = 70(g/h) \quad \text{(A.10)}$$

2. Determine the desired dosage load:

   The desired concentration of alkalinity is 200 mg/L of $CaCO_3$ which means the desired load is two times more than the current load; knowing that the flow rate is constant:

   $$200(mg/L) * 0.7(m^3/h) * 1(g)/10^3(mg) * 10^3(L)/(m^3) = 140(g/h) \quad \text{(A.11)}$$

   Assuming 100 mg/L of alkalinity to be dosed, the molarity of $CaCO_3$ with a molecular weight of 100.08 g/mole is:

   $$mmol/LCaCO_3 = 100(mg/LCaCO_3)/100.08(g/molCaCO_3) = 0.99(mmol/L) \quad \text{(A.12)}$$

   Knowing that the number of equivalents per mole of $CaCO_3$ is 2, the equivalents per liter needed are calculated as follows:

   $$meq/LCaCO_3 = meq/mmolCaCO_3 * mmol/LCaCO_3 \quad \text{(A.13)}$$

   $$meq/LCaCO_3 = 2.00 * 0.99 = 1.99(meq/L) \quad \text{(A.14)}$$

   An equivalent is the amount of a substance that reacts with (or is equivalent to) an arbitrary amount of another substance in a given chemical reaction. By this definition, an equivalent is the number of moles of an ion in a solution, multiplied by the valence of that ion. The equivalent weight of a compound can be calculated by dividing the molecular weight by the number of positive or negative electrical charges that result from the dissolution of the compound (Wikipedia, 2020).

   Therefore, the equivalent weight of $CaCO_3$ and $NaHCO_3$ is calculated as follows:

   $$g/eqCaCO_3 = MWCaCO_3/nofions = 100.08/2 = 50.04(g/eq) \quad \text{(A.15)}$$

   $$g/eqNaHCO_3 = MWNaHCO_3/nofions = 84.00/1 = 84.00(g/eq) \quad \text{(A.16)}$$

3. Determine the concentration of the solution:

4. In view of implementing the alkalinity addition to the PST, different experiments were carried out to understand the solubility and the saturation concentration of baking soda in tap water. The set-up conditions were as follows:

   - 250 g of baking soda (Arm and Hammer), 100 % pure $NaHCO_3$
   - 5 L of tap water, gently poured in the bucket
   - Supernatant sampled at different time intervals and analysed with Titrino to measure the alkalinity.

   The evolution of the solubilization of $NaHCO_3$ in a batch experiment is shown in Figure A.3. The saturation concentration obtained is 30 g$CaCO_3$/L.

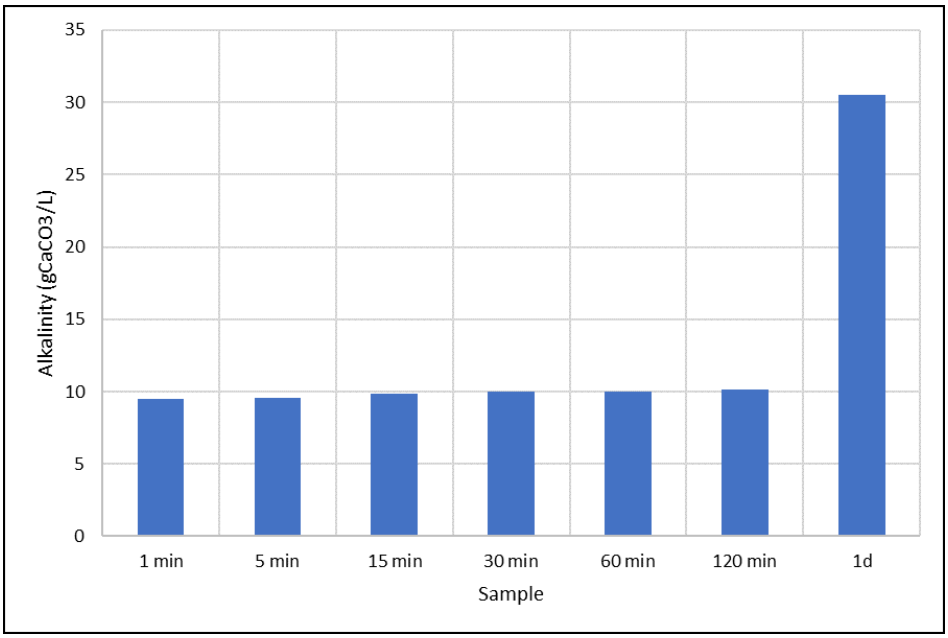

Figure A.3: $NaHCO_3$ solubilization over time

The equivalent saturation concentration of $NaHCO_3$ is calculated as follows:

$$\begin{aligned} g/LNaHCO_3 &= 84(g/eqNaHCO_3) * 30(g/LCaCO_3)/50.04(g/eqCaCO_3) \\ &= 50.36(g/L) \end{aligned} \tag{A.17}$$

The latter will be used to calculate the needed flow rate. However, in order to calculate the flow rate, the equivalent concentration of the substrate is another necessary parameter.

Knowing the equivalents per liter of the solution, the concentration of the substrate should be defined:

$$\begin{aligned} mg/LNaHCO_3 &= 84(g/molNaHCO_3) * 1.99(meq/LCaCO_3)/1(eq/LCaCO_3) \\ &= 167.87(mg/L) \end{aligned} \tag{A.18}$$

Therefore, the mass of $NaHCO_3$ needed per hour with the above concentration and the constant inlet flow rate of 0.7 m3/h is:

$$g/hNaHCO_3 = 167.86(mg/LNaHCO_3) * 0.7(m^3/h) = 117.50(g/h) \tag{A.19}$$

Thus, the mass loaded within a day will be:

$$g/dNaHCO_3 = 117.50(g/hNaHCO_3) * 24(h) = 2820.18(g/d) \tag{A.20}$$

Now, using the mass loaded per hour and the saturation concentration, the minimum volume of solution to be added per hour/day/min is calculated as follows:

$$L/hNaHCO_3 = 117.50(g/hNaHCO_3)/50.36(g/LNaHCO_3) = 2.33(L/h) \tag{A.21}$$

$$L/dNaHCO_3 = 2.33(L/hNaHCO_3) * 24(h)/1(d) = 56.00(L/d) \tag{A.22}$$

$$mL/minNaHCO_3 = 56(L/d)*1(d)*1000(mL/L)/60(min)*24(h) = 38.88(mL/min) \tag{A.23}$$

The calculated minimum flow rate of the solution to be added is 38.88 mL/min, thus the flow rate of the peristatic pump is adjusted to pump 40 mL of solution per minute to the PST. As such, the flow rate of the solution dosed per day by the pump is:

$$L/dNaHCO_3 = 40(mL/min) * 60(min) * 24(h)/1(d) * 1000(mL/L) = 57.6(L/d) \tag{A.24}$$

5. Determine the required chemical amount:

Assuming a storage retention time of 5 days for the tank, the total mass of baking soda to be added is:

$$kgNaHCO_3 = 2820.18(g/dNaHCO_3) * 1(kg)/1000(g) * 5(d) = 14.10(kg) \tag{A.25}$$

Thus, in case of substrate dosage to the PST a slightly higher mass of 15 kg is determined as dosage mass. The total volume of baking soda with density of

2.2 kg/L is:

$$LNaHCO_3(solid) = 14.10(kgNaHCO_3)/2.2(kg/LNaHCO_3) = 6.41(L) \quad \text{(A.26)}$$

6. Determine the volume of the solution: To determine the volume of the dissolution tank an HRT of 1 day should be imposed, since the baking soda needs one day of retention time to reach saturation (see Figure A.3). Knowing the HRT and the flowrate, one can calculate the volume of the solution to be prepared.

   An HRT of 1 day can be considered for the solution tank, since the baking soda needs one day of retention time to be saturated (see Figure A.3. Knowing the HRT and the flowrate, one can calculate the volume of the solution to be prepared.

$$HRT = V/Q \quad \text{(A.27)}$$

$$LNaHCO_3(aq) = 57.6(L/dNaHCO_3) * 1(d) = 57.6(L) \quad \text{(A.28)}$$

Note that this value represents the volume of the solution for 1 day of HRT. Therefore, in the beginning of the dosing when the baking soda has not yet dissolved, the total volume of the tank should be:

$$LNaHCO_3(total) = 57.6(L) + 6.41(L) = 64.01(L) \quad \text{(A.29)}$$

This volume includes the volume of the solid baking soda as well as the volume of the water (solvent) needed to dissolve this amount. It ensures that the baking soda is not under/over saturated. Therefore, a total volume of 64 L should be prepared in the tank.

A.4 Solution preparation

The solutions can be prepared by dissolving the desired amount of solute (e.g. substrate-acetate) into a specific volume. Also, stock solutions can be used for dilution to solutions of lower concentration for experimental use.

A.4.1 Preparing a standard solution from a solid

First, the required mass of solid chemical is weighed in a small beaker. A small amount of solvent is added to the beaker and the solution is stirred until the solid is dissolved. The amount of solid to be added should lower than the solubility of the chemical. The solution is then transferred into a volumetric flask with a specific volume corresponding to the required dilution. Before adding additional solvent to the flask, the beaker and stirring rod must be rinsed carefully with the solvent and the washings added to the volumetric flask to make sure all remaining traces of the solution have been transferred. Finally, additional solvent is added

to the flask until the liquid level reaches the volume mark. The flask is capped and inverted until the contents are thoroughly mixed.

In the case of substrate feeding into the SST, the required volume is higher than can be prepared with a volumetric flask. For that reason, a concentrated acetate solution should be prepared by using a volumetric flask and then it should be diluted to the desired concentration.

For the example given above, it is known that only 400 g of sodium acetate can be dissolved in a 2 L volumetric flask as explained above. Then, it can be transferred into a bucket and completed to 10 L.

In the alkalinity dosage example, it was calculated that the total volume of the tank in which the baking soda is continuously dissolved to saturation, is 64 L. To supply a saturated solution for 5 days, 15 Kg of baking soda needs to be added to the tank. As calculated earlier, to ensure that the solution leaves saturated, a minimum volume of 56.7 L of water should be provided (HRT = 1 day). To maintain the concentration of the solution saturated, the volume of the solution should remain constant over time. For this, a toilet syphon was used to continuously add tap water to the solution, maintaining the level of water at a desired height. Once the tank was filled with 65 L of solution, the syphon was fixed at the water surface. In addition, a mixer was added to ensure the homogeneity of the solution. The alkalinity solution was dosed to the primary clarifier with a peristaltic pump.

A.4.2 Diluting a solution of known concentration

Dilution is the addition of more solvent to produce a solution of reduced concentration. Most often a diluted solution is created from a small volume of a more concentrated stock solution. To make such a solution, a volumetric pipet is used to deliver an exact amount of the stock solution into a clean volumetric flask, which is then further filled up to the required volume. Caution: This procedure is reversed if the addition of the concentrated solution to solvent causes heating (an exothermic reaction). For example, if the solution will be done with an acid, first distilled water should be put into the flask, then the acid should be added slowly.

A.5 Conclusion

Within this SOP, the preparation of substrate dosage into wastewater treatment systems is explained and the crucial points of dosage calculations are presented. All required steps are explained with examples: substrate feeding into a secondary settling tank and alkalinity addition to PST influent. The order of the calculation steps can be changed depending on the aim of the dosage and the chemical that will be used. The following issues are suggested to be considered carefully when preparing substrate dosage:

- Solubility of substrate/chemical

- Necessary feeding flowrate
- Applicable feeding flowrate
- Feeding period
- Total volume of the solution
- Reservoir to keep the solution
- Refill period of the reservoir if necessary